The Flexible Alternating Current Transmission System (FACTS) devices affect the performance of the pre-existing protective distance relays on the transmission line. These devices make the distance relay to either under reach or over reach their protection zone and trip boundaries especially when they are located within the fault loop. This dissertation dealt on the mitigation of the effects of a series FACTS device, Thyristor Controlled Series Capacitor (TCSC), on the distance relays used in the protection of transmission lines. The simulation model of the Thyristor Controlled Series Capacitor, a series FACTS device was implemented in the Nigeria power system using MATLAB/ Simulink software tool so as to bring to fore the impact of these compensation devices on the performance of distance relays on the transmission line. The apparent impedance of the Nigeria 330kV transmission network was calculated based on the symmetrical components of voltage and current. The results from the case system for different fault types at various locations were generated from system modelling and simulations for conditions without TCSC, with TCSC and with Metal Oxide Varistor (MOV) protection. For the case without TCSC, the relay tripped a 50km fault at 50.03km for relay A and 229.47km for relay B indicating zone 1 and zone 2 protection zone respectively. For a 100km fault, the relay tripped at 100.1km for relay A and 181.9km for relay B indicating zone 1 protection for both relays. Also for a 250km fault, the relay tripped the fault at 250.17km for relay A and 29.15km for relay B indicating zone 2 and zone 1 protection zone respectively. This base case without TCSC indicates that the distance relay operated accurately and tripped the fault at the correct protection zones. When TCSC was incorporated in the system under different fault conditions, the relay overreached its protection zone; for a 50km fault, the relay tripped the fault at 51.15km for relay A and 117.6km for relay B indicating both relays tripping in protection zone 1. For a 100km fault, the relay tripped at 100.1km for relay A and 67.46km for relay B. Also for a 250km fault, relay A tripped at 138.2km and relay B tripped at 30.02km indicating both relays tripping in zone 1. These tripping zones for TCSC incorporation show inaccurate relay zone coordination. The introduction of protective MOV with TCSC considering line distributed parameters resulted to further relay mal-operation. Implementing the developed adaptive relay algorithm, a 50km fault tripped correctly at 50.01km for relay A and 229.77km for relay B, 100km fault tripped at 100.1km for relay A and 180.01km for relay B also 250km fault tripped at 250.10km for relay A and 29.50km for relay B. These indicate correct and accurate protection zone tripping. Thus, the results from the developed adaptive relay algorithm proved very effective in adjusting the settings of the relay to accurately trip with respect to the location and direction of faults in the Nigeria power system.

The Flexible Alternating Current Transmission System (FACTS) devices affect the performance of the pre-existing protective distance relays on the transmission line. These devices make the distance relay to either under reach or over reach their protection zone and trip boundaries especially when they are located within the fault loop. This dissertation dealt on the mitigation of the effects of a series FACTS device, Thyristor Controlled Series Capacitor (TCSC), on the distance relays used in the protection of transmission lines. The simulation model of the Thyristor Controlled Series Capacitor, a series FACTS device was implemented in the Nigeria power system using MATLAB/ Simulink software tool so as to bring to fore the impact of these compensation devices on the performance of distance relays on the transmission line. The apparent impedance of the Nigeria 330kV transmission network was calculated based on the symmetrical components of voltage and current. The results from the case system for different fault types at various locations were generated from system modelling and simulations for conditions without TCSC, with TCSC and with Metal Oxide Varistor (MOV) protection. For the case without TCSC, the relay tripped a 50km fault at 50.03km for relay A and 229.47km for relay B indicating zone 1 and zone 2 protection zone respectively. For a 100km fault, the relay tripped at 100.1km for relay A and 181.9km for relay B indicating zone 1 protection for both relays. Also for a 250km fault, the relay tripped the fault at 250.17km for relay A and 29.15km for relay B indicating zone 2 and zone 1 protection zone respectively. This base case without TCSC indicates that the distance relay operated accurately and tripped the fault at the correct protection zones. When TCSC was incorporated in the system under different fault conditions, the relay overreached its protection zone; for a 50km fault, the relay tripped the fault at 51.15km for relay A and 117.6km for relay B indicating both relays tripping in protection zone 1. For a 100km fault, the relay tripped at 100.1km for relay A and 67.46km for relay B. Also for a 250km fault, relay A tripped at 138.2km and relay B tripped at 30.02km indicating both relays tripping in zone 1. These tripping zones for TCSC incorporation show inaccurate relay zone coordination. The introduction of protective MOV with TCSC considering line distributed parameters resulted to further relay mal-operation. Implementing the developed adaptive relay algorithm, a 50km fault tripped correctly at 50.01km for relay A and 229.77km for relay B, 100km fault tripped at 100.1km for relay A and 180.01km for relay B also 250km fault tripped at 250.10km for relay A and 29.50km for relay B. These indicate correct and accurate protection zone tripping. Thus, the results from the developed adaptive relay algorithm proved very effective in adjusting the settings of the relay to accurately trip with respect to the location and direction of faults in the Nigeria power system.

CHAPTER ONE

INTRODUCTION

1.1 Back Ground of the Study

Generally, the asynchronous machines are basically alternating current (a.c) electrical machine, which run at speed other than the synchronous speed of the rotating magnetic field developed by the stator currents in the stator windings. Like other electrical machines, the asynchronous machines are reversible, in that they can operate at a time as either motors or generators. The mode of operation of the machine is principally determined by the rotating magnetic field in relation to the rotor. Strictly speaking, all asynchronous machines are based on induction principle. Categorically, asynchronous machines are of two types viz;

i) the Normal induction motor(I M)

ii) the Transfer-field reluctance machine (TFM)

1.1.1 The transfer field reluctance Machine

In its broad definition, a reluctance machine is an electric machine in which torque is produced by the tendency of a movable part to move into a position where the inductance of an energized phase winding is a maximum.

Structurally, the transfer field machine is basically a reluctance machine. It differs from the simple reluctance machine in two important aspects viz;

i) it has two set of windings instead of one, as obtainable in simple reluctance machine

ii) each winding has a synchronous reactance which is independent of rotor position, while the winding reactance of simple reluctance machine varies cyclically (L.A Agu 1984).

The transfer field machine comprises basically a stator, with current carrying windings which produce a rotating magnetic field as in normal induction motor and a second member, the rotor, which is magnetically anisotropic; meaning that the reluctance to the passage of flux along one axis is a minimum and along a second axis, at ninety electrical degree to the first is maximum. The operation of the machine depends on the tendency of the low-reluctance axis to align itself with the axis of the rotating magnetic field. In its most elementary form, it comprises two identical salient-pole machines whose rotors are mechanically coupled together but with their axis displaced by 0.5π electrical radians.

The main windings are connected in series, while the auxiliary winding are connected in series but transposed between the two machine sections. There are no windings on the rotor of either of the composite machines.

This machine induces negative sequence e.m.fs of frequency (2s-1) ω_0 in the auxiliary windings which will in turn circulate a current excluded from the supply.

The interaction of the main and auxiliary winding magnetomotive forces (mmfs), will produce an interference wave with beat frequency ω, which is equal to the rotor frequency. Hence a reluctance torque is developed in the rotor as a result of its interaction with the interference wave and this creates a turning effect on the rotor segment of the machine. This however gives the implication that a transfer-field machine is an energy converter and like the normal induction motoris asynchronous and may or may not be self starting depending on the machine type and the nature of a.c supply. The transfer-field machine is very useful in control systems, electrical gear, low speed drives etc. It has the outstanding advantage that its auxiliary winding terminals which correspond to rotor conductors in normal induction motor is available without requiring slip-rings or current collection gear, thereby making it applicable

in harsh environment. More interestingly, the machine can also be used to supply a d.c load through rectifier, a function which has not been performed satisfactorily by induction motor, because the output wave forms of induction motors tend to be increasingly distorted as the load current increases.

1.2 Statement of Problem

This research work becomes imperative due to;

i. the major set backs of the existing three phase transfer field motor without rotor winding, which includes the low output torque, low output power and lower power factor.
ii. these poor output characteristics of the motor make it very much inferior to those of conventional three-phase induction motor counterpart of comparable size and rating. This is the attribute of its excessive leakage reactance.

1.3 Aim and Objectives of the research work.

The aim of this dissertation is to improve the performance indices of a three-phase transfer field reluctance motor through induced rotor current.

The objectives are to;

i. develop models of the machine necessary to explain its behaviour under steady-state and dynamic state conditions.
ii. derive mathematical equations necessary for the formation of the machine's equivalent circuits
iii. derive the machine's output characteristics equations from the equivalent circuits.
iv. establish the machine's circuit parameters necessary for the output characteristic plots through simulations for the analysis of the machine's output.

1.4 Significance of the research work

The significant of this research work lies on the improvement of the performance characteristics of the existing three phase transfer field reluctance motor by the introduction of rotor windings to the salient poles structures. These characteristics include; the output torque, power factor and starting current.

It is common knowledge that a low speed machine will find numerous applications in domestic and industrial appliance requiring low speed drives, such as grinding machines for perishables etc.

1.5 Motivation

This work is motivated by the fact that the new configuration of three phase transfer field relucantce motor has the potential of replacing the induction motor counterpart which incorporates inverters for low speed operations for industrial and domestic purposes.

1.6 Scope of the research work

The study circles within the analysis of the effect of the introduction of rotor windings on three-phase transfer field reluctance motor, followed by derivation of mathematical models/equations necessary for the formulation of machines equivalent circuits. Simulations of the derived equations from the models for analysis of the motor characteristics and comparison of its characteristics with those of the existing three phase transfer field reluctance motor without rotor winding were made, so also the presentation and discussion of the achieved results.

CHAPTER TWO

LITERATURE REVIEW

2.1 The Brief history of invention of induction motor(IM)

The induction motor is a well known machine with a long history of invention. The basic principles of electromagnetic induction were discovered in the early 19th century by Oersted, Guass and Faraday.

The first electric motors were simple electrostatic devices created by the Scottish monk Andrew Gordon in the 1740s. The theoretical principle behind the production of mechanical force by the interactions of an electric current and magnetic field (Amperes force law) was discovered later by Andre-Marie Ampere in 1820.

The conversion of electric energy into mechanical energy by electromagnetic means was demonstrated by British Scientist Michael Farady in 1821. He discovered the electromagnetic induction law around 1831 and Maxwell formulated the laws of electricity (Maxwell's equations) around 1860. This discovery and formulation, led to the invention of the induction motor generally credited to two Persons namely Galileo Farraris (1885) and Nicola Tesla (1886) (Ion Boldea et al 2011). Their induction machines are as shown in fig 2.1 and fig 2.2 respectively

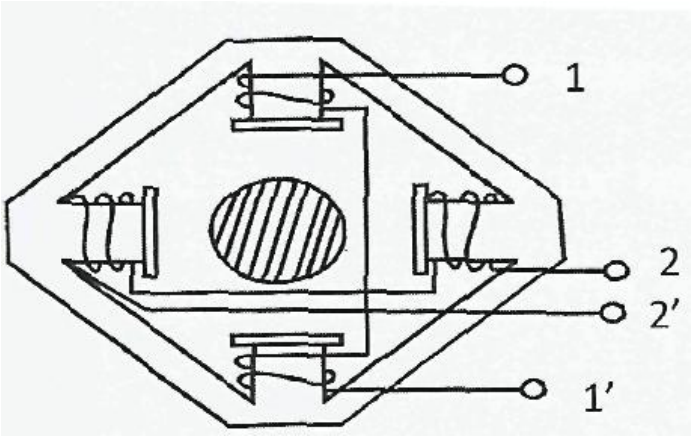

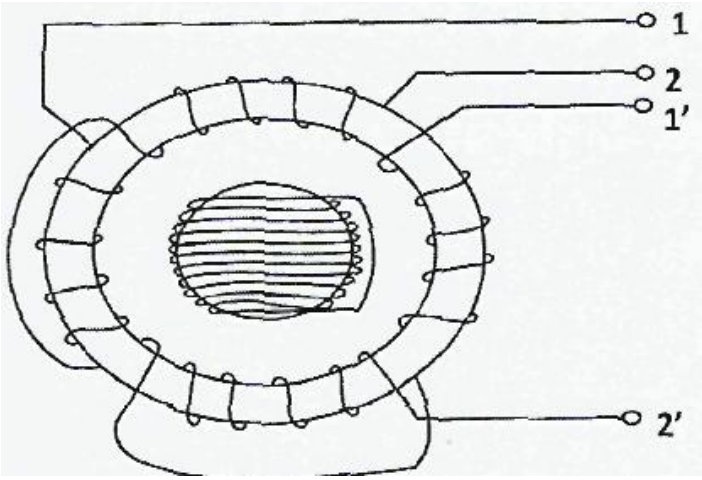

Fig 2.1 – Ferrari's induction motor **Fig 2.2 – Tesla's induction motor**

Both motors have been supplied from a two-phase a-c power source and thus contained two phase concentrated coil windings $1 - 1^1$ and $2 - 2^1$ on the ferromagnetic stator core. In Ferrari's patent, the rotor was made of a copper cylinder while in the Tesla's Patent, the rotor was made of a ferromagnetic cylinder provided with a short –circuited winding (P. Alger 1970).

Though the contemporary induction motors have more elaborate topologies and their performance is much better, the principle has remained basically the same.

The three-phase a-c power grid capable of delivering energy at a distance to induction motors and other consumers was put forward by Dolivo-Dobrovolsky around 1880. In the year 1889-1890, he introduced first ever cage rotor version of three phase induction motor. Interestingly, these type of motors are used till date for commercial purposes. Driven by his own invention, Dobrovolsky made a claim that motor by Tesla was unfit for practical use due to two phased pulsations.

In the year 1892, Westing House was successful in achieving his first induction motor that could be used practically. He developed GOHertz induction motor Lien 1893, but all of these early motors were two phased motors.

The General Electric started producing three phased induction motor by the year 1894. In some years time, in 1896, Westing house and General Electric signed agreement for production of squirrel cage rotor.

In 1905, Alfred Zehaden described linear induction motor that could be used in the lift or trains in a patent form. It took around thirty years from then for Kemper to build the linear induction motor for use in 1935. This motor was further improvised by Laithwaite.

He was the one to introduced first ever full sized working model of the induction motor. It is amazing to witness how conventional motors have progressed to be strong-horse powered motors today.

Basically the induction motor converts electric power to mechanical power in its rotor (rotating part). Its power is supplied to the rotating device by means of electromagnetic induction (Gupter, 2009). It is used in a wide variety of applications as a means of converting electric power to mechanical work. It is without doubt the work horse of electric power industry (Broad Way 1973). The reasons are its low cost, simple and rugged construction, absence of brushes (which are needed in most d.c. motors) and lastly and most importantly, its speed can be readily controlled by modern power electronic devices. In its normal working range, the speed of the induction motor remains reasonably constant, varying slightly with load. Hence, it is seen as a constant speed motor. Its major demerit is the inherent low lagging power factor. Another distinguishing feature of such motor is that they are singly excited machines, although such machines are equipped with both field and armature windings. In

such a machine, the field (stator) winding is connected to an a.c. supply and there is no electrical connection from the armature (rotor) to any source of supply. Currents are made to flow in the armature conductors by induction, which interacts with the field produced by the field winding and thereby producing a net unidirectional torque. Such motor are also called asynchronous motors as they run at a speed other than the synchronous speed of rotating filed developed by the stator currents. Like other electrical machines, the asynchronous machine is reversible meaning that it can either run as a generator or a motor at a time, depending on the nature of its slip. When run faster than its synchronous speed, an induction motor runs as an induction generator (Theraja 2002). It converts the mechanical energy it receives into electrical energy and this energy is released by the stator.

However, induction motor can be reversed as induction generator without running it faster than synchronous speed by connecting capacitor which makes it operate with leading power factor, or by allowing its rotor to be rotated by a prime mover. However, induction generators have restricted applications as a source of power supply.

In terms of the rotor type and constructional arrangements, induction motor can be classified into two types viz; Squirrel cage and Wound rotor induction motor.

The squirrel cage rotor windings are perfectly symmetrical and have the advantage of being adaptable to any number of pole pairs. The distribution of currents due to electromagnetic induction in the rotor bars varies from bar to bar sinusoidally and depends upon the position and time, assuming sinusoidal distribution of radial flux density in space and also the applied voltage to be varying sinusoidally with time. There is no possibility of adding any external resistance in the rotor circuit since the rotor winding is permanently short-circuited in the cage construction.

In wound rotor induction motor, the rotor is wound with an insulated winding similar to that of the stator except that the number of slots is smaller and fewer turns per phase of a heavier conductor are used. Some motors are provided with brush lifting and slip-ring short-circuiting arrangement for starting and running conditions. Since the connection of the wound secondary to the external terminal is made through slip-rings and brushes, so wound secondary motors often are caled slip-ring induction motors.

More-still, induction motor can also be classified depending upon the type of input supply. These are;

(i) Poly phase (usually three phase) induction motor

(ii) Single phase induction motor

2.2 The Poly Phase induction motor

The poly-phase induction motors are majorly the three phase type. The most popular ac motor for applications exceeding a few horse power is the three-phase induction motor. It is simple, extremely reliable, powerful for its size and has few moving parts. The field of the induction motor is in the stator, and the armature is on the rotor. The field has pairs of pole pieces onto which stator coils are wound. The simplest three-phase induction motor is the two-pole motor, which has pairs of poles, one pair for each phase.

The motor comprises a stator and a rotor mounted on bearings and separated from the stator air gaps. The stator consists of a magnetic core made up of laminations carrying slot-embedded conductors which constitute the stator windings. These windings can be connected in either a delta or three – or four wire star scheme. (See plates 4 and 5). the rotor of induction motor is cylindrical and carries either conducting bars short-circuited at both ends by end rings (See plate 6(a/b) or a poly phase winding connected in a predetermined manner with

terminals brought out of slip rings for external connections and short circuited (see plate 7(a/b).

2.2.1 Operation of three-Phase induction motor

For the principle of operation of three-phase induction motor, let us consider a two-pole, three-phase, star connected, symmetrical induction motorshown in fig. 2.3

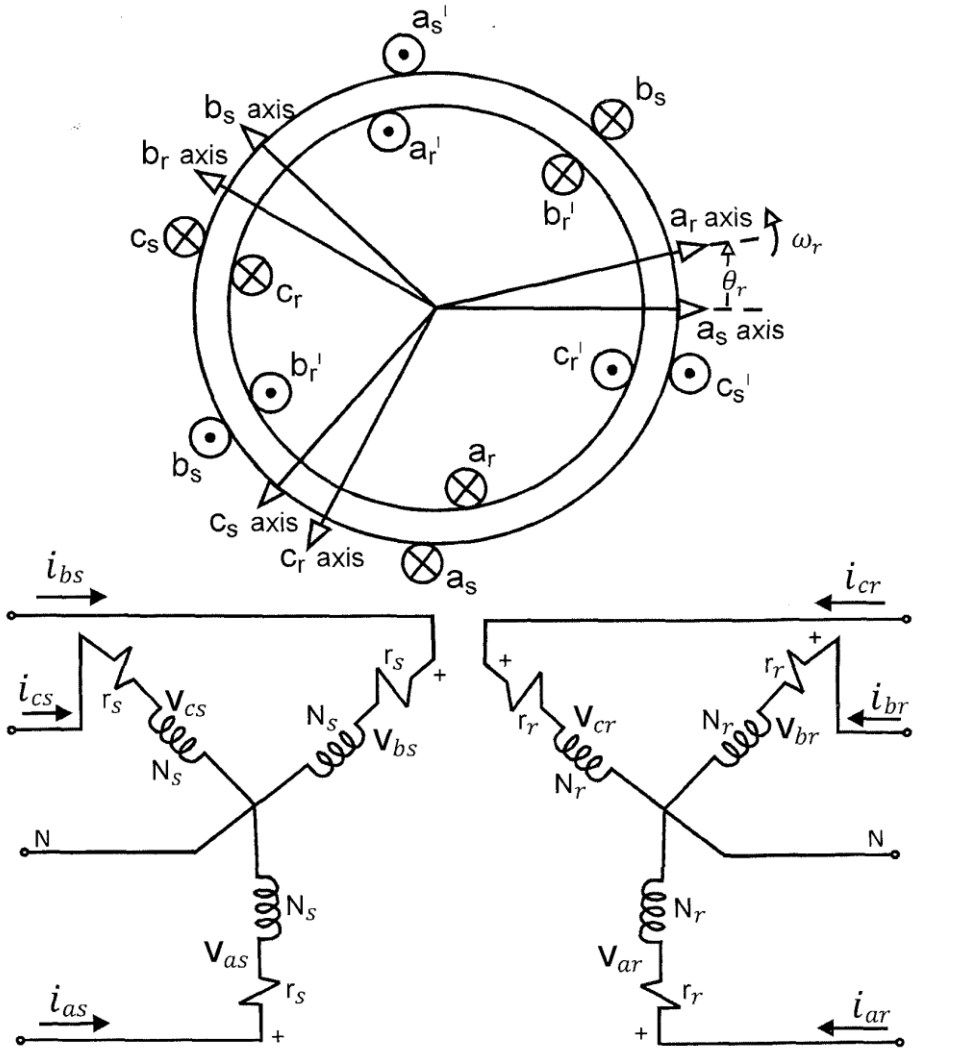

Fig 2.3: Two pole 3 – phase, star-connected symmetrical induction machine

The fundamental idea behind the operation of an induction motoris simple. In this work, qualitative description of the principles of operation of the machine is adopted. A three phase induction motorof the type provided in fig 2.3, comprises two major parts namely the stator and the rotor.

The phase displacement between the voltages applied on the stator windings produces a travelling MMF or rotating magnetic field in the uniform air gap.

This field links the short-circuited rotor winding and the relative motion induces short-circuit currents in them, which move about the rotor in exact synchronism with the rotating magnetic field. Obviously, any induced current will react in opposition to the flux linkages producing it, resulting herein a torque on the rotor in the direction of the rotating field. This torque causes the rotor to revolve so as to reduce the rate of change of flux linkages reducing the magnitude of the induced current and the rotor frequency.

If the rotor were to revolve at exactly synchronous speed, there would be no changing flux linkages about the rotor coils and no torque would be produced. However, the practical motor has friction losses requiring some electromagnetic torque, even at no load, and the system will stabilize with the rotor revolving at slightly less than synchronous speed. A mechanical shaft load will cause the rotor to decelerate, but this increases the rotor current, automatically increasing the torque produced, and stabilizing the system at a slightly reduced speed.

The difference in speed between rotor and rotating magnetic field is termed “slip”. Slip varies from a fraction of one percent at no-load to a maximum value of three or four percent under full load conditions for most properly designed machines. The speed change between no-load and full-load is so small that the squirrel-cage motor is often termed a constant –speed machine.

2.2.2 Induced Rotor Voltage

From the fundamental theory on rotating fields, passing balanced three-phase currents through a balanced three-phase winding can produce a rotating MMF wave. Speed of rotation is set by supply frequency and the number of poles in the machine. In an induction machine, the air-gap of the machine is designed to be constant, therefore the rotating MMF will produce a rotating flux density. The stator flux density can be defined in terms of either mechanical or electrical quantities as (T.A Lipo et al 1985);

$$\text{Bs} = \text{B Cos}\,\frac{p}{2}\left[(\theta_m - \emptyset_m - \omega_s t\,\right] = \text{B cos}\left[(\theta_e + \emptyset e - \omega_s t\,\right] \qquad (2.1)$$

In the above equation, ϕ_{m} and ϕ_{e} are arbitrary phase angle in mechanical and electrical angles respectively. They are normally set to zero. θ is the location at which the flux density wave form is observed. At a given location, the flux density varies sinusoidally with time and at a given time, it varies sinusoidally with location. To understand fully the workability of an induction machine, we need to consider the flux density seen by a conductor on the rotor.

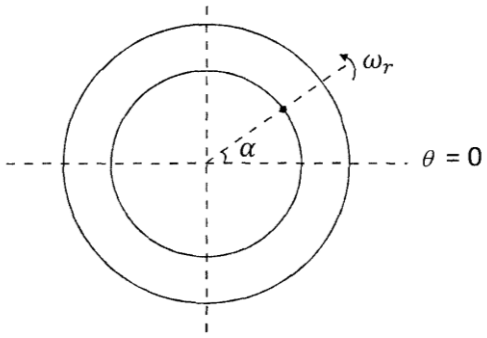

Fig 2.4; Image of a rotating MMF wave

In the image of a rotating MMF wave shown above, there is a rotor conductor at position $\theta_{\text{m}} = \alpha$. If the rotor is stationary then the rotor will observe the stator flux density as (T.A Lipo et al 1985);

$B_c = B_s \text{ Cos } \left[\frac{P}{2}(\alpha - \omega_s t)\right]$ (2.2)

Assuming the rotor is rotating at mechanical speed, ω_m, the location of the conductor becomes;

$\theta_m = \alpha + \omega_m t$ (2.3)

The flux density seen by the conductor becomes;

$B_c = B_s \cos \left[\frac{P_n}{2}\{\alpha + (\omega_m - \omega_s)t\}\right]$

$= B_s \cos \left[\frac{P_n}{2}(\alpha - s\omega_s t)\right]$

$= B_s \cos \left[\frac{P_n}{2}\alpha - \frac{P_n}{2}s\omega_s t\right]$

$= B_s \cos \left[\frac{P_n}{2}\alpha - s\omega_e t\right]$

$= B_s \cos \left[\frac{P_n}{2}\alpha - \omega_{sl} t\right]$ (2.4)

Where;

B_s = stator flux density

B_c = flux density as seen by the conductor

P_n = number of pole

ω_e = supply frequency in rad/s

$\omega_{sl} = s\omega_e$ = slip frequency in rad/s

Now the voltage induced in a conductor of length L, moving with velocity V, perpendicular to a magnetic field density B is given by (I. Mckenzie et al 1971);

$e = BLV \sin 90^0 = BLV$ (2.5)

The relative velocity V_r of conductor through the magnetic field is given by;

$$V_r = r\omega_{sl} = rs\omega_e \quad (2.6)$$

Therefore the voltage induced in the rotor conductor is obtained by substituting equations (2.4) and (2.6) into equation (2.5) which gives;

$$e = r\ L\ s\omega_e\ B_s \cos\left[\frac{P_n}{2}\ \alpha - s\omega_e t\right] \quad (2.7)$$

where; r is the radius of the conductor

2.2.3 Rotor Current and field

Without the knowledge of the full details of the rotor circuit some assumptions about the circuit can be made to enable us understand the behaviours of the induction machine. The assumption is that the motor conductor is part of a circuit with constant resistance R_R and inductance L_R, (T.A. Lipo et al 1985).

Now if the slip is low ($s \rightarrow o$), then the reactance associated with the inductance will be negligible and is given by the expression;

$$X_R = S\omega_e L_R \quad (2.8)$$

In this case, though induced voltage is small, the induced current may be significant, since the conductors are short-circuited, and so, R_R is low. Also the currents will be approximately in phase with the induced voltage. If the slip is high ($S \rightarrow 1$), then the rotor reactance will be significant due to the increase in induced voltage, rotor current will be high but will lag the induced voltage significantly due to the inductance of the rotor (Fitzgerald A.E. et al 2003).

The flux density produced by a set of a.c. currents rotates at a speed given by;

$N_s = \frac{120 f_e}{P_n}$ rpm (2.9)

In the case of rotor currents, equation (2.9) gives the speed of rotation relative to the conductors. However, the actual speed of rotation of the flux density will be given by;

$\omega_r = \omega_s (1-s)$ rad/s. (2.10)

That is, the rotor magnetic field rotates at synchronous speed.

We can get a better understanding of the relative position of the rotor and stator fields by drawing phasor diagrams. The phasor diagram of the stator flux density can be drawn from either a stator reference frame where it rotates at electrical speed, ω_e or from the rotor reference frame, where it rotates at electrical speed $s\omega_e$.

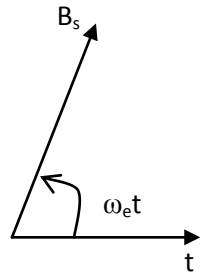

(a) Stator phasor observed from stator

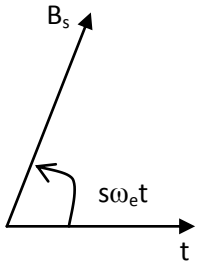

(b)**Stator phasor observed from rotor**

Fig. 2.5

We first consider the case where slip s is low. Under this condition induced current lags induced voltage slightly while the rotor flux density is almost 90^0 electrically behind the stator flux density. This is as illustrated in fig 2.6 below;

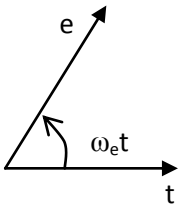

(a) Rotor induced voltage at low slip

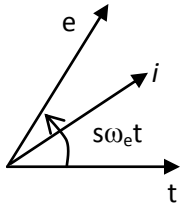

(b) Rotor current at low slip

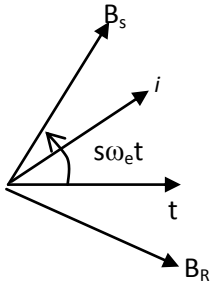

(c) Rotor current at low slip

Fig 2.6: Phasors for rotor induced voltage, current and flux density at low slip

From fig 2.6, it is seen that at low slip, the angle between the flux density phasors is almost 90^0. The rotor torque will be approximately proportional to induced voltage and therefore proportional to slip. When the slip is very high, mechanical speed is close to zero.

Under this condition, rotor current lags induced voltage and the angle between rotor nad stator flux densities is much greater. This is illustrated in figure 2.7

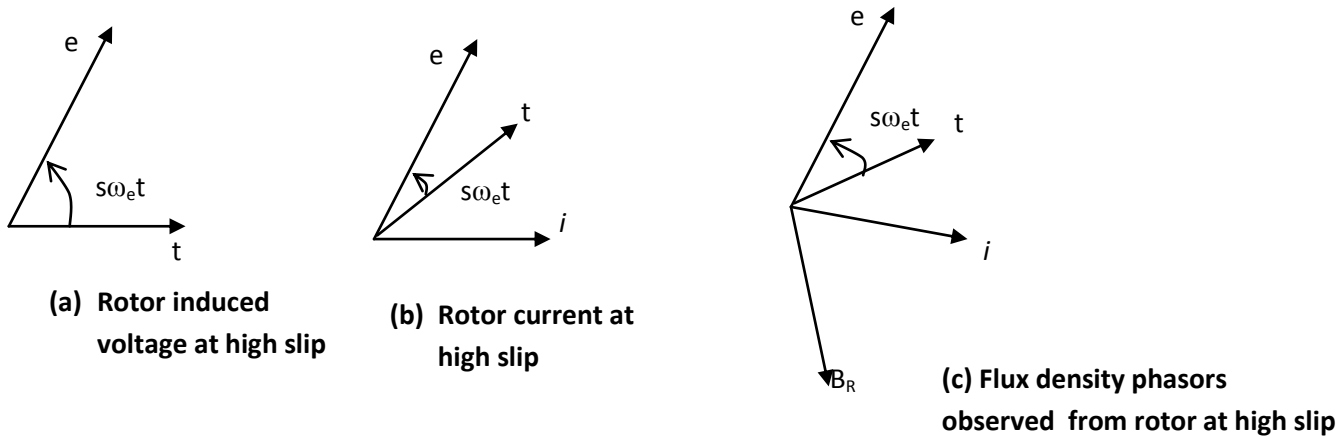

Fig 2.7: Phasors for rotor induced voltage, current and flux density at high slip

From the torque equation, even though the magnitude of the induced currents is higher and the rotor flux density phasor has a high magnitude, torque will not necessarily be higher than it is at low slip (Fitzgerald A.E et al 2003).

2.2.4 The inductance matrix and transformation of stator quantities to arbitrary q-d-o reference frame

The winding arrangement of a 2-pole, 3-phase, star connected symmetrical induction motoris shown in figure 2.3. The stator windings are identical with equivalent turns, (N_s) and resistance (r_s). The rotor windings which may be wound or forged as a squirrel cage winding can also be approximated as identical windings with equivalent turns (N_r) and resistance (r_r)

The air gap of an induction motoris uniform and the stator and rotor windings may be approximated as having a sinusiodally distributed windings

The stator inductance L_s is given as,

$$L_s = \begin{bmatrix} L_{Ls} + L_A - L_B \cos 2\theta_r & -\tfrac{1}{2} L_A - L_B \cos 2\left(\theta_r - \frac{\pi}{3}\right) & -\tfrac{1}{2} L_A - L_B \cos 2\left(\theta_r - \frac{\pi}{3}\right) \\ -\tfrac{1}{2} L_A - L_B \cos 2\left(\theta_r - \frac{\pi}{3}\right) & L_{Ls} + L_A - L_B \cos 2\left(\theta_r - \frac{2\pi}{3}\right) & -\tfrac{1}{2} L_A - L_B \cos 2(\theta_r + \pi) \\ -\tfrac{1}{2} L_A - L_B \cos 2\left(\theta_r + \frac{\pi}{3}\right) & -\tfrac{1}{2} L_A - L_B \cos 2(\theta_r + \pi) & L_{Ls} + L_A - L_B \cos 2\left(\theta_r + \frac{2\pi}{3}\right) \end{bmatrix} \quad (2.11)$$

Where; $L_{Ls} + L_A - L_B \cos 2\theta r = La_s a_s$ = Stator self inductance in winding **a** (2.12)

$L_{Ls} + L_A - L_B \cos 2\left(\theta_r - \frac{2\pi}{3}\right) = L_{bs} b_s$ = Stator self inductance in winding **b** (2.13)

$L_{Ls} + L_A - L_B \cos 2\left(\theta_r + \frac{2\pi}{3}\right) = L_{cs}\, c_s$ = Stator self inductance in winding **c** (2.14)

$-\tfrac{1}{2} L_A - L_B \cos 2\left(\theta_r - \frac{\pi}{3}\right) = L_{as} b_s$ (2.15)

$-\tfrac{1}{2} L_A - L_B \cos 2\left(\theta_r + \frac{\pi}{3}\right) = L_{as}\, c_s$ (2.16)

$-\tfrac{1}{2} L_A - L_B \cos 2(\theta_r + \pi) = L_{bs}\, c_s$ (2.17)

From equation 2.11, it is evident that all stator self inductances are equal.

That is; $L_{as}\, a_s = L_{bs}\, b_s = L_{cs}\, c_s = L_{cs}\, c_s$ and $L_{as}\, a_s = L_{Ls} + L_{ms}$ (2.18)

Where;

L_{Ls} = Stator leakage inductance, L_{ms} = Stator magnetizing inductance

The stator magnetizing inductance, (L_{ms},) corresponds to L_A in equation (2.12) through equation (2.14), and is mathematically expressed as;

$$L_{ms} = \left(\frac{N_S}{2}\right)^2 \frac{\pi \mu_o r_s l}{g} \quad (2.19)$$

Where; N_s = stator equivalent turns, μ_o = permeability of free space, r_s = stator resistance, r_s = stator winding length

g = length of uniform gap

Like the stator self inductances, the stator – to stator mutual inductances are also equal.

This implies that;

$L_{as}\, b_s = L_{as}\, c_s = L_{bs}\, c_s = -\frac{1}{2} L_{ms}$ (2.20)

This corresponds to $-\frac{1}{2} L_A$ in equation (2.15) through equation (2.17) with $L_B = 0$. Consequently, equation 2.11 is now rewritten as;

$$L_s = \begin{bmatrix} L_{LS} + L_{mS} & -\frac{1}{2} L_{ms} & -\frac{1}{2} L_{ms} \\ -\frac{1}{2} L_{ms} & L_{LS} + L_{LS} & -\frac{1}{2} L_{ms} \\ -\frac{1}{2} L_{ms} & -\frac{1}{2} L_{ms} & L_{LS} + L_{ms} \end{bmatrix} \quad (2.21)$$

In a related manner, the rotor inductance matrix is obtained as;

$$L_r = \begin{bmatrix} L_{Lr} + L_{mr} & -\frac{1}{2} L_{mr} & -\frac{1}{2} L_{mr} \\ -\frac{1}{2} L_{mr} & L_{Lr} + L_{Lr} & -\frac{1}{2} L_{mr} \\ -\frac{1}{2} L_{mr} & -\frac{1}{2} L_{mr} & L_{Lr} + L_{mr} \end{bmatrix} \quad (2.22a)$$

Whereas in stator, the rotor self inductances are equal that is,

$L_{ar}\, a_r = L_{br}\, b_r = L_{cr}\, c_r = L_{Lr} + L_{mr}$ (2.22b)

The rotor magnetizing inductance, L_{mr} is given as;

$$L_{mr} = \left(\frac{N_S}{2}\right)^2 \frac{\pi \mu_o r l}{g} \quad (2.23)$$

The rotor – to-rotor mutual inductances are equal and expressed as;

$L_{ar}\, b_r = L_{ar}\, c_r = L_{br}\, c_r = -\frac{1}{2} L_{mr}$ (2.24)

The mutual inductances between the stator and the rotor windings are obtained as follows;

i) The mutual inductances $L_{as}\, a_r = L_{bs}\, b_r$ and $L_{cs}\, c_r$ are equal, and is given by the expression;

$$L_{as}\, a_r = L_{bs}\, b_r = L_{cs}\, c_r = L_{sr}\, c_r = L_{sr} \cos \theta r \qquad (2.25)$$

ii) The mutual inductances $L_{as}\, b_r$, $L_{bs}\, c_r$ and $L_{cs}\, a_r$ are equal; and is given by the expression

$$L_{as}\, b_r = L_{bs}\, c_r = L_{cs}\, a_r = L_s \cos\left(\theta_r + \frac{2\pi}{3}\right) \qquad (2.26)$$

iii) The mutual inductances $L_{as}\, c_r$, $L_{bs}\, a_r$ and $L_{cs}\, b_r$ are equal; and is given by the expression;

$$L_{as}\, c_r = L_{bs}\, a_r = L_{cs}\, b_r = L_{sr} \cos\left(\theta_r - \frac{2\pi}{3}\right) \qquad (2.27)$$

Equation (2.25) through equation (2.27), gives one expression for the mutual inductance between the stator and the rotor windings of an induction motorexpressed as;

$$L_{sr} = L_{sr}\begin{bmatrix} \cos\theta r & \cos\left(\theta_r + \frac{2\pi}{3}\right) & \cos\left(\theta_r - \frac{2\pi}{3}\right) \\ \cos\left(\theta r - \frac{2\pi}{3}\right) & \cos\theta r & \cos\left(\theta_r + \frac{2\pi}{3}\right) \\ Cos\left(\theta r + \frac{2\pi}{3}\right) & Cos\left(\theta_r - \frac{2\pi}{3}\right) & Cos\,\theta r \end{bmatrix} \qquad (2.28)$$

The L_{sr} on the right hand side of equation (2.28) represents the amplitude of the mutual inductances between the stator and rotor windings and is given by the expression;

$$L_{sr} = \left(\frac{N_s}{2}\right)\left(\frac{N_r}{2}\right)\left(\frac{\pi \mu_o r l}{g}\right) \qquad (2.29)$$

2.2.5– Transformation to arbitrary q-d-o reference frame

The voltage equation in machine variables for the stator and the rotor of a star-connected symmetrical induction motorshown in figure 2.3 are expressed as follows;

$$\left.\begin{aligned} V_{as} &= i_{as}\, r_s + p\lambda_{as} \\ V_{bs} &= i_{bs}\, r_s + p\lambda_{bs} \\ V_{cs} &= i_{cs}\, r_s + p\lambda_{cs} \end{aligned}\right\} \qquad (2.30)$$

Similarly, for the rotor voltage equations;

$$\left.\begin{aligned} V_{ar} &= i_{ar}\, r_r + p\lambda_{ar} \\ V_{br} &= i_{br}\, r_r + p\lambda_{br} \\ V_{crs} &= i_{cr}\, r_r + p\lambda_{cr} \end{aligned}\right\} \qquad (2.31)$$

In both equations, P = d/dt, the s subscripts denotes variables and parameters associated with the stator circuits and the r subscripts denotes variables and parameters associated with the rotor circuits. Both r_s and r_r are diagonal matrices each with equal non zero elements (Krause et al 1995).

For a magnetically linear system, the flux linkages can be expressed as;

$$\begin{bmatrix} \lambda_s^{abc} \\ \lambda_r^{abc} \end{bmatrix} = \begin{bmatrix} L_{ss}^{abc} & L_{sr}^{abc} \\ L_{rr}^{abc} & L_{rr}^{abc} \end{bmatrix} \begin{bmatrix} i_s^{abc} \\ i_r^{abc} \end{bmatrix} \text{ wb.turn} \qquad (2.32)$$

For an idealized inductance machine, six first order differential equations are used to describe the machine, one differential equation for each machine winding. The stator-to- rotor coupling terms are functions of rotor position and hence when the rotor rotates, the coupling terms vary with time (Chee-mum-ong 1997).

In the analysis of induction machine, it is also desirable to transform the abc variables with the symmetrical rotor windings to the arbitrary q do reference frame (Krause et al 1995).

The transformation equation from the abc quantities to the q do reference frame is given by (Chec-mum-ong 1997).

$$\begin{bmatrix} f_q \\ f_d \\ f_o \end{bmatrix} = \left[T_{qdo}\ (\theta)\right] \begin{bmatrix} f_a \\ f_b \\ f_c \end{bmatrix} \tag{2.33}$$

Where the variable f can be the phase voltage, current or flux linkages of the machine.

$$\left[T_{qdo}\ (\theta)\right] = \frac{2}{3} \begin{bmatrix} \cos\theta & \cos\left(\theta - \frac{2\pi}{3}\right) & \cos\left(\theta + \frac{2\pi}{3}\right) \\ sin\theta & sin\left(\theta - \frac{2\pi}{3}\right) & sin\left(\theta + \frac{2\pi}{3}\right) \\ \frac{1}{2} & \frac{1}{2} & \frac{1}{2} \end{bmatrix} \tag{2.34}$$

and the inverse of equation (2.34) is

$$\left[T_{qdo}\ (\theta)\right]^{-1} = \begin{bmatrix} cos\theta & sin\theta & 1 \\ \sin\left(\theta - \frac{2\pi}{3}\right) & \sin\left(\theta - \frac{2\pi}{3}\right) & 1 \\ \cos\left(\theta + \frac{2\pi}{3}\right) & \sin\left(\theta + \frac{2\pi}{3}\right) & 1 \end{bmatrix} \tag{2.35}$$

2.2.6 Voltage equations in q-d-o reference frame

From equation (2.30), the stator winding abc voltage equations can be expressed as;

$$V_s^{abc} = r_s^{abc}\ \ i_s^{abc} + p\lambda_s^{abc} \tag{2.36}$$

Applying the transformation, $\left[T_{qdo}\ (\theta)\right]$, to equation (2.36), yields;

$$V_s^{qdo} = \left[T_{qdo}\ (\theta)\right] r_s{}^{abc} \left[T_{qdo}\ (\theta)\right]^{-1} \left[i_s^{qdo}\right] + \left[T_{qdo}\ (\theta)\right] p\left[T_{qdo}\ (\theta)\right]^{-1} \left[\lambda_s^{qdo}\right] \tag{2.37}$$

The above equation (2.37), simplifies to ;

$$V_s^{qdo} = r_s^{qdo}\ \ i_s^{qd0} + \rho\lambda_s^{qd0} + \omega \begin{bmatrix} 0 & 1 & 0 \\ -1 & 0 & 0 \\ 0 & 0 & 0 \end{bmatrix} \lambda_s^{qdo} \tag{2.38}$$

Where; $r_s^{qdo} = r_s \begin{bmatrix} 1 & 0 & 0 \\ 0 & 1 & 0 \\ 0 & 0 & 1 \end{bmatrix}$; p = d/dt; ω= $\frac{d\theta}{dt}$

Similarly, the rotor quantities must be transformed into the same q-d-o frame. Now the transformation angle for the rotor phase quantities is (θ-θr). When the transformation Tqdo (θ-θr) is applied to the rotor voltage equation in the same manner as the stator, we have;

$$V_r^{qdo} = r_r^{qdo} \; i_r^{qdo} + p\lambda_r^{qdo} + (\omega - \omega r) \begin{bmatrix} 0 & 1 & 0 \\ -1 & 1 & 0 \\ 0 & 0 & 0 \end{bmatrix} \lambda_r^{qdo} \qquad (2.39)$$

2.2.7 Flux Linkage in q-d-o reference frame

From equation (2.32), the stator and rotor flux linkages are given as;

$$\lambda_s^{abc} = L_s^{abc} \; i_s^{abc} + L_{sr}^{abc} \; i_r^{abc} \qquad (2.40)$$

$$\lambda_r^{abc} = L_{rs}^{abc} \; i_s^{abc} + L_{rr}^{abc} \; i_r^{abc} \qquad (2.41)$$

The stator flux linkages in q-d-o reference frame are obtained by applying T_{qdo} (θ) to equation (2.40) to give;

$$\lambda_s^{qdo} = \left[T_{qdo}\ (\theta)\right] \left[L_{ss}^{abc} \; i_s^{abc} + L_{sr}^{abc} \; i_r^{abc}\right]$$

$$= T_{qdo}\ (\theta)\ L_{ss}^{abc} \; T_{qdo}{}^{-1}(\theta)\ i_s^{qdo} + T_{qdo}\ (\theta)\ L_{rs}^{abc} \; T_{qdo}{}^{-1}(\theta)\ i_r^{qdo} \qquad (2.42)$$

Equation (2.42) simplifies to (Chee – Mum ong 1997);

$$\begin{bmatrix} \lambda_{qs} \\ \lambda_{ds} \\ \lambda_{0s} \end{bmatrix} = \begin{bmatrix} L_{Ls} + \frac{3}{2} L_{ss} & 0 & 0 \\ 0 & L_{Ls} + \frac{3}{2} L_{ss} & 0 \\ 0 & 0 & L_{Ls} \end{bmatrix} \begin{bmatrix} i_{qs} \\ i_{ds} \\ i_{os} \end{bmatrix} + \begin{bmatrix} \frac{3}{2} L_{sr} & 0 & 0 \\ 0 & \frac{3}{2} L_{sr} & 0 \\ 0 & 0 & 0 \end{bmatrix} \begin{bmatrix} i_{qr} \\ i_{dr} \\ i_{or} \end{bmatrix} \qquad (2.43)$$

In a similar manner, if the transformation, T_{qdo} (θ – θ_r) is applied to equation (2.41) the rotor q-d-o flux linkage becomes;

$$\lambda_r^{qdo} = \left[T_{qdo}\ (\theta - \theta r)\right] L_{rs}^{abc} \left[T_{qdo}\ (\theta - \theta r)\right]^{-1}\ i_s^{qdo} + \left[T_{qdo}\ (\theta - \theta r)\right] L_{rr}^{abc} \left[T_{qdo}\ (\theta - \theta r)\right]^{-1}\ i_r^{qdo} \quad (2.44)$$

Equation 2.44 can be simplified as;

$$\begin{bmatrix}\lambda_{qr}\\ \lambda_{dr}\\ \lambda_{0r}\end{bmatrix} = \begin{bmatrix}\frac{3}{2}L_{sr} & 0 & 0\\ 0 & \frac{3}{2}L_{sr} & 0\\ 0 & 0 & 0\end{bmatrix}\begin{bmatrix}i_{qs}\\ i_{ds}\\ i_{os}\end{bmatrix} + \begin{bmatrix}L_{Lr}+\frac{3}{2}L_{rr} & 0 & 0\\ 0 & L_{Lr}+\frac{3}{2}L_{rr} & 0\\ 0 & 0 & L_{Lr}\end{bmatrix}\begin{bmatrix}i_{qr}\\ i_{dr}\\ i_{or}\end{bmatrix} \quad (2.45)$$

Merging equation (2.43) and (2.45). gives the stator and rotor flux linkage equations in q-d-o reference frame as depicted in equation (2.46)

$$\begin{bmatrix}\lambda_{qs}\\ \lambda_{ds}\\ \lambda_{0s}\\ \acute{\lambda}_{qr}\\ \acute{\lambda}_{dr}\\ \acute{\lambda}_{0r}\end{bmatrix}\begin{bmatrix}L_{Ls}+L_m & 0 & 0 & L_m & 0 & 0\\ 0 & L_{Ls}+L_m & 0 & 0 & L_m & 0\\ 0 & 0 & L_{Ls} & 0 & 0 & 0\\ L_m & 0 & 0 & \acute{L}_{Lr}+L_m & 0 & 0\\ 0 & L_m & 0 & 0 & \acute{L}_{Lr}+L_m & 0\\ 0 & 0 & 0 & 0 & 0 & \acute{L}_{Lr}\end{bmatrix}\begin{bmatrix}i_{qs}\\ i_{ds}\\ i_{as}\\ \acute{\imath}_{qr}\\ \acute{\imath}_{dr}\\ \acute{\imath}_{ar}\end{bmatrix} \quad (2.46)$$

In equation (2.46), the primed quantities are rotor values referred to the stator side and are related thus;

$$\left.\begin{aligned}\acute{\lambda}_{qr} &= \frac{N_s}{N_r}\lambda_{qr}\\ \acute{\imath}_{dr} &= \frac{N_s}{N_r}\lambda_{dr}\end{aligned}\right\} \quad (2.47)$$

$$\left.\begin{aligned}\acute{\imath}_{qr} &= \frac{N_r}{N_s}i_{qr}\\ \acute{\imath}_{dr} &= \frac{N_r}{N_s}i_{dr}\end{aligned}\right\} \quad (2.48)$$

Also from equation (2.46), L_m is the magnetizing inductance on the stator side and can be expressed as;

$$L_m = \frac{3}{2} L_{ss} = \frac{3}{2}\frac{N_r}{N_s} L_{sr} = \frac{3}{2}\frac{N_s}{N_r} L_{rr} \quad (2.49)$$

2.2.8 Steady – State analysis of 3-phase induction motor

In steady state operation of the three phase induction motor(IM), the derivative terms in the voltage equations become zero.

Referring to equation (2.42) earlier expressed as;

$$V_s^{qdo} = r_s^{qdo} i_s^{qdo} + p\lambda_s^{qdo} + \omega \begin{bmatrix} 0 & 1 & 0 \\ -1 & 0 & 0 \\ 0 & 0 & 0 \end{bmatrix} \lambda_s^{qdo}$$ and substituting,

$$r_s^{qdo} = r_s \begin{bmatrix} 1 & 0 & 0 \\ 0 & 1 & 0 \\ 0 & 0 & 1 \end{bmatrix}$$, gives;

$$\begin{bmatrix} V_{qs} \\ V_{ds} \\ V_{os} \end{bmatrix} = \begin{bmatrix} r_s & 0 & 0 \\ 0 & r_s & 0 \\ 0 & 0 & r_s \end{bmatrix} \begin{bmatrix} i_{qs} \\ i_{ds} \\ i_{0s} \end{bmatrix} + p \begin{bmatrix} \lambda_{qs} \\ \lambda_{ds} \\ \lambda_{0s} \end{bmatrix} \begin{bmatrix} 0 & \omega & O \\ -\omega & 0 & 0 \\ 0 & 0 & 0 \end{bmatrix} \begin{bmatrix} \lambda_{qs} \\ \lambda_{ds} \\ \lambda_{0s} \end{bmatrix} \quad (2.50)$$

Equation (2.50) suggests that;

$$\left.\begin{aligned} V_{qs} &= r_s i_{qs} + p\lambda_{qs} + \omega\lambda_{ds} \\ V_{ds} &= r_s i_{ds} + p\lambda_{ds} + \omega\lambda_{qs} \\ V_{0s} &= r_s i_{os} + p\lambda_{os} \end{aligned}\right\} \quad (2.51)$$

Also considering equation (2.35) in the same way as above gives;

$$\left.\begin{aligned} \acute{V}_{qs} &= \acute{r}_r \acute{i}_{qr} + p\acute{\lambda}_{qr} + (\omega-\omega_r)\acute{\lambda}_{dr} \\ \acute{V}_{ds} &= \acute{r}_r \acute{i}_{dr} + + p\acute{\lambda}_{dr} - (\omega-\omega_r)\acute{\lambda}_{qr} \\ \acute{V}_{as} &= \acute{r}_r \acute{i}_{ar} + p\acute{\lambda}_{as} \end{aligned}\right\} \quad (2.52)$$

When the derivation terms (P=d/dt) are set equal to zero and is applied to the stator and rotor voltage equation (2.51) and (2.52) for the q-axis, we have;

$$V_{qs} = r_s\, i_{qs} + \omega\lambda_{ds} \tag{2.53}$$

$$\acute{V}_{qr} = \acute{r}_r\, \acute{\imath}_{qr} + (\omega-\omega_r)\, \acute{\lambda}_{dr} \tag{2.54}$$

Since q and d are in space quadrature, if we apply the transformation $F_{ab} = jF_{qs}$ to equation (2.53) and (2.54), we have;

$$V_{qs} = r_s\, i_{qs} + j\omega\lambda_{qs} \tag{2.55}$$

$$\acute{V}_{dr} = \acute{r}_r\, \acute{\imath}_{qr} + (\omega-\omega_r)\, \acute{\lambda}_{qr} \tag{2.56}$$

From equation (2.46), the stator flux linkage along the q-axis is;

$$\lambda_{qs} = (L_{Ls} + L_m)\, i_{qs} + L_m\, \acute{\imath}_{qr}$$

$$= L_{Ls}\, i_{qs} + L_m\, i_{qs} + L_m\, \acute{\imath}_{qr}$$

$$\Rightarrow \lambda_{qs} = L_{Ls}\, i_{qs} + L_m\, (i_{qs} + \acute{\imath}_{qr}) \tag{2.57}$$

Also, the rotor flux linkage along the q-axis, is,

$$\acute{\lambda}_{qr} = L_m\, i_{qs}\, (\acute{L}_{Lr} + L_m)\, \acute{\imath}_{qr}$$

$$= L_m\, i_{qs} + \acute{L}_{Lr} + \acute{\imath}_{qs} + L_m\, \acute{\imath}_{qr}$$

$$\Rightarrow \acute{\lambda}_{qr} = \acute{L}_{Lr}\, i_{qr} + L_m\, (i_{qs} + \acute{\imath}_{qr}) \tag{2.58}$$

Substituting equation (2.57) back into equation (2.55), we have;

$$V_{qs} = r_s\, i_{qs} + j\omega\, [L_{Ls}\acute{\imath}_{qr} + L_m\, (i_{qs} + \acute{\imath}_{qr})]$$

$$= r_s\, i_{qs} + j\omega\, L_{Ls}\, i_{qs} + j\omega\, L_m\, (i_{qs} + \acute{\imath}_{qr})$$

$\Rightarrow V_{qs} = r_s\, i_{qs} + jX_{LLs}\, i_{qs} + jX_{Lm}\, (i_{qs} + \acute{\imath}_{qr})$ (2.59)

But from equation (2.56), we have that;

$\acute{V}_{qr} = \acute{r}_r\, \acute{\imath}_{qr} + \mathrm{j}\,(\omega-\omega_r)\, \acute{\lambda}_{qr}$

$\Rightarrow \acute{V}_{qr} = \acute{r}_r\, \acute{\imath}_{qr} + \mathrm{js}\omega\, \acute{\lambda}_{qr}$

$= \acute{r}_r\, \acute{\imath}_{qr} + \mathrm{js}\omega\, [L\acute{}_{Lr} + L_m\, (i_{qs} + \acute{\imath}_{qr}]$

$= \acute{r}_r\, \acute{\imath}_{qr} + \mathrm{js}\omega\, L\acute{}_{Lr}\, \acute{\imath}_{qr} + js\omega\, L_m\, (i_{qs} + \acute{\imath}_{qr})$

$\Rightarrow \acute{V}_{qr} = \acute{r}_r\, \acute{\imath}_{qr} + \mathrm{js}\, \acute{X}_{LLr}\, \acute{\imath}_{qr} + \mathrm{js}X_{Lm}\, (i_{qs} + \acute{\imath}_{qr})$ (2.60)

Where s = slip of the induction motor.

If we let us suppose that the q-axis is aligned with phase **a** of the induction motor such that;

$V_{qs} = V_{as}$; $\acute{V}_{qr} = \acute{V}_{ar}$

$i_{qs} = i_{as}$; $\acute{\imath}_{qr} = \acute{\imath}_{ar}$, then equation (2.59) boils down to;

$V_{as} = r_s\, i_{as} + jX_{Ls} + \mathrm{j}X_{Lm}\, (i_{as} + \acute{\imath}_{as})$ (2.61)

Similarly, equation (2.60) yields;

$\acute{V}_{ar} = \acute{r}_r\, \acute{\imath}_{ar} + js\acute{X}_{LLr}\, \acute{\imath}_{ar} + \mathrm{js}X_{Lm}\, (i_{as} + \acute{\imath}_{ar})$ (2.62)

Dividing equation (2.62) through by the slip(s), we have;

$\frac{\acute{V}_{ar}}{s} = \frac{\acute{r}_r}{s}\, i_{\acute{a}r} + j\acute{X}_{LLr}\, \acute{\imath}_{ar} + \mathrm{j}X_{Lm}\, (i_{as} + \acute{\imath}_{ar})$ (2.63)

Equations (2.61) and (2.63) are used to draw the steady state equivalent circuit of an induction motor as depicted in figure (2.8)

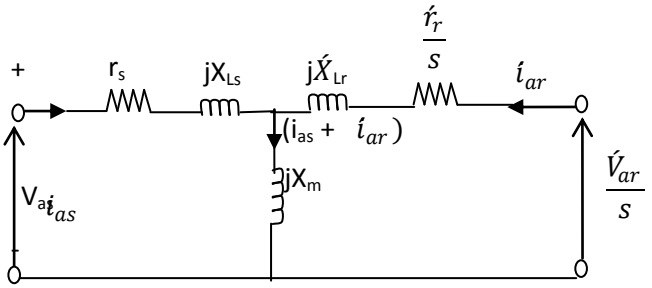

Fig 2.8 – Per phase equivalent circuit of an induction motor

Normally, for an induction motor, (squirrel cage type) the rotor conductors (windings) are short-circuited. Hence, rotor voltage $V_{ar}^{\prime}$ is equal to zero. The per phase equivalent circuit of figure (2.8) with the rotor short circuited, yields;

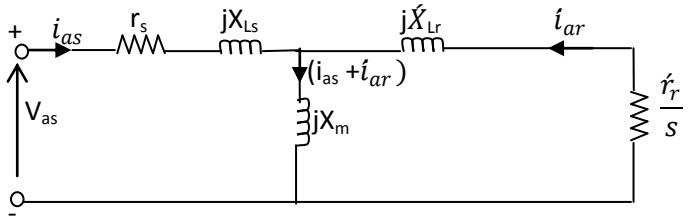

Fig 2.9 – Per phase equivalent circuit of an induction motor at run condition with (s<1) the rotor short circuited

To account for the copper loss $(\acute{\imath}_{ar})^2_r$ in the rotor circuit, figure (2.17) is redrawn as shown in fig (2.10)

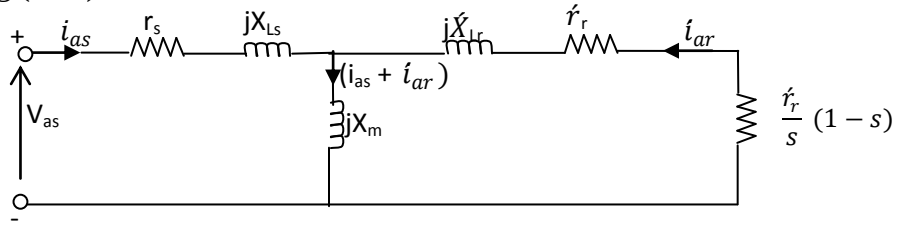

Fig 2.10 – Per phase equivalent circuit of an induction motor which account for copper loss $(\acute{\imath}_{ar})^2_r$ in the rotor circuit.

With reference to figure 2.9, under run condition of the motor the rotor speed (n_r)>0, and s<1. Hence the load resistance $\acute{r}_r$ is affected by slip (s).

2.2.9 Power across air gap, output power and Electromechanical torque

With reference to the equivalent circuit o fig 2.9, the power, crossing the terminals of the shunt mutual inductance (jX_m) is the electrical power input per phase minus the stator losses (stator copper and iron loss). It is the power that is transferred from the stator to the rotor through the air-gap magnetic field. This is known as the power across the air gap(P_g). Its 3-phase value (Pg) is given by (Eleanya et al 2017);

$$P_g = 3(\acute{\imath}_{ar})^2 \frac{\acute{r}_r}{s} \text{ Watts} \quad (2.64)$$

Similarly, rotor Copper loss (P_{cr}) as in figure 2.10 $= 3(\acute{\imath}_{ar})^2 \acute{r}_r$ Watts (2.65)

From equations (2.64) and (2.65);

Power across the air gap $P_g = \frac{P_{cr}}{s}$

$$\Rightarrow P_{cr} = sP_g \text{ Watts} \quad (2.66)$$

The mechanical (gross) Output power (P_m) of the motor is obtained by subtracting equation 2.66 from 2.64 as below;

$$P_m = P_g - P_{cr} = 3(\acute{\imath}_{ar})^2 \frac{r_r}{s} - 3(\acute{\imath}_{ar})^2 r_r$$

$$= 3(\acute{\imath}_{ar})^2 \frac{r_r}{s} (1-s) \text{ Watts} \quad (2.67)$$

Similarly, the electromagnetic torque (T_e) developed by the motor is given by;

$$T_e = \frac{P_g}{\omega_r} = \frac{(1-s)P_g}{\omega_s(1-s)} = \frac{P_g}{\omega_s}$$

$$\Rightarrow T_e = \frac{3(\acute{\imath}_{ar})2 \frac{\acute{r}_r}{s}}{\omega_s} \text{ N-m} \quad (2.68)$$

Where $\omega_r = 2\pi n_r$ = rotor speed in mechanical radian per second, $\omega_s = 2\pi n_s$ = synchronous speed in mechanical radian per second

More-still, the mechanical net power or shaft power (P_{sh}) = P_m – mechanical losses (friction and windage losses)

$\Rightarrow$ Output or shaft torque (T_{sh}) of the motor is given by;

$$T_{sh} = \frac{P_{sh}}{(1-s)\omega_s} \text{ N-m} \qquad (2.69$$

Equation (2.68) is an interesting and significant result according to which torque is obtained from the power across the air gap by dividing it with synchronous speed (ω_s) in rad/s as if power was transferred at synchronous speed.

2.2.10 Torque/slip characteristics of an induction motor.

The torque – slip performance indices of an induction motor can be studied for better if the per-phase equivalent circuit of figure 2.9 is slightly modified as in fig 2.11 below;

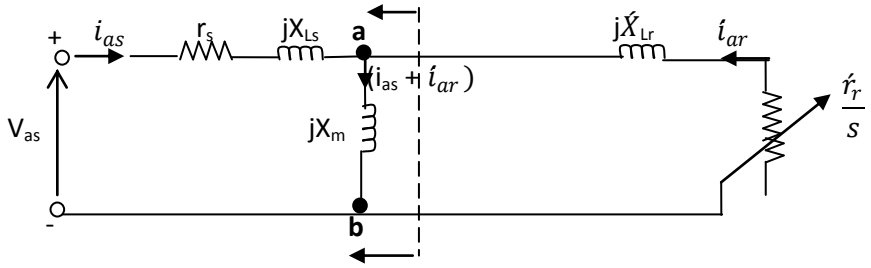

Fig 2.11 – Modified per –phase equivalent circuit of an induction motor at run condition.

The expression for torque-slip characteristics is easily obtained by finding the Thevenin equivalent of the circuit of figure 2.11, to the left of **ab**, as shown below

$Z_{TH} = R_{TH} + jX_{TH}$

$= (r_s + jX_{Ls}) \,//\, jX_m$

$= \frac{(r_s + jX_{Ls})jX_m}{(r_s + jX_{Ls} + jX_m)}$

$= \left[\frac{(r_s + jX_{Ls})jX_m}{(r_s + j(X_{Ls} + X_m))}\right] \Omega$ (2.70)

Assuming $X_{Ls} + X_m >>> r_s$ then;

$Z_{TH} = \left(\frac{r_s X_m}{X_{Ls} + X_m} + \frac{jX_{Ls} X_m}{X_{Ls} + X_m}\right) \Omega$ (2.71)

$\Rightarrow R_{TH} = \frac{r_s X_m}{X_{Ls} + X_m}$ (real component of Z_{TH})

$X_{TH} = \frac{jX_{ls} X_m}{X_{Ls} + X_m}$ (imaginary component of Z_{TH}) (2.72)

Similarly, $V_{TH} = \left[\frac{jX_m}{(r_s + jX_{Ls} + X_m)}\right] V_{as}$ volts (2.73)

For negligible value of r_s compared to $j(X_{Ls} + X_m)$;

$V_{TH} = \left[\frac{jX_m}{(jX_{Ls} + X_m)}\right] V_{as}$ volts (2.74)

Hence, the circuit of figure (2.11), reduces to that of figure (2.12), in which it is convenience to take V_{TH} as the reference voltage.

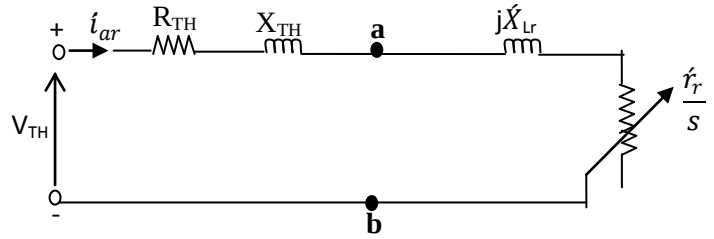

Fig 2.12 – Thevenin equivalent of 3 – phase induction motor circuit model

From figure 2.12;

$$\acute{\imath}_{ar} = \frac{V_{TH}}{\left[\left(R_{TH} + \frac{r_r}{s}\right) + j\ (X_{TH} + X_{Lr})\right]} \quad \text{Amperes} \tag{2.75}$$

Putting equation (2.75) into (2.68) we obtain;

$$T_e = \frac{3\acute{r}_r}{S\omega_s}\left[\frac{(V_{TH})^2}{\left(R_{TH} + \frac{r_r}{s}\right)^2 + j\ (X_{TH} + X_{Lr})^2}\right] \text{N-m} \tag{2.76}$$

Table 2.1 – The machine parameters

Parameter	Value
$L_s = L_r$	5.79mH
$r_s = \acute{r}_r$	1.10Ω
V	220V
F	$50H_z$
P	2

Further-still, equation (2.76) is the expression for torque developed as a function of voltage and slip.

2.2.11 Efficiency/slip characteristics of a conventional 3-phase induction motor

With reference to squirrel cage induction motor type, the resistance is fixed, and less compared to its reactance. There is no provision for addition of external resistance efficiency (ε) of the machine is given by;

$$\varepsilon = \frac{Power\ \ Output}{Power\ \ input} \tag{2.77}$$

For the per-phase equivalent circuit of an induction motorof fig 2.11

The input impedance looking at the input terminals is given by;

$$Z = r_s + jX_{ls} + \left[\frac{(jX_{mq})\left(jX_{lr} + \frac{r_{\acute{r}}}{s}\right)}{\frac{r_{\acute{r}}}{s} + j(X_m + X_{lr})}\right] \quad (2.78)$$

The current in the main (stator) winding; $i_{as} = \frac{V_{as}}{Z}$ (2.79)

The current in the rotor winding is given by; $i_{\acute{a}r} = \left[\frac{jX_m}{\frac{r_{\acute{r}}}{s} + j(X_m + X_{lr})}\right] i_{as}$ (2.80)

Copper losses in the stator and rotor windings = $3\, r_{\acute{r}}\, (i_{as} + i_{\acute{a}r})^2$ (2.81)

For the machine;

Input power = Output power + copper losses in stator and rotor windings, excluding windage and frictional losses. (2.82)

Adding equation 2.67 to equation 2.82, we have;

Input power = $3\, r_{\acute{r}} \left(\frac{1-s}{s}\right) (i_{\acute{a}r})^2 + 3\, r_{\acute{r}}\, (i_{ar} + i_{\acute{a}r})^2$

$$= 3\, r_{\acute{r}} \left[\left(\frac{1-s}{s}\right)(i_{\acute{a}r})^2 + (i_{ar} + i_{\acute{a}r})^2\right] \quad (2.83)$$

$\therefore$ From equation 2.77;

Efficiency $\varepsilon = \frac{3\, r_{\acute{r}} \left(\frac{1-s}{s}\right) (i_{\acute{a}r})^2}{3\, r_{\acute{r}} \left[\left(\frac{1-s}{s}\right)(i_{\acute{a}r})^2 + (i_{ar} + i_{\acute{a}r})^2\right]}$

$$= \frac{\left(\frac{1-s}{s}\right) (i_{\acute{a}r})^2}{\left(\frac{1-s}{s}\right)(i_{\acute{a}r})^2 + (i_{ar} + i_{\acute{a}r})^2} \quad (2.84)$$

2.2.12 Power factor/Slip characteristics of a conventional 3-phase induction motor

From the Thevenin equivalent of a 3-phase induction motorcircuit model of fig 2.12, the machine's power factor (cosθ) is given as;

$$\text{Power factor } (\cos\theta) = \frac{Real\ (Z)}{\sqrt{Real\ (Z)^2 + Imag\ (Z)^2}}$$

$$= \frac{R_{TH} + \frac{r_{\acute{r}}}{s}}{\sqrt{(R_{TH} + \frac{r_{\acute{r}}}{s})^2 + (X_{TH} + X_{Ir})^2}} \qquad (2.85)$$

2.2.13 Rotor current ($i_{\acute{d}r}$)-Slip(s) Characteristics of Conventional 3-Phase induction Motor. This can be explained using equation 2.75.

2.2.14 The dynamic Model of 3-Phase induction motor

The dynamic analysis of a 3-phase induction motor can be done using, three particular cases of the generalized mode in arbitrary reference frames. They are of general interest and they include;

i) Stator reference frame model

ii) Rotor reference frame model

iii) Synchronously rotating reference model

The dynamic analysis of the induction motor is carried out in the d-q-rotor reference frame. As earlier derived in the steady state analysis of equations (2.51) and (2.52), the stator and rotor voltage equation in the arbitrary reference frames are expressed as;

$$
\begin{aligned}
V_{qs} &= r_s i_{qs} + P\lambda_{qs} + \omega\lambda_{ds} \\
V_{ds} &= r_s i_{ds} + P\lambda_{ds} - \omega\lambda_{qs} \\
V_{os} &= r_s i_{ds} + P\lambda_{0s} \\
\acute{V}_{qr} &= \acute{r}_r \acute{\imath}_{qr} + P\acute{\lambda}_{qr} + (\omega-\omega_r)\,\acute{\lambda}_{dr} \\
\acute{V}_{dr} &= \acute{r}_r \acute{\imath}_{dr} + P\acute{\lambda}_{dr} - (\omega-\omega_r)\,\acute{\lambda}_{qr} \\
\acute{V}_{or} &= r_r i_{or} + P\lambda_{or}
\end{aligned}
\qquad (2.86)
$$

While the stator and rotor flux linkages in the arbitrary reference frame are given as;

$$
\begin{aligned}
\lambda_{qs} &= (L_{Ls} + L_m)i_{qs} + L_m \acute{\imath}_{qr} \\
\lambda_{ds} &= (L_{Ls} + L_m)i_{ds} + L_m \acute{\imath}_{dr} \\
\acute{\lambda}_{qr} &= L_{Ls}\, i_{os} \\
\acute{\lambda}_{qr} &= (\acute{L}_{Lr} + L_m)\,\acute{\imath}_{qr} + L_m\, i_{qs} \\
\acute{\lambda}_{dr} &= (\acute{L}_{Lr} + L_m)\,\acute{\imath}_{dr} + L_m\, i_{ds} \\
\acute{\lambda}_{qr} &= L_{Lr}\, i_{or}
\end{aligned}
\qquad (2.87)
$$

With equations (2.86) and (2.87), the dynamic equivalent circuits of an induction motor in the arbitrary reference frame is as shown in figure 2.15.

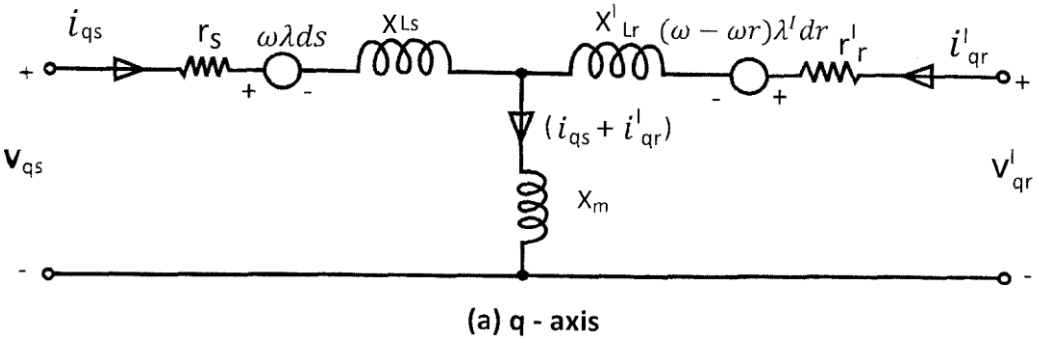

X

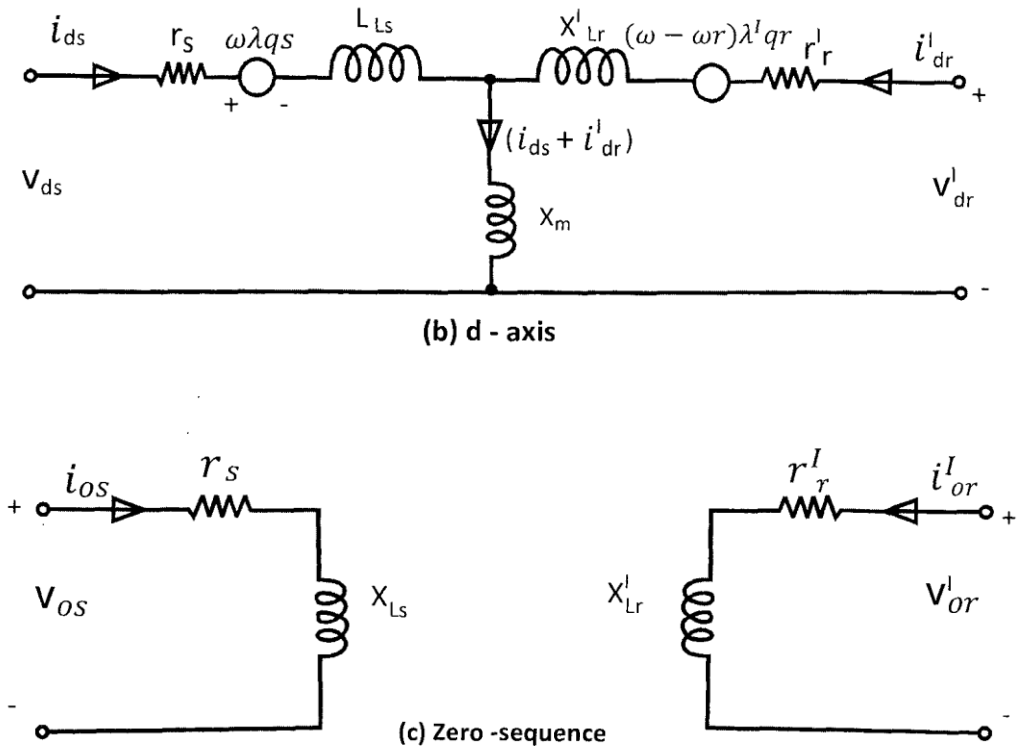

Fig 2.17 – Dynamic equivalent circuit for 3-phase symmetrical induction machine in an arbitrary reference frame

Substituting the flux linkage values into the voltage equations gives;

$$
\left.
\begin{aligned}
V_{qs} &= (r_s + L_s P)\, i_{qs} + \omega_{Ls}\, i_{ds} + L_m P \acute{\imath}_{qr} + \omega_{Lm}\, \acute{\imath}_{dr} \\
V_{ds} &= \omega_{Ls}\, i_{qs} (r_s + L_s P)\, i_{ds} + \omega L_m\, \acute{\imath}_{qr} + L_m P \acute{\imath}_{dr} \\
V_{os} &= (r_s + L_{Ls} P)\, i_{as} \\
\acute{V}_{qr} &= L_m P\, i_{qs} + (\omega - \omega_r) L_m\, i_{ds} + (\acute{r}_r + \acute{L}_r P) \acute{\imath}_{qr} + (\omega - \omega_r)\, \acute{L}_r\, \acute{L}_{dr} \\
\acute{V}_{dr} &= (\omega - \omega_r) L_m\, i_{qs} + L_m P\, i_{ds} - (\omega - \omega_r)\, \acute{L}_r\, \acute{\imath}_{qr} + (\acute{r}_r + \acute{L}_r P) \acute{\imath}_{dr} \\
\acute{V}_{or} &= (\acute{r}_r + L_{Lr} P)\, \acute{\imath}_{0r} \\
\text{Where, } L_s &= L_{Ls} + L_m,\ \acute{L}_r = \acute{L}_{Lr} + L_m
\end{aligned}
\right\} \qquad (2.88)
$$

From equation (2.87) through equation (2.88), it can be observed that only leakage inductance and phase resistances influence the zero-sequence voltages and currents unlike in the d-q-component variables which are influenced by the self and mutual inductances and phase

resistances. Again in a balances 3-phase machine, the sum of the three-phase current is zero which leads to a zero sequence current of zero value (R.krishnan, 2001).

This therefore implies that the analysis can be carried out with the voltage and flux linkage equations ignoring the Zero-sequence components. And when this is done, the flux linkage equation of (2.87) can be rewritten as;

$$\begin{bmatrix}\lambda_{qs}\\ \lambda_{ds}\\ \acute{\lambda}_{qr}\\ \acute{\lambda}_{dr}\end{bmatrix}=\begin{bmatrix}(L_{Ls}+L_m) & 0 & L_m & 0\\ 0 & (L_{Ls}+L_m) & 0 & L_m\\ L_m & 0 & (\acute{L}_{Lr}+L_m) & 0\\ 0 & L_m & 0 & (\acute{L}_{Lr}+L_m)\end{bmatrix}\begin{bmatrix}i_{qs}\\ i_{ds}\\ \acute{\imath}_{qr}\\ \acute{\imath}_{0r}\end{bmatrix} \quad (2.89)$$

The voltage equation for the induction motor in the arbitrary reference frame becomes;

$$\begin{bmatrix}V_{qs}\\ V_{ds}\\ \acute{V}_{qr}\\ \acute{V}_{dr}\end{bmatrix}=\begin{bmatrix}(r_s+L_sP) & \omega_{Ls} & L_mP & \omega_{Lm}\\ -\omega L_s & (r_s+L_sP) & -\omega L_m & L_mP\\ L_mP & (\omega-\omega_r)L_m & (\acute{r}_s+\acute{L}_rP) & (\omega-\omega_r)\acute{L}_r\\ -(\omega-\omega_r)L_m & L_mP & -(\omega-\omega_r)\acute{L}_r & (\acute{r}_r+\acute{L}_rP)\end{bmatrix}\begin{bmatrix}i_{qs}\\ i_{ds}\\ \acute{\imath}_{qr}\\ \acute{\imath}_{dr}\end{bmatrix} \quad (2.90)$$

In q-d-rotor reference frame $\omega=\omega_r$.

Substituting this into equation (2.90), we have;

$$\begin{bmatrix}V_{qs}\\ V_{ds}\\ \acute{V}_{qr}\\ \acute{V}_{dr}\end{bmatrix}=\begin{bmatrix}(r_s+L_sP) & \omega_r L_s & L_mP & \omega_r L_m\\ -\omega_r L_s & (r_s+L_sP) & -\omega_r L_m & L_mP\\ L_mP & 0 & (\acute{r}_r+\acute{L}_rP) & 0\\ 0 & L_mP & 0 & (\acute{r}_r+\acute{L}_rP)\end{bmatrix}\begin{bmatrix}i_{qs}\\ i_{ds}\\ \acute{\imath}_{qr}\\ \acute{\imath}_{dr}\end{bmatrix} \quad (2.91)$$

The transformation from **a-b-c** to **q-d-o** variables is still the same and given as;

$$[T_{abc}] = {}^{2}/_{3}\begin{bmatrix}\cos\theta_r & \cos\left(\theta_r-\frac{2\pi}{3}\right) & \cos\left(\theta_r+\frac{2\pi}{3}\right)\\ \sin\theta_r & \sin\left(\theta_r-\frac{2\pi}{3}\right) & \sin\left(\theta_r+\frac{2\pi}{3}\right)\\ \frac{1}{2} & \frac{1}{2} & \frac{1}{2}\end{bmatrix} \quad (2.92)$$

The inverse matrix is;

$$[T_{abc}]^{-1} = \begin{bmatrix} \cos\theta_r & \text{Sin}\,\theta_r & 1 \\ \cos\left(\theta_r - \frac{2\pi}{3}\right) & \sin\left(\theta_r - \frac{2\pi}{3}\right) & 1 \\ \cos\left(\theta_r - \frac{2\pi}{3}\right) & \sin\left(\theta_r + \frac{2\pi}{3}\right) & 1 \end{bmatrix} \quad (2.93)$$

The electromagnetic torque for the d-q-rotor reference is expressed as;

$$T_e = \frac{3}{4} P_n L_m (i_{qs} i_{dr} - i_{ds} i_{qr}) \quad (2.94)$$

Also, the electromechanical (rotor) dynamic equation is given by;

$$T_e = J \frac{dw_m}{dt} + T_L + B\omega_m \quad (2.95)$$

Where;

J = moment of inertia of motor, T_L = Load torque, B = friction coefficient of the load and motor, ω_m = mechanical rotor speed.

2.2.15 Dynamic Simulation of the motor

The dynamic simulation of the 3-phase induction motoris carried out with parameters and constants for a slip, 220v, 4 pole, 3-phase, 50Hz star-connected induction motor as tabulated below;

2.2 Review of Related Literature

Reluctance machine in the familiar form is a three phase machine with a salient pole rotor. The machine has a squirrel cage which is included only for the purpose of enabling it to start as an asynchronous machine and then pull into synchronism at full speed. It delivers output torque or power only at synchronous speed (Ijeomah et al 1994).

Under certain conditions, a reluctance machine can operate stably synchronous without any cage or winding on the rotor. This was first noted by Gorges Han. He observed the stable operation of a Poly-Phase induction motor at one-half normal speed by means of unbalanced impedance in the secondary circuit (Georges 1896). He equally observed that operation of an induction motorwith electric asymmetry, which is achieved by loading the rotor winding of a wound rotor induction motorwith unbalanced load results in a drive running close to half synchronous speed. This effect, later called "Gorges Phenomenon" was most pronounced when a phase of the rotor circuit was open-circuited. The torque/speed characteristics was determined and its determination implies that depending on loading, the reluctance machine can run asynchronously at close to half-speed or synchronously at half-speed. Due to some draw-backs of his scheme, his finding failed to attract industrial acceptance.

An attempt to improve Georges work was carried out by Schenfer (Schenfer 1926). He attempted using the machine as a half-speed industrial drive. He placed two windings on the stator, feeding them separately, one with a balanced three-phase a.c and the other with d.c. The rotor had short-circuited windings to enhance starting. The machine thus started synchronously and was then synchronized at half-speed by the stationary field established by the d.c.

Further development generally centered around synchronous operation, each adopting Schenfer's method and developing a different and more effective and/or economical means of feeding both the a.c and d.c for synchronous operation.

Russel and Norseworthy adopted the machine for synchronous operation and improved Schenfer's scheme by employing a single stator winding to carry the two currents (d,c, and a.c) simultaneously. In the synchronous operation as described above, a drive comparable to

conventional synchronous machine was achieved with high output and power factor (Norsworthy K.H 1958).

In the preceding schemes described so far, the unbalance impendence results in the electrical asymmetry in the secondary circuit. On the other way round, this electrical asymmetry can be brought about by using rotors, whose reluctance to the passage of flux along one axis is a maximum and a minimum along a second axis of $\frac{\pi}{2}$ electrical radians to the first.

A synchronous operation of the reluctance machine attracted little attention and industrial acceptance due to the following operational lapses;

(i) Undesirable (2s-1)wo frequency harmonics induced in the mains supply by the operation

(ii) Poor output and low power factor

(iii) Excessive vibration and noise.

A configuration which improved the industrial acceptance of the half speed machine by coupling two machine elements mechanically together and appropriately connecting their winding in parallel to the supply, was developed by Broadway. Broadway's scheme combined both electrical and magnetic asymmetry in the secondary (Broadway 1973). Owing to the combination of both electric and magnetic asymmetry in Broadway's machine, the machine was able to produce an output characteristics in both synchronous and asynchronous modes comparable to conventional induction motorcounterpart. Broadway and Co. endeavoured to adapt the machine as a feasible variable speed industrial drive by operating it asynchronously. This they did by coupling rotors of two identical cage machines and feeding their stator windings in parallel.

Operating at $\propto + \beta = \pi/2$ rad, the $(2s-1)\omega_o$ harmonic existed only in the loop formed by the stator windings. Thus, it was effectively eliminated from the supply. The output characteristics were enhanced while vibration and noise were considerably reduced. At slip, s = 1/2 the set, with d.c excitation incorporated, operates as a synchronous machine. Within the range $1 < s < 1/2$ it operates as a motor, and as a generator in the $1/2 < s < 8$ range if the rotor shaft is driven beyond the half-speed synchronous point by a mechanical drive system.

The set's operation resembles that of an induction motorwith its entire operational mode compressed within $0 \leq S \leq 1$ instead of $-1 \leq S \leq 1$. Thus, although each unit of the set operates on reluctance principle, their combined operation markedly differs from a normal reluctance machine. As distinct from the conventional polyphase reluctance machine therefore, this machine is described as "Reluctance Effect Machine" or briefly, REM-

Broadway and Co. discovered that the machine was self-starting even without the rotor cage. However, the electrical asymmetry in the rotor circuit enhanced the performance of the machine, and in fact provided the larger proportion of the total machine output.

Though successful on synchronous operation, the scheme still depended on the complex technique of feeding both a.c and d.c through a single stator winding. Consider the conflicting current limiting requirements for a.c and d,, c. The reactance of a winding is normally higher than its resistance and effectively limits the a.c. This does not however apply to the d.c which is only sensitive to coil resistance.

Thus, the set losses its flexibility in order to achieve a winding design effective for both a.c and d.c. Although external resistors could be incorporated in the d.c circuit as current limiter, they result in high operational losses.

For asynchronous operation, the terminals of the. stator winding are not accessible for control as in wound rotor induction motors. Thus, control or speed adjustments was not easily achieved.

To achieve all of the advantanges of the Broadway set and also overcome the adverse effect of high leakage reactance in reluctance effect machines Agu, L. A. proposed a set of two equivalent reluctance machines. This is an evolution of a new configuration of a two element machine popularly known as the "Transfer-field reluctance machine". This was configured to operate asynchronously as coupled poly-phase reluctance machine. In this scheme, there are two stator windings in each machine elements known as main and auxiliary windings (Agu L.A. 1997). The Agu's configuration, unlike Broadway's version has no rotating (rotor) conductors (windings).

In furtherance to the existing configuration of the new machine, study on the contribution of the net torque of the machine by the constituent elements was carried out (Agu L.A. et al 2002), so also the magnetic of the machine in its idealized form (Anih L.U 2009).

All the studies on this machine quoted so far have been centered on steady state analysis derived from circuit theory approaches (Anih L.U et al 2009). For a more general analysis, a d-q-o modeling is necessary.

Some authors studied the dynamic models of synchronous machines with two poly phase windings in a stator displaced by an arbitrary angle. Fuchs and Rosenberg derived the d-q equations (Fuch's E.F. et al 1974), while Schiferl and Ong included the effect of mutual leakage inductances and performed an analog simulation for the machine supplying an ac and a rectifier load simultaneously (Schiferl R.F. et al 1983).

In the steady-state performance of the double-wound machine was reported as a high voltage generator (Touma-Holmberg. M et al 2000), while Obe E.S**.** and Senjyu T, presented a d-q model using space vector approach (Obe E.S et al 2006). The work presented by the two researchers couples two of such machine and interconnects their windings. They also studied the machines dynamic and steady-state behavior as a low speed motor. The effect of mutual leakage coupling first introduced in Schiferl R.F and Ong C.M's work is ignored here since these values are always very low when the windings are symmetric. The torque enhancement of a reluctance effect machine by slip-frequency secondary voltage injection was reported by Ijeomah (Ijeomah et al 1994). In their scheme, the enhancement technique used include;

(i) Secondary voltage injection scheme

(ii) Double fed operation scheme

Additionally, the enhancement of the output power and power factor of a transfer field machine operating in the synchronous mode by direct capacitance injection in the auxiliary winding of the machine was reported by Obe and Anih (E.S. Obe et al 2014). It was shown that by proper turning of the injected capacitance, the torque and output power of the machine is markedly enhanced at improved power factor. Such turning of the capacitive load, the $\frac{x_d}{x_q}$ ratio can be theoretically varied from zero to infinity without manipulation of the rotor geometry at very good power factor including unity.

Most recently, the enhancement of the output power of transfer field machine by introduction of parallel path winding was reported by Eze and Anih (Eze I.N. et al 2016). In their study, additional identical main and auxiliary windings were respectively introduced on both halves of the machine elements. The scheme is conceived to reduce the excessive leakage reactance of the machine.

2.3 Summary of Review of Related Literature

Ijeomah (1996) evolved a configuration which enhanced the output power of the conventional transfer field motor by injecting slip frequency voltage in the auxillary winding. The injected voltage in the auxillary winding is made to be in time phase with the induced voltage in the auxillary windings, thus leading to enhanced circulating current in the winding. The enhanced current actually made the main winding to draw an additional current for mmf balance. The scheme enhanced the maximum power and hence maximum torque of the machine but with negligible effect on the starting torque. This is due to its cageless nature, for all cageless machines produce lower load (rotor) currents.

Obe and Anih (2001) enhanced the output power of transfer field machine by balanced capacitance injection technique into the auxillary winding to neutralize reactance. The scheme improved the power factor, and hence maximum torque. However, there was no significant improvement in the starting torque.

The enhancement of the output power of transfer field machine by introduction of parallel path windings to both the stator and rotor sections as reported by Eze and Anih (2001), though is conceived to reduce the excessive leakage reactance of the machine and thus enhance both the maximum torque and starting torque. This is to the detriment of the stator and rotor sizes and weights due to increase in their slots for their windings.

CHAPTER THREE

Research Methodology

The new configuration of 3-phase transfer field reluctance motor is intended to minimize the excessive leakage reactance associated with the existing three phase transfer filed motor. To achieve the afore-mention goal, the following methods were adopted, viz;

(1) Method – Analytical calculation

Tool - Matlab plots

Procedure:

(i) Development of mathematical model of the motor, necessary to explain its behaviour under steady-state and dynamic state condition

(ii) Derivation of mathematical equations from the model, necessary for the formation of the machine's equivalents circuit diagrams

(iii) Derivation of the machine's output characteristics equations from the equivalent circuit diagrams

(iv) Establishment of the machines circuit parameters.

(v) Simulation of the derived equations as in (iii) and (iv)

(vi) Generation of the machine plots (graphs) from (v) for analysis of the machine's output characteristics

(2) **Modification Method:** Here, the existing three-phase transfer field motor without rotor windings is modifed by optimizing the rotor design. This is achieved by introducing rotor windings at the rotor sections of the machine sets (M/C A and M/C B). The idea is that when resistance (in the form of coils) are added to the rotor circuit the rotor power factor is improve, which inturn results in improved starting torque. This of course increases the

rotor impedance and therefore decreases the value of rotor current, but the effect of improved power factor predominates and the starting torque is increased (V.K Mehta et al 2000). To bring down the effect of such reduction in rotor-induced current, the main windings of the machine sections are connected in series and then connected to the utility supply. The auxiliary and cage (rotor) windings of both machine sections are connected in parallel but transposed between the two sections of the machine halves and short circuited.

The fact that when impedances are connected in parallel, the resultant impedance will be lower than the least impedances and when impedances are reduced, higher current will flow into the circuit and output power increases, thereby resulting in higher electromagnetic torque which forms the basis of research methodology of this study.

The analytical method adopted to achieve the results in this work follows the chronological order as below;

(i) Analysis of three-phase transfer field reluctance motor (T.F.M) without rotor windings.
(ii) Analysis of three-phase transfer field reluctance motor with the introduction of rotor windings
(iii) Analysis and comparism of results.

3.2 Analysis of the three-phase transfer field reluctance motor (T.F.M) without rotor windings

The three-phase transfer field reluctance machine is a new breed of electrical machine which operates under synchronous and asynchronous mode. It has the dual characteristics of both machines depending on the mode of operation.

3.2.1 Motor description/Physical Configuration

The transfer field reluctance motor (TFM) as shown in Plate 1, comprises a two stack machine in which the rotor is made up of two identical equal halves whose pole axes are $\pi/2$ radians out of phase in space. They are housed in their respective induction motor type stators.

There are no windings in the rotor. The stator has two physically isolated but magnetically coupled identical windings known as the main and auxiliary windings. The axes of the main windings are the same in both halves of the machine, whereas the axes of the auxiliary windings are transposed in passing from one half of the machine to the other. Both sets of windings are distributed in the stator slots and occupy the same slots for perfect coupling and have the same number of poles. The two sets of windings of the transfer field machine are essentially similar and may be connected in parallel which of course double its output.

The stator and rotor of the machine are wound for the same pole number and both are star connected as in fig 3.1.

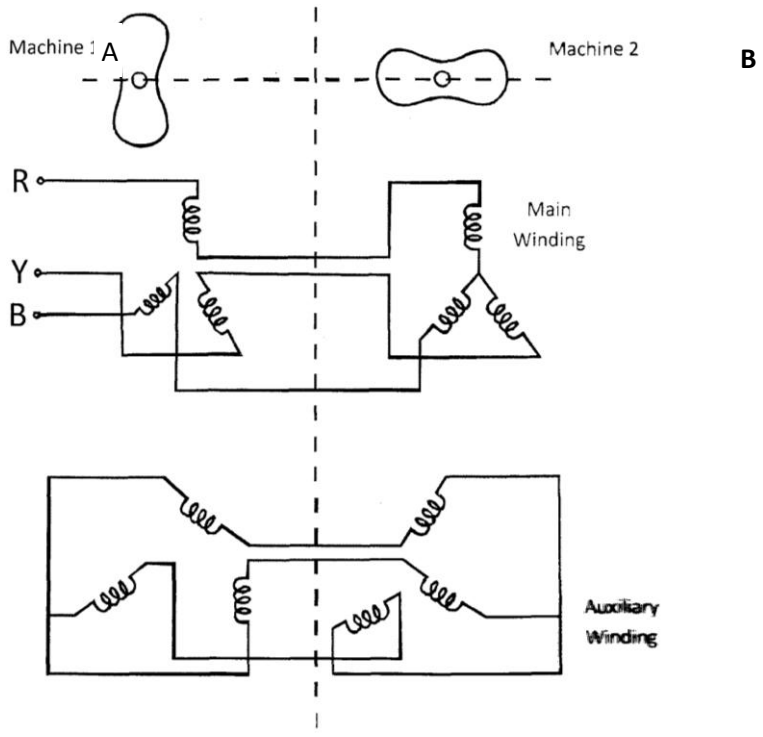

Fig 3.1 Connection diagram for a three phase transfer field reluctance motor without rotor windings

3.2.2 The Machine Model

The per-phase coupled coil representation of the Transfer Field reluctance motor is shown in fig 3.2 below

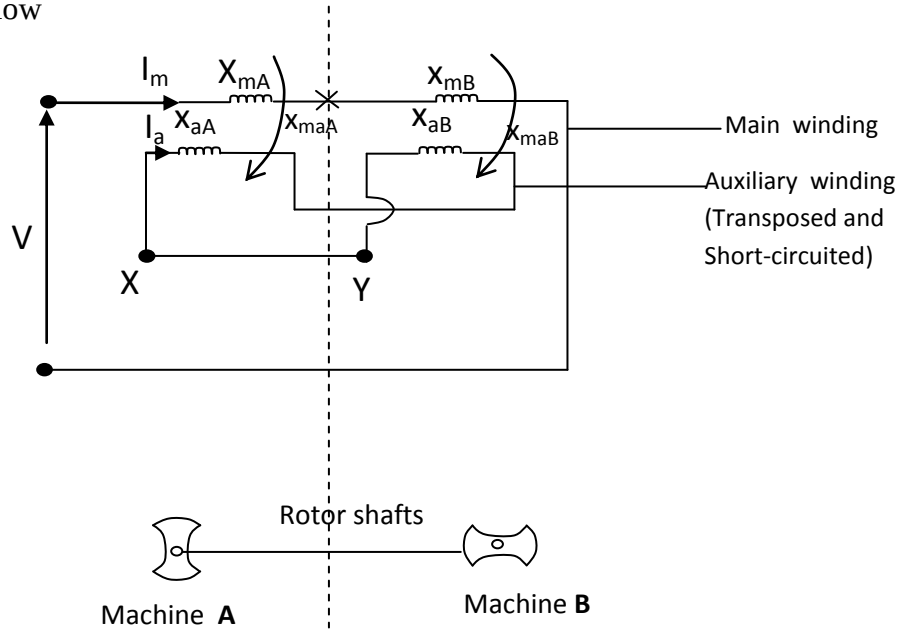

Fig 3.2: Per phase coupled coil representation of a T.F. Motor without rotor windings

Each machine half is similar in features to the conventional synchronous machine. The major unorthodox characteristics of the machine are;

i) the stator and rotor are arranged in two identical halves; and hence the machine may be treated as two separate reluctance machines whose stator windings are connected in series.

ii) there are no windings in the rotor

iii) the pole axes of the two pole half are mutually in space quadrature

iv) there is second set of poly-phase stator windings (auxiliary windings) whose conductor side are shifted electrical by 180^0 (anti-series), by passing through one section of the machine to another. The main and the auxiliary windings are identical in all respects and

occupy the same electrical position in the stator slot, thus ensuring a perfect coupling between the windings.

3.2.3 Principle of Operation and analysis

The analysis of the three-phase transfer-field reluctance motor derived from the studies on coupled machines (Anih L.U. et al 2001).

In its operation, when the main windings of machine **A** is connected to an **a.c** supply voltage, V, with the auxiliary windings open circuited, it draw a magnetizing current $\mathbf{I_o}$ at the supply frequency $\boldsymbol{\omega_o}$.

This magnetizing current produces an magnetomotive force (mmf) distribution on both units of the machine (A and B) which may be expressed as (Anih L.U. et al 2008);

Magnetizing (mmf) $m_o = M_o \cos (x - \omega_o t)$ (3.1)

Where; m_0 = Instantaneous value of the magnetizing mmf

M_o = Peak amplitude of the instantaneous magnetizing mmf

x = Angular distance measured from the reference axis, which is taken as the center line of the stator poles

t = Time in seconds

ω_0 = Supply angular frequency.

The air-gap permeance of the rotor in one unit machine, say unit A, may be expressed as;

$P_A = P_o + P_V \text{ Cos } 2 (x-\omega t)$ (3.2)

Where;

P_A = Rotor permeance distribution for unit area of air-gap of machine **A** half.

P_v = the amplitude of the variable part of the permeance distribution.

ω = the speed of rotor of unit machine

Similarly, the air-gap rotor permeance distribution in unit **B** machine, whose pole axis is in space quadrature with unit A machine may be expressed as;

$$P_B = P_o + P_v \text{ Cos } 2 (x - \omega t - 90^0)$$

$$= P_o - P_v \text{ Cos } 2 (x - \omega t) \quad (3.3)$$

The flux density produced by this mmf at the instant when its axis coincides with the pole axis of the rotor of machine A is given by;

$$B_{AO} = m_o P_A$$

$$= M_0 \cos (x-\omega_o t) [P_o + P_V \text{ Cos } 2 (x-\omega t)]$$

$$= M_o P_o \text{ Cos } (x-\omega_o t) + M_o P_V \text{ Cos } (x-\omega_o t) \text{ Cos } 2 (x-\omega t)$$

$$= M_o P_o \text{ Cos } (x-\omega_o t) + 0.5 M_o P_V \text{ Cos } [x - (2\omega - \omega_o)t] + 0.5 M_o P_V$$

$$\text{Cos } (3x- \omega t - \omega t) + \text{third harmonics} \quad (3.4)$$

Similarly, the corresponding flux density distribution produced in machine **B** is expressed as;

$$B_{BO} = M_o P_o \text{ Cos } (x-\omega_o t) - 0.5 M_o P_o \text{ Cos } [x + (\omega_o - 2\omega)t]$$

$$+ \text{third space harmonics} \quad (3.5)$$

It should be noted at this juncture that the first components of equations (3.4 and 3.5) will induce emfs E_1 in the main windings which is additive and tend to oppose the voltage supply. The e.mf's they induce in the auxiliary windings cancel out. These e.m.fs are equal in magnitude and in time phase.

The second components of equations (3.4 and 3.5), will induce voltages E_2, in the main windings which are equal and opposite and in consequence, cancel each other (anti-phase).

However, in the auxiliary winding, these induced voltages, E_2 will add up because of the transposition of the auxiliary windings. See fig 3.3 for illustration.

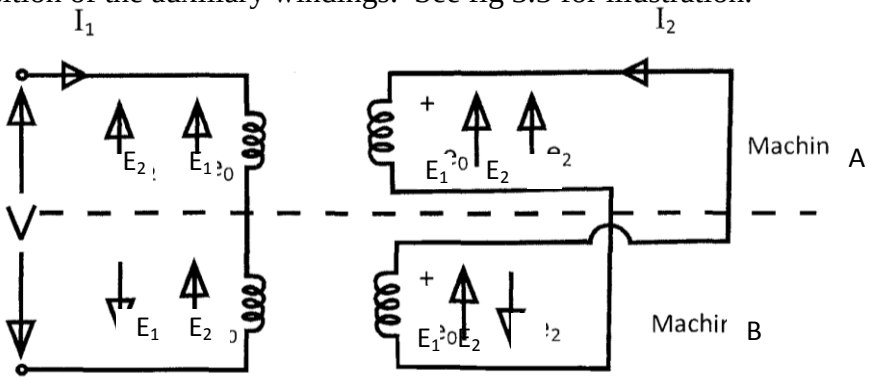

Fig 3.3 Induced voltage, E_1, E_2 in the main and auxiliary winding

The direction of emf E_1 induced in the main winding conductor in both halves of the machine A, B such as $\boldsymbol{a_1}$ and $\boldsymbol{\acute{a}_1}$ by this flux is as shown in fig 3.3 in full lines. These emfs E_1 are both equal in magnitude and in time phase in both sections of the machine and will oppose the supply voltage **V** in both sections.

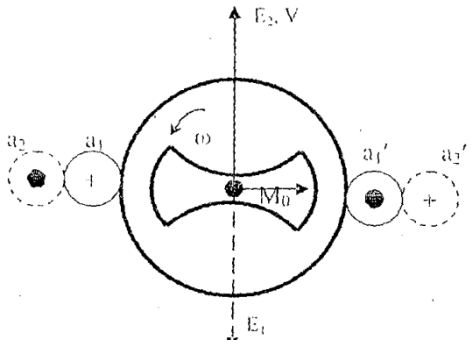

Fig 3.4a - Section A part of the machine showing the induced e.m.f s in the stator windings

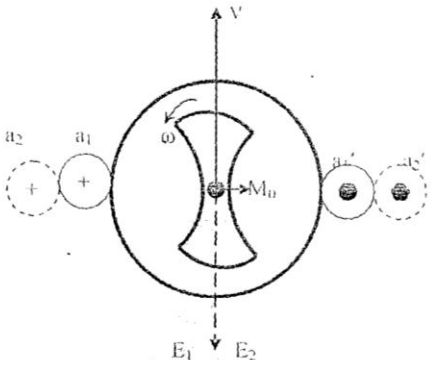

Fig 3.4b - Section Ba part of the machine showing the induced e.m.f s in the stator windings (Source-Anih/Agu 2008)

The emfs induced by the third space harmonics cancel out if the windings are star connected. If however, the windings are desired to be connected in delta, the winding pitch must be chosen such that the emf induced by harmonics of flux is eliminated.

The average value of the second components of the flux in equation (3.4 and 3.5);

ie $\pm 0.5\ M_o\ P_o\ \text{Cos}\ [x + (\omega_o - 2\omega)t] = 0$

More-still, the average of this flux as seen by the auxiliary windings, whose conductors are transposed between the two machine halves is expressed as;

$$B_{AO} - B_{BO} = 0.5\ M_o\ P_V\ \text{Cos}\ [x + (\omega_o - 2\omega)t] \qquad (3.6)$$

This flux density distribution rotates in the negative clockwise direction for $\omega < \frac{\omega_o}{2}$

The direction of emf E_2 induced in the auxiliary windings by this flux will be in anti-phase in both halves of the machine (see fig 3.3), because of the transposition of the auxiliary windings as shown in the dotted circles in fig 3.4b It therefore follows that in section A half, E_2 will be diametrically opposed to E_1 and in section B half E_2 will be in phase with E_1 (see fig.3.3)

3.2.4 Short Circuiting of the Auxiliary Winding

If the terminals (XY) of fig 3.2 is bridged as in fig 3.3, it is said to be short –circuited. If this occurs, emf will be induced in it (auxiliary windings), at $(\omega_o - 2\omega)$ frequency, and is given by;

$$e_a = E_{2m} \cos [(\omega_o - 2\omega)\ t - 0.5\ \pi) \qquad (3.7)$$

Where;

e_a = Instantaneous voltage induced in the auxiliary windings

E_{2m} = Peak amplitude of the instantaneous voltage (e_a)

E_2 = r.m.s value of the instantaneous voltage induced in the auxiliary windings

This induced emf of equation (3.7), will circulate current (i_a) say at the same frequency in the short – circuited winding and this induced current is inversely proportional to its leakage impedance and is expressed as;

$$i_a = \frac{E_{2m}\ Cos\ [\ (\omega_o - 2\omega)t - 0.5\pi]}{\{r_a^2 + [(\omega_o - 2\omega)L]^2\}^{1/2}} \quad \tan^{-1}\left[\frac{(\omega_o - 2\omega)L}{r_a}\right]$$

$$= I_{2m}\ Cos\ [((\omega_o - 2\omega)t - 0.5\pi - \phi]\ [\tan^{-1}\left[\frac{(\omega_o - 2\omega)L}{r_a}\right] \qquad (3.8)$$

Where,

I_{2m} = Peak amplitude of the instantaneous current in the auxiliary windings (i_a)

r_a = Resistance of the auxiliary windings

L = Inductance of the auxiliary windings

ϕ = Impedance angle = $\tan^{-1}\left[\frac{(\omega_o - 2\omega)L}{r_a}\right]$

The distribution of mmf in the auxiliary winding of machine A say, due to this current (i_a) has the form;

$$m_a = M_2\ Cos\ [x + (\omega_o - 2\omega)t - 0.5\ \pi\text{-}\phi] \qquad (3.9)$$

Where;

m_a = instantaneous mmf distribution in the auxiliary winding

m_2 = Peak value of the instantaneous mmf distribution in the auxiliary winding

Similarly, in machine B, the corresponding auxiliary winding mmf will be expressed as;

$$m_a = -\ M_2\ Cos\ [x + (\omega_o - 2\omega)t + 0.5\ \pi\text{-}\phi] \qquad (3.10)$$

Equation 3.10 arises due to transposition of auxiliary winding as in fig 3.2/3.3.

The flux density distribution in machine A half due to its rotating mmf is given by;

$$B_{2A} = m_a\ [P_o + P_v\ Cos\ 2\ (x - \omega t)]$$

$$= M_2 \text{ Cos } [x + (\omega_o - 2\omega)t - 0.5\ \pi\text{-}\phi]\ (P_o + P_v \text{ Cos } 2\ (x - \omega t)] \quad (3.11)$$

Similarly, in machine B half, the corresponding flux density distribution is given by;

$$B_{2B} = - m_a\ [P_o\ P_v \text{ Cos } 2\ (x - \omega t)]$$

$$= -m_2 \text{ Cos } [x + (\omega_o - 2\omega)t - 0.5\ \pi\text{-}\phi]\ [P_o\ P_v \text{ Cos } 2\ (x - \omega t)] \quad (3.12)$$

Hence, the total flux density over the two machine halves is the combination of equation 3.10 and 3.12. This is given by;

$$B_{2T} = B_{2A} + B_{2B}$$

$$= M_2 \text{ Cos } [x + (\omega_o - 2\omega)t - 0.5\ \pi\text{-}\phi]\ [P_o + P_v \text{ Cos } 2\ (x - \omega t)]$$

$$- M_2 \text{ Cos } [x + (\omega_o - 2\omega)t - 0.5\ \pi\text{-}\phi]\ \{P_o + P_v \text{ Cos } 2\ (x + \omega t)] \quad (3.13)$$

$$= M_2\ P_v \text{ Cos } (x - \omega_o t + 0.5\ \pi + \phi) + \text{third space harmonics} \quad (3.14)$$

In both equation (3.4, 3.5 and 2.14), the third harmonics are eliminated because the machine is star connected (see fig 3.1)

The presence of (i_a) in the auxiliary winding leads to an additional current (i_m) to be drawn by the primary in a manner similar to what is obtainable in transformers and induction motors, in order to neutralize the effect of the auxiliary current (i_a). The primary flux needed to neutralize the secondary flux is produced by the primary current (i_m).

3.2.5 Magnetomotive Force (mmf) Balance of the Machine

The auxiliary winding load current mmf (i_a) has been given in equation (3.8). The flux of the m_a linking the primary winding has been expressed in equation (3.9).

This flux must be opposed and balanced by the primary load current flux. The primary (main winding) mmf is expressed as;

$m_m = M_1 \text{ Cos } (x - \omega_o t - \alpha)$ (3.15)

The self-flux of m_m is given by;

$m_m P_o = M_1 P_0 \text{ Cos } (x-\omega_o t - \alpha)$ (2.16)

For mmf balance;

$B_{2T} = m_m P_o$

Also, $m_m p_o = -B_{2T}$

$\Rightarrow M_1 P_o \text{ Cos } (x-\omega_o t - \alpha) = - M_2 P_v \text{ Cos } (x - \omega_o t + 0.5 \pi + \phi)$

$= M_2 P_v \text{ Cos } (x- \omega_o t - 0.5 \pi + \phi)$ (2.17)

$\therefore M_1 P_o = M_2 P_v$ (2.18)

Assuming $\alpha = 0.5 \pi - \phi$,

$\therefore m_m = M_1 \text{ Cos } (x- \omega_o t - 0.5 \pi + \phi)$ (2.19)

Where,

m_m = Instantaneous mmf distribution of the primary (main) winding of the machine

M_1 = Peak amplitude of the instantaneous mmf distribution of the primary (main) winding.

The role of primary and auxiliary windings can be exchanged. If we now use the auxiliary winding as the primary winding and vice-versa, and if the mmf is M_2, then the primary, now the secondary (auxiliary) will have mmf (M_1).

$\Rightarrow M_1P_v = M_2P_o$ (2.20)

Combining equations (3.17 and 3.19) we have; $|M_1| = |M_2|$ (2.21)

Fig 3.5, at a certain instant in time shows the mmf distribution phasors in the two halves of the Transfer Field Machine.

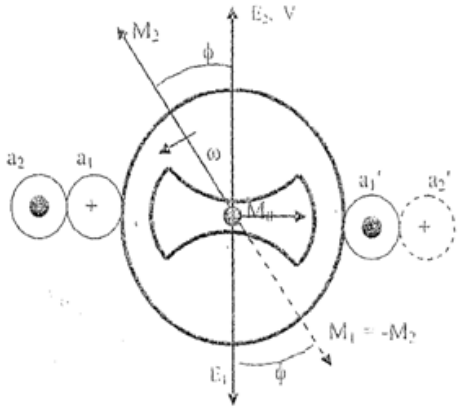

Fig 3.5a – Half Part (Machine A) of the TF Machine, showing mmfs, M_o, M_i, M_2 (Anih/Agu 2008)

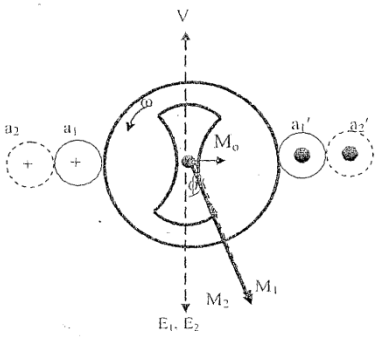

Fig 3.5b – Half Part (Machine A) of the TF Machine, showing mmfs. M_o, M_i, M_2 (Anih/Agu 2008)

In machine A, M_1 and M_2 are equal in magnitude but in anti-phase, whilst in machine B, M_1 and M_2 are equal in magnitude and in phase because of the transposition of the machine windings (see fig 3.3)

3.2.6 Per Unit Slip (s)

The slip of the primary (main) winding field with respect to the rotor is expressed as;

$s_m = \omega_o - \omega$

But generally, $s = \frac{\omega_o - \omega}{\omega_o}$

$\Rightarrow \omega = \omega_o (1-s)$

$\therefore s_m = \omega_o - [\omega_o (1-s)]$

$= \omega_o - \omega_o + s\omega_o$

$= s\omega_o$ (3.22)

Similarly, the corresponding auxiliary winding field slip (S_a) with respect to the rotor is given by;

$s_a = \omega_o - \omega_o$

$= [\omega_o (1-s)] - \omega_o$

$= \omega_o - s\omega_o - \omega_o$

$= - s\omega_o$ (3.23)

Equation (3.22 and 3.23) give the implication that the main winding mmf M_1 and the excitation current mmf M_o will rotate at the speed ($S\omega_o$) with respect to the rotor whilst the auxiliary winding mmf M_2 will rotate at the speed ($- S\omega_o$) with respect to the rotor. Thus, the

combination of M_o and M_1 gives $M_o + M_1 = \acute{M}$, rotating at the same speed as M_2 relative to the rotor but in the opposite direction.

3.2.7 Mechanism of Torque Production in TF Machine

When the terminals (X Y) of fig 2.2 is not bridged (under open circuit condition), the machine does not develop torque. This is on the account of;

i) the absence of a rotor winding which would produce induction motor type torque

ii) the impedance of the winding does not change with rotor angular position, so there is no reluctance torque.

However, the component of the primary winding flux that induces e.m.f in the auxiliary winding rotates in the negative sense relative to the rotating magnetizing mmf of the primary (main) winding. That is, M_0 and M_1 rotate at the speed $S\omega_0$ while the auxiliary current mmf M_2 rotates at the same speed relative to the rotor but in the opposite sense. Let us examine as instance in time when the axes of the magnetizing mmf M_o concides with the d – axis of the rotor – pole in machine A and hence with q – axis of the machine B, both being in space quadrature. The magnetizing flux in machine A will be maximum, and that in machine B, is negligible compared to that of machine A. The effective magnetizing flux would therefore be almost entirely of that produced by machine A. In fig, 3.6a, shows section A part of the machine. The mmf phasor M_1 and M_2 are shown to be equal in magnitude but in phase opposition and with the resultant of M_o and M_1 producing $\acute{M}$, which rotates at the speed $S\omega_o$, whislt M_2 rotates at $– s\omega_0$. The resultant mmf in section A part of the machine ($M_{Ra} = \acute{M} + M_2$) acts at the leading pole tip of the rotor as shown in fig 3.6a. In section B half of the machine, the direction of M_2 phasor would have reversed due to the transposition of the auxiliary winding.

Therefore, the phasors M_1 and M_2 will now be in phase and the resultant mmf ($M_{RB} = \acute{M}+M_2$) acts at the leading rotor pole tip. Since in both halves of the TF Machine A, B respectively, their resuctant mmfs, M_{RA} and M_{RB} act at the leading pole tips. Consequently, their targential components will exert a reluctance torque in the positive anticlockwise sense in both halves of the TF Machine which will pull the rotor forward.

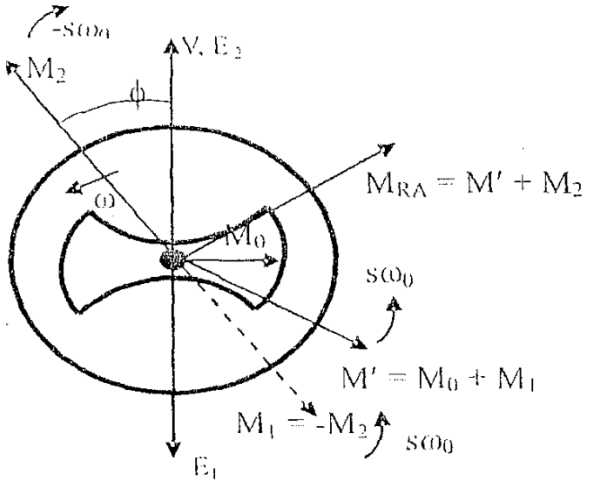

Fig 3.6a Machine A part of the TF machine showing the resultant mmf (M_{RA}) acting on the leading rotor pole tip.

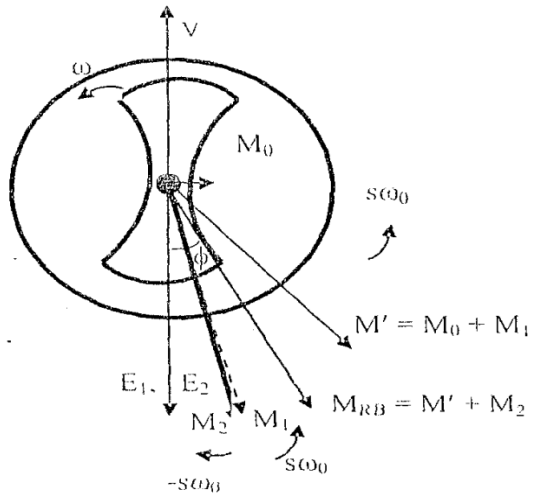

Fig 3.6b Machine A part of the TF machine showing the resultant mmf (M_{RB}) acting on the leading rotor pole tip.

Obviously, the intensity of the resultant mmfs and hence flux is greater in machine B than in machine A at this instant t_0 say as shown in fig 3.6a and b.

Thus, machine B produces the greater proportion of the net torque of the TF machine. As time progresses, M_2 and M_1 will be moving apart in machine B, thus weakening the resultant mmf M_{RB}, but moving closer in machine A, thereby strengthening the resultant mmf M_{RA} and hence flux at this instant t_2 say. The combination of M_1 and M_2 will coincide at a point leading the axis of the rotor pole by ϕ after each of them has traveled a distance of 0.5π electrical radians.

Since torque is directly proportional to the square of mmf and hence flux, each section of the T.F machine that produces the greater proportion of the flux will produce the greater proportion of the net torque that transfer cyclically from one machine half to the other. When the torque in one machine half is increasing, the torque from the other half is decreasing while the net torque remains constant. Infact, when the torque in one half is maximum, it will be zero in the other. This phenomenon can be explained quantitatively by considering the combination mmfs in the air gaps of each machine half of the TF machine.

In section A machine half, the combination mmfs is expressed as;b

$$\text{Mmfs}_A = M_o \cos(x-\omega_o t) + M_1 \cos(x-\omega_o t - 0.5\pi - \phi + \phi)$$

$$+ M_2 \cos(x+(\omega_o - 2\omega) - 0.5\pi - \phi) \quad (3.24)$$

$$= \acute{M} \cos(x-\omega_o t - \sigma) + M_2 \cos[x + (\omega_o - 2\omega)\, t - 0.5\pi - \phi \quad (3.25)$$

$$= (\acute{M} - M_2) \cos(x- \omega_o t - \sigma) + M_2 \cos(x- \omega_o t - \sigma)$$

$$+ M_2 \cos[x + (\omega_o - 2\omega) - 0.5\pi - \phi) \quad (3.26)$$

$$= (\acute{M} - M_2) \cos(x - \omega_o t - \sigma) + 2\, M_2 \cos[x- \omega t - 0.5(\sigma + \phi + 0.5\pi)]$$

$$\cos [(\omega - \omega_o)t - 0.5 (\sigma - \phi - 0.5\pi)] \quad (3.27)$$

Where σ = Primary input power factor angle.

The torque component of equation (3.27) is a wave that rotates round the air gap at the speed of the rotor ω, whose amplitude is modulated as slip frequency by cos $[(\omega-\omega_2)t-0.5 (\sigma-\phi-0.5\pi)]$, can consequently impart a reluctance torque on the rotor in the forward anticlockwise direction.

The first component of equation 3.27 cannot produce torque since it rotate at a speed different from that of the rotor.

Similarly, the mmf combination in section B half of the machine is given by;

$$Mmfs_B = (\acute{M}-M_2) \cos (x-\omega_o t - \sigma) + 2M_2 \sin [x-\omega t - o.5 [(\sigma+\phi + 0.5\pi)] \sin [(\omega-\omega_o)t - 0.5 (\sigma-\phi-o.5\pi)] \quad (3.28)$$

Just as in equation (3.27), the second component of equation (3.28) is a wave that rotates round the air-gap at the speed of the rotor ω, hence can impart a reluctant torque on the rotor.

It can be inferred from the two equations, (3.27 and 2.28) that the amplitude of each torque producing mmf in the two halves of the machine has same space phase displacement with respect to the corresponding rotor axis. The variations of the amplitudes of the waves are in time quadrature. The out ward interpretation of this is that the torque swings cyclically between the two sections of the machine, while the net torque remains constant.

The machine's self-starting characteristics can be inferred from the gross mmfs in both halves of the machine, that is equations (3.26 and 3.27) which are non-zero at starting (ie at ω = 0) (L.U Aniih/ L.A. Agu 2008).

3.2.8 Effect of Auxiliary Winding Power Factor

Assuming the auxiliary winding is loaded such that the power factor is reversed as in fig.3.7, it will be discovered that the axes of the resultant mmfs M_{RA} and M_{RB} in both halves of the

machine will intersect at the trailing rotor poles tips as shown in fig, 3.7, and thus leading to an electromagnetic torque in the opposite direction to the rotation of the rotor.

The machine in this case will require an external mechanical agency as a prime mover and this corresponds to generator operation mode.

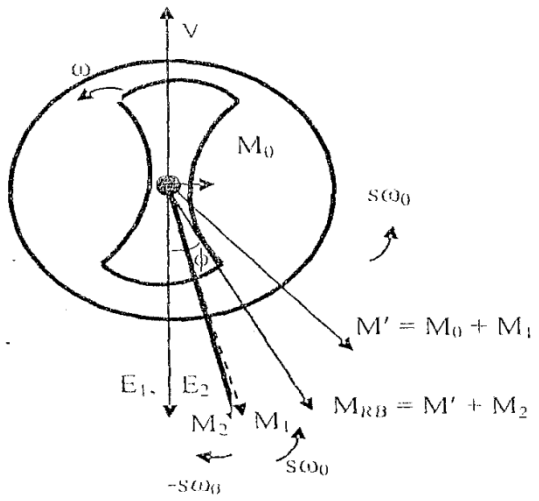

Fig 3.7(a) The mmf phasor of machine A part of the T.F machine, illustrating generator operation

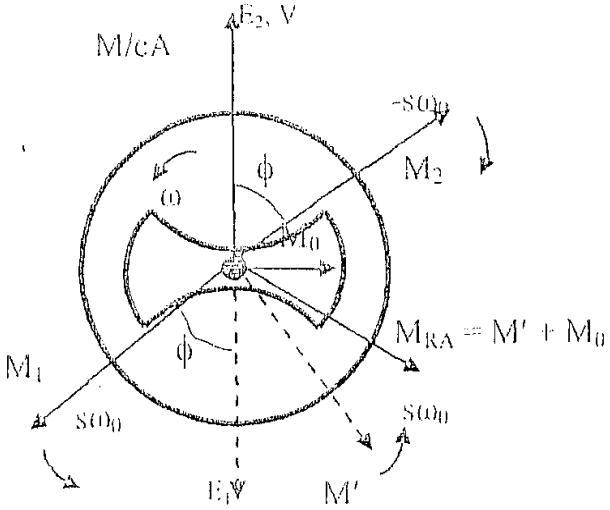

Fig 3.7(b) The mmf phasor of machine B part of the T.F machine, illustrating generator operation

3.2.9 The dynamic model of 3-phase transfer field machine

For the stator windings of the three-phase TF machine, the mathematical model of the voltage equation is given by;

$$V_A = r_A i_A + P\lambda_A \quad (3.29)$$

$$V_B = r_B i_B + P\lambda_B \quad (3.30)$$

$$V_C = r_C i_C + P\lambda_C \quad (3.31)$$

Where $V_A = V_R$ (Red)

$V_B = V_Y$ (yellow)

V_C = V_B (Blue) are the three phase balance voltage which rotate at the supply frequency (ω) at the main winding.

For the rotor, the flux linkages rotate at the speed of the rotor (ω_r).

Therefore for the auxiliary winding of the machine, we have;

$$V_a = r_a i_a + \rho\lambda_a \quad (3.32)$$

$$V_b = r_b i_b + \rho\lambda_b \quad (3.33)$$

$$V_c = r_c i_c + \rho\lambda_c \quad (3.34)$$

Equations (3.29 – 3.34) can be written in a compact form as;

$$V_{ABC} = r_{ABC} i_{ABC} + \rho\lambda_{ABC} \quad (3.35)$$

$$V_{abc} = r_{abc} i_{abc} + \rho\lambda_{abc} \quad (3.36)$$

where ;

$\rho = d/dt$ (derivative term, as usual)

$$(V_{ABC})^T = [V_A, V_B, V_C] \quad (3.37)$$

$$(V_{abc})^T = [V_a, V_b, V_c] \quad (3.38)$$

$$r_{ABC} = \text{diag}([r_A r_B r_C]) \quad (3.39)$$

$$r_{abc} = \text{diag}([r_a r_b r_c]) \quad (3.40)$$

In the above two equations (3.37) and (3.38), "ABC" subscript denotes variables and parameters associated with the main winding and the subscript "abc" denotes variables and parameters associated with the auxiliary winding. Both r_{ABC} and r_{abc} are diagonal matrices each with equal non zero element. For a magnetically linear system, the flux linkages may be expressed as (Anih L.U. 2009);

$$\begin{bmatrix}\lambda_{ABC}\\ \lambda_{abc}\end{bmatrix} = \begin{bmatrix}L_{GG} & L_{GH}\\ L_{HG} & L_{HH}\end{bmatrix} \begin{bmatrix}i_{ABC}\\ i_{abc}\end{bmatrix} \text{ wb turn} \quad (3.41)$$

Where,

$$\left.\begin{aligned} \lambda_{ABC} &= (\lambda_A, \lambda_B, \lambda_C,)^t \\ \lambda_{abc} &= (\lambda_a, \lambda_b, \lambda_c,)^t \\ i_{ABC} &= (i_A, i_B, i_C,)^t \\ i_{abc} &= (i_a, i_b, i_c,)^t \end{aligned}\right\} \quad (3.42)$$

The super-script **t** of equation (3.42) denotes the transpose of the array.

The inductance matrices term L_{GG} , L_{GH}, and L_{HH} are obtained from inductance sub-matrices L_{11}, L_{12}, L_{21} and L_{22} for machines A and B, defined as;

$$\left.\begin{aligned} L &= \begin{bmatrix} L_{11} & L_{12} \\ L_{21} & L_{22} \end{bmatrix} \\ L_{11} &= \begin{bmatrix} L_{AA} & L_{AB} & L_{AC} \\ L_{BA} & L_{BB} & L_{BC} \\ L_{CA} & L_{CB} & L_{CC} \end{bmatrix} \\ L_{12} &= \pm \begin{bmatrix} L_{Aa} & L_{Ab} & L_{Ac} \\ L_{Ba} & L_{Bb} & L_{Bc} \\ L_{Ca} & L_{Cb} & L_{Cc} \end{bmatrix} \\ L_{21} &= \pm \begin{bmatrix} L_{aA} & L_{aB} & L_{aC} \\ L_{bA} & L_{bB} & L_{bC} \\ L_{cA} & L_{cB} & L_{cC} \end{bmatrix} \\ L_{22} &= \begin{bmatrix} L_{aa} & L_{ab} & L_{ac} \\ L_{ba} & L_{bb} & L_{bc} \\ L_{ca} & L_{cb} & L_{cc} \end{bmatrix} \end{aligned}\right\} \quad (3.43)$$

Where;

L = The augmented matrix, for the inductance matrix for machine A and B

L_{11} and L_{22} are "self" inductances of main and auxiliary windings respectively.

L_{12} and L_{21} are the "mutual" inductances between the main and auxiliary windings.

L_{GG} is obtained by adding L_{11} for machine A and L_{11} for machine B.

This will yield;

$$L_{GG}\begin{bmatrix} (2L_{Ls}+L_{md}+L_{mq}) & -\frac{1}{2}(L_{md}+L_{mq}) & -\frac{1}{2}(L_{md}+L_{mq}) \\ -\frac{1}{2}(L_{md}+L_{mq}) & (2L_{Ls}+L_{md}+L_{mq})a & -\frac{1}{2}(L_{md}+L_{mq}) \\ -\frac{1}{2}(L_{md}+L_{mq}) & -\frac{1}{2}(L_{md}+L_{mq}) & (2L_{Ls}+L_{md}+L_{mq}) \end{bmatrix} \quad (3.44)$$

L_{GH} is obtained by adding L_{12} for machine A to L_{12} for machine B to give

$$L_{GH} = (L_{mq} - L_{md}) \begin{bmatrix} \cos 2\,\theta r & \cos(2\,\theta r - \alpha) & \cos(2\,\theta r + \alpha) \\ \cos(2\,\theta r - \alpha) & \cos(2\,\theta r + \alpha) & \cos 2\,\theta r \\ \cos(2\,\theta r + \alpha) & \cos 2\,\theta r & \cos(2\,\theta r - \alpha) \end{bmatrix} \quad (3.45)$$

Where $\alpha = \frac{2\pi}{3}$

By applying the same method, L_{HG} and L_{HH} are obtained. So far the main and auxiliary windings in both machine halves are identical, L_{GG} is observed to be equal to L_{HH}. So also L_{GH} and L_{HG}. Owing to this observation of equality, auxiliary winding parameters do not change values when they are referred to the main winding.

Equations (3.44) and (3.45) resemble the inductance expressions for a wound rotor induction machine, even though the individual machine making up the composite machine possesses salient pole rotors with no conductors.

3.2.10 Machine Model in arbitrary q-d-o reference frame

In order to remove the rotor position dependence on the inductance seen in equation (3.45), the voltage equations (3.35) and (3.36) need to be transferred to **q-d-o** reference frame.

The technique is to transform all the state variables to an arbitrary reference frame. Equation (3.41) is then rewritten in **q-d-o** frame as;

$$\begin{bmatrix} (\lambda_Q & \lambda_D & \lambda_O) \\ (\lambda_q & \lambda_d & \lambda_o) \end{bmatrix}^T = \begin{bmatrix} K_G L_{GG}\,(k_G)^{-1} & K_G L_{GH}\,(k_H)^{-1} \\ K_G L_{GH}\,(k_G)^{-1} & K_G L_{HH}\,(k_H)^{-1} \end{bmatrix} \begin{bmatrix} (I_Q & I_D & I_O) \\ (I_q & I_d & I_o) \end{bmatrix} \quad (3.46)$$

$$\left.\begin{aligned} \text{Here, } K_G &= \frac{2}{3} \begin{bmatrix} \cos\phi & Cos\,(\phi - \alpha) & Cos\,(\phi + \alpha) \\ \sin\phi & Sin\,(\phi - \alpha) & Sin\,(\phi + \alpha) \\ \frac{1}{2} & \frac{1}{2} & \frac{1}{2} \end{bmatrix} \\ K_H &= \frac{2}{3} \begin{bmatrix} \cos\beta & Cos\,(\beta - \alpha) & Cos\,(\beta + \alpha) \\ \sin\beta & Sin\,(\beta - \alpha) & Sin\,(\beta + \alpha) \\ \frac{1}{2} & \frac{1}{2} & \frac{1}{2} \end{bmatrix} \end{aligned}\right\} \quad (3.47)$$

Where, θ_r = rotor position

β = speed of rotation of the arbitrary reference frame.

As $\beta = 2\theta_r = \theta$, as in equation (3.45), the time varying inductance frame, the voltage equation will be totally eliminated.

Hence, the voltage equations (3.35) and (3.36) will after the transformation yield;

$$V_Q = \omega\lambda_D + \rho\lambda_Q + rI_Q \quad (3.48)$$

$$V_D = \omega\lambda_Q + \rho\lambda_D + rI_D \quad (3.49)$$

$$V_O = \rho\lambda_O + rI_O \quad (3.50)$$

Doing like-wise for the rotor quantities (auxiliary windings) yield;

$$V_q = (\omega - 2\omega_r)\lambda_d + \rho\lambda_q + rI_q \quad (3.51)$$

$$V_d = (\omega - 2\omega_r)\lambda_q + \rho\lambda_d + rI_d \quad (3.52)$$

$$V_o = (\omega - 2\omega_r)\rho\lambda_o + rI_o \quad (3.53)$$

Also, the flux linkages of equation (3.45) are expressed as;

$$\lambda_Q = (2L_1 + L_{mq} + L_{md})I_Q - (L_{md} - L_{mq})I_q$$

$$= 2L_1 I_Q + L_{mq} I_Q + L_{md} I_Q - L_{md} I_q + L_{mq} I_q$$

$$= 2L_1 I_Q + L_{mq} I_Q + L_{md} I_Q + L_{md} I_Q - L_{md} I_Q - L_{md} I_q + L_{mq} I_q$$

$$= 2L_1 I_Q + 2L_{md} I_Q + L_{mq} I_Q - L_{md} I_Q - L_{md} I_q + L_{mq} I_q$$

$$= 2(L_1 + L_{md}) I_Q + [I_Q (L_{mq} + L_{md}) + I_q (L_{mq} - L_{md})]$$

$$= 2(L_1 + L_{md}) I_Q + (I_Q + L_q)(L_{mq} - L_{md})$$

$$\Rightarrow \lambda_Q = 2(L_1 + L_{md}) I_Q + (I_Q + I_q)(L_{mq} - L_{md}) \quad (3.54)$$

Similarly

$$\lambda_D = (2L_1 + L_{mq} + L_{md}) I_D + (L_{md} - L_{mq}) I_d$$

$$\Rightarrow \lambda_D = 2(L_1 + L_{mq})\, I_D + (I_D - I_d)\,(L_{md} - L_{mq}) \quad (3.55)$$

$$\lambda_O = 2L_1\, I_O \quad (3.56)$$

Also

$$\lambda_q = (2L_1 + L_{mq} + L_{md})\, I_q - (L_{md} - L_{mq})\, I_Q$$

$$= 2(L_1 + L_{md})\, I_q + (L_{mq} - L_{md})\,(I_Q + I_q) \quad (3.57)$$

$$\lambda_d = (2L_1 + L_{mq} + L_{md})\, I_d + (L_{md} - L_{mq})\, I_D$$

$$= 2(L_1 + L_{mq})\, I_d + (L_{md} - L_{mq})\,(I_D + I_d) \quad (3.58)$$

$$\lambda_O = 2L_1 I_O \quad (3.59)$$

As before, equations (3.54 – 3.56) represent the flux linkages of the main winding circuit while equations (3.57 – 3.59) represent the flux linkages of the auxiliary winding, and **r** in equations (3.48 – 3.53) is the sum of the resistances of the main or auxiliary windings in both machine halves.

Hence, equation (3.54) can be put into equation (3.48), and equations (3.58) into equation (3.51) to yield;

$$V_Q = \omega\lambda_D + \rho\,[2(L_1 + L_{md})\, I_Q + (L_{mq} - L_{md})\,(I_Q + I_q)] + rI_Q$$

$$= \omega\lambda_D + j\omega\,[2(L_1 + L_{md})]\, I_Q + j\omega\,(L_{mq} - L_{md})\,(I_Q + I_q) + rI_Q \quad (3.60)$$

$$\Rightarrow V_q = (\omega - 2\omega_r)\,\lambda_d + \rho\,[2(L_1 + L_{md})\, I_q] + (L_{mq} - L_{md})\,(I_Q + I_q)] + rI_q$$

$$\therefore V_q = (\omega - 2\omega_r)\,\lambda_d + j\omega\,[2(L_1 + L_{mq})]\, I_q + j\omega\,(L_{mq} - L_{md})\,(I_Q + I_q) + rI_q \quad (3.61)$$

Equation (3.60) and (3.61) result the T equivalent circuit shown below in figure 3.8.

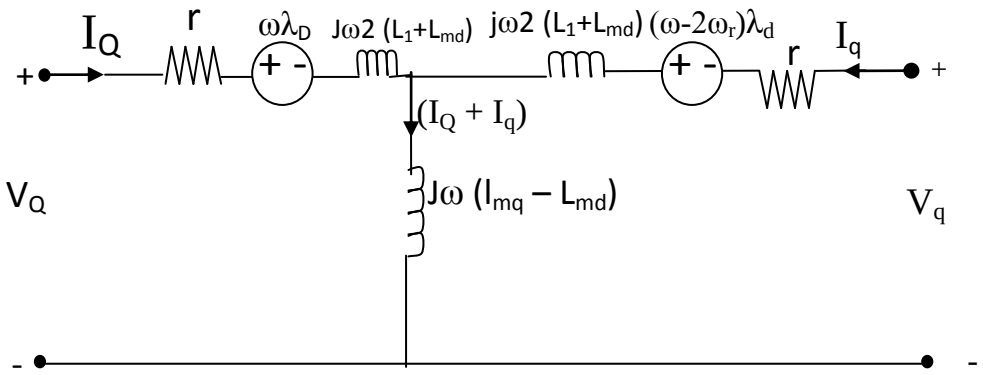

Fig 3.8 Arbitrary reference frame equivalent circuit for a 3-phase symmetrical transfer field reluctance motor in the q-variable.

Applying the same method to equation (3.55) and (3.49) and then equations (3.57) and (3.52) we have;

$$V_D = - \omega\lambda_Q + \rho\ [2(L_1+ L_{mq}) + (L_{md} - L_{mq})\ (I_D+I_d)] + rI_D$$

$$= - \omega\lambda_Q + j\omega 2\ (L_1+ L_{mq})\ I_D + j\omega\ (L_{md}- L_{mq})\ (I_D+I_d) + rI_D \qquad (3.62)$$

$$V_d = - (\omega - 2\omega_r)\ \lambda_q + \rho\ [2(L_1+ L_{mq})\ I_{q\,+} (L_{md} - L_{mq})\ (I_D+I_d)] + rI_d$$

$$= - (\omega - 2\omega_r)\ \lambda_q + j\omega 2\ (L_1+ L_{mq})\ I_{q\,+} j\omega\ (L_{md} - L_{mq})\ (I_D+I_d)] + rI_d \qquad (3.63)$$

Equations (3.62) and (3.63) result the Tequivalent circuit shown below in figure 3.9.

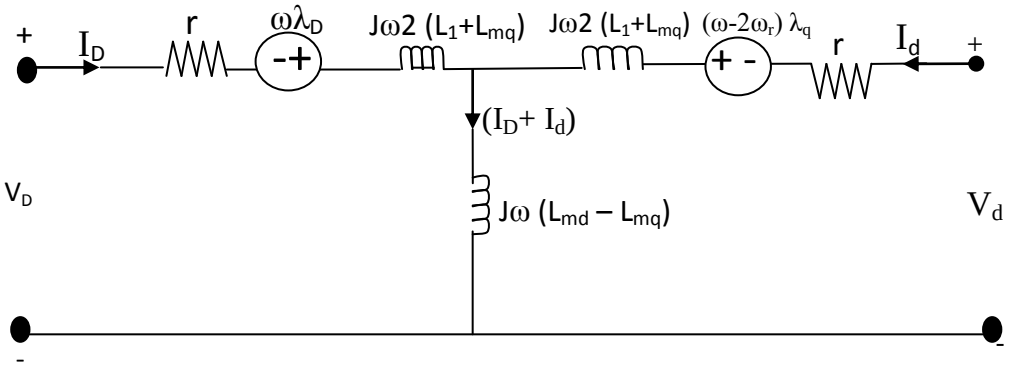

Fig 3.9 Arbitrary reference frame equivalent circuit for a 3-phase symmetrical transfer field motor in the d-variables

More still, from equation (3.50) and (3.54)

$V_o = \rho\lambda_o + rI_o$

$= \rho(2L_1\ I_o) + rI_o$ (3.64)

$V_{or} = \rho\lambda_o + rI_o$

$= \rho(2L_1\ I_o) + rI_o$ (3.65)

Equations (3.64) and (3.65) result the T equivalent circuit shown in fig 3.10.

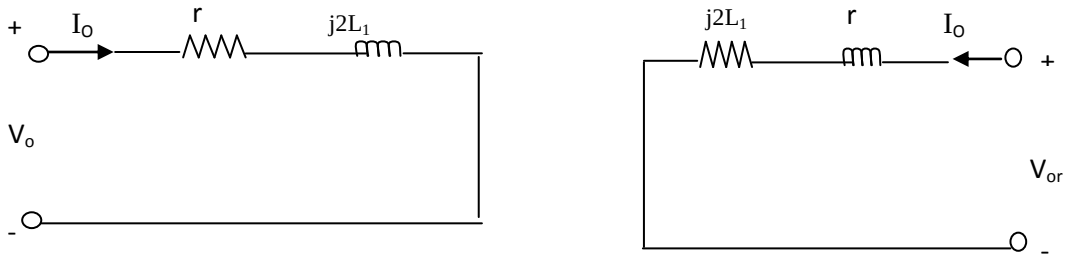

Fig 3.10 Arbitrary reference frame equivalent circuit for a 3 – phase symmetrical transfer field reluctance motor in the 0 – variable

3.2.11 q-d-o Torque Equation

The expression for electromagnetic torque is obtained from energy considerations and derived to be (Anih L.U 2009);

$$T_e = \frac{P_n}{2}\left[K_G\begin{pmatrix} I_A \\ I_B \\ I_C \end{pmatrix}\right]^T \left[\frac{\partial}{\partial\theta}\ [L_{GH}]\right]\left[K_G\begin{pmatrix} I_a \\ I_b \\ I_c \end{pmatrix}\right] \quad (3.66)$$

Equation (3.66) can be shown to yield;

$$T_e = \frac{3}{4} P_n\ (L_{md} - L_{mq})\ (I_Q\ I_d - I_q\ I_D) \quad (3.67)$$

Equation (3.67) shows that currents in both the main and auxiliary windings contribute positively to torque production, therefore, there is no copper penalty limitation of space for auxiliary winding conductor is utilized.

The electromechanical (rotor) dynamic equation for the machine is expressed as;

$$J\frac{d\omega_m}{dt} = T_e - T_L \quad (3.68)$$

Where;

P_n = Number of poles

T_L = motor shaft load torque in N-m

T_e = Electromagnetic torque in N-m

J = Moment of inertia of motor in kg – m^2

ω_m = Mechanical rotor speed in $rads^{-1}$

3.2.12 Steady state analysis of 3-phase transfer field reluctance motor model in arbitrary q-d-o reference frame

The steady state equivalent circuit of a three-phase transfer field machine may be derived from the **d-q-o** equivalent circuit. This can be achieved with the understanding that all the derivative terms of equation (3.48) through equation (3.54) are set to zero, and the following relations exist between the **q-axis** and **d-axis** variables.

$F_D = jF_Q$ (Main winding circuit)

$F_d = -jF_Q$ (Auxiliary winding circuit)

$V_Q = V_A$, $I_Q = I_A$, $V_q = V_a$, $I_q = I_a$

As the machine is half speed type with synchronous speed $\omega^1 = \frac{\omega}{2}$; the per slip $\acute{s}$ is given by;

$$\acute{s} = \frac{\acute{\omega} - \omega_r}{\acute{\omega}} \quad (3.69)$$

$$= \frac{0.5\omega - \omega_r}{0.5\omega}$$

$$= \frac{\omega - 2\omega_r}{\omega}$$

$$\Rightarrow \acute{s}\omega = \omega - 2\omega_r \quad (3.70)$$

But for the normal induction motorcounterpart;

$s = \frac{\omega - \omega_r}{\omega}$

$\Rightarrow \omega_r = \omega - s\omega$ (3.71)

Putting equation (3.71) into equation (3.70), yields;

$\acute{s} = 2s - 1$ (3.72)

It can be recalled from equations (3.48 – 3.54) that;

$V_Q = \omega\lambda_D + \rho\lambda_Q + rI_Q$

$= \omega\lambda_D + (0)\lambda_Q + rI_Q$

$= \omega\lambda_D + rI_Q$

$\Rightarrow V_Q = \omega\lambda_D + rI_Q$

$= j\omega\ [2\ (L_1 + L_{mq})\ I_D + (L_{md} - L_{mq})\ (I_D + I_d)] + rI_Q$

$= j[2\ (x_1 + x_{mq})\ I_D + (x_{mq} - x_{md})\ (I_D + I_d)] + rI_Q$

$\Rightarrow V_A = [j2(x_1 + x_{mq}) + r]\ I_A + j\ (x_{md} - x_{mq})\ (I_A + I_a)$ (3.73)

Similarly

$V_q = (\omega - 2\omega_r)\ \lambda_d + \rho\ \lambda_d + rI_q$

$= (\omega - 2\omega_r)\ \lambda_d + (0)\lambda_q + rI_q$

$= (\omega - 2\omega_r)\ \lambda_d + rI_q$

$= \acute{s}\omega\ \lambda d + rI_q$

$= j\acute{s}\omega\ [2(L_1 + L_{mq}))\ I_d + (L_{md} - L_{mq})\ (I_D + I_d)] + rI_q$

$= j\acute{s}\ [2(x_1 + x_{mq}))\ I_d + (x_{md} - x_{mq})\ (I_D + I_d) + rI_q$

Dividing both sides by $\acute{s}$, we have;

$\Rightarrow \frac{V_q}{\acute{s}} = j\ [2(x_1 + x_{mq}))\ I_d + (x_{md} - x_{mq})\ (I_D + I_d) + \frac{rI_q}{\acute{s}}$

$\Rightarrow \frac{V_a}{\acute{s}} = [j2(x_1 + x_{mq})I_a] + j(x_{md} - x_{mq})(I_A + I_a) + \frac{rI_a}{\acute{s}}$

$= [2j(x_1 + x_{mq}) + \frac{r}{\acute{s}}]I_a + j(x_{md} - x_{mq})(I_A + I_a)]$

Referring to equation (3.72);

$$\frac{V_a}{2S-1} = [j2(x_1 + x_{mq}) + \frac{r}{2s-1}] I_a + j[(x_{md} - x_{mq})(I_A + I_a)] \quad (3.74)$$

Equations (3.73) and (3.74) result a per phase T – equivalent circuit as shown in figure 3.11.

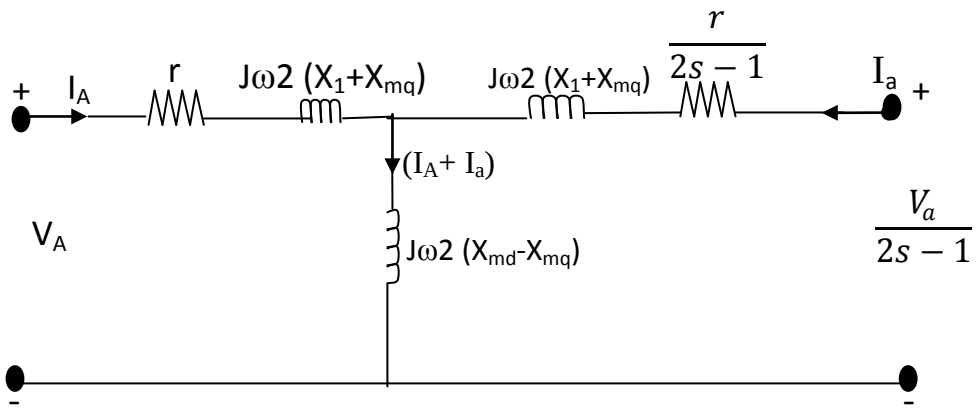

Fig 3.11 Per phase steady state T – equivalent circuit of a 3-phase transfer field reluctance motor, using the q-variable.

The rotor (auxiliary) is usually short circuited and hence from figure 2.36, $\frac{V_a}{2S-1} = 0$

Also, $\frac{r}{2S-1} = r + \frac{2r(1-s)}{2S-1}$ (3.75)

Hence, figure 3.11 can be redrawn for better as in figure 3.12 to suit equation (3.75) as below.

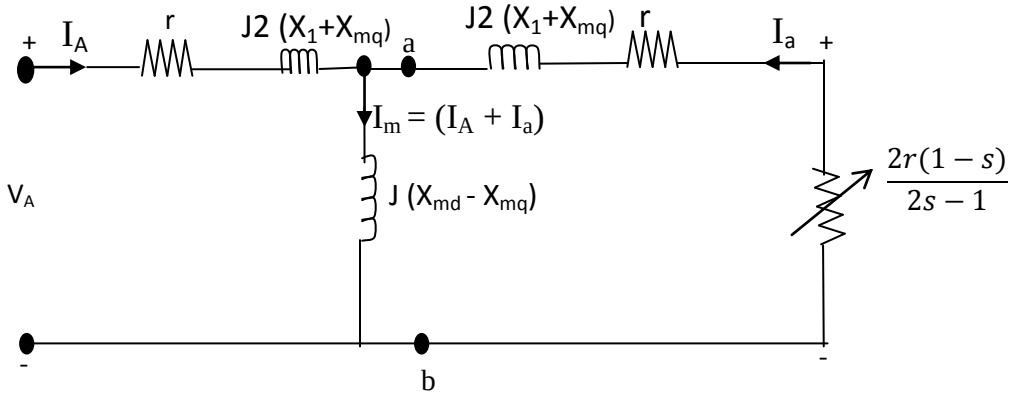

Figure 3.12 Per phase steady state T - equivalent circuit of a 3-phase transfer field reluctance motor.

N-B - Figure 3.12 can also be obtained using the d-variable of equation (3.49) and (3.52).

3.2.13 Power across air – gap, Torque and power output in 3-phase Transfer field reluctance motor

With reference to the equivalent circuit of figure (3.12), the power crossing the terminals (**ab**) in the circuit is the electrical power input per phase minus the stator losses (stator copper and iron losses) and hence, is the power that is transferred from the stator (main windings) to the rotor (auxiliary windings) through the air-gap magnetic field. This is known as the power across the air gap. Its 3-phase value is symbolized as P_G.

From figure 3.12,

$$P_G = 3(I_a)^2 \frac{r}{2S-1} \quad (3.76)$$

The Auxiliary winding copper loss $P_{c(aux)} = 3(I_a)^2 r$ (3.77)

∴ From equations (3.76) and (3.77);

$$P_G = \frac{P_c\,(aux)}{2S-1}$$

$\Rightarrow P_c$ (aux) = (2S-1)P_G (3.78)

If equation (3.77) is subtracted from equation (3.76), we have;

$P_G - P_c$ (aux) = P_m (Mechanical output (gross) power)

$\Rightarrow P_m = [\ 3(I_a)^2 \frac{r}{2S-1}] - [\ 3(I_a)^2 r]$

$= 6(I_a)^2 \quad \frac{r(1-s)}{2S-1}$

$\Rightarrow P_m = 2P_G (1-s)$ (3.79)

From the equations established so far, it is evident that high slip (s) operation of the transfer field machine would be highly inefficient, hence, transfer field motor just as the induction motor counterpart are therefore designed to operate at low slip at full load.

3.2.14 Torque/Slip characteristic of a 3-phase transfer field reluctance motor without rotor windings

The torque- slip characteristic of a 3-phase transfer field reluctance motor without rotor windings can be studied for clarity if the per phase steady-state equivalent circuit of figure (3.12) is modified as shown fig 3.13 below; **taking $x_1 + x_{mq} = x_q$**

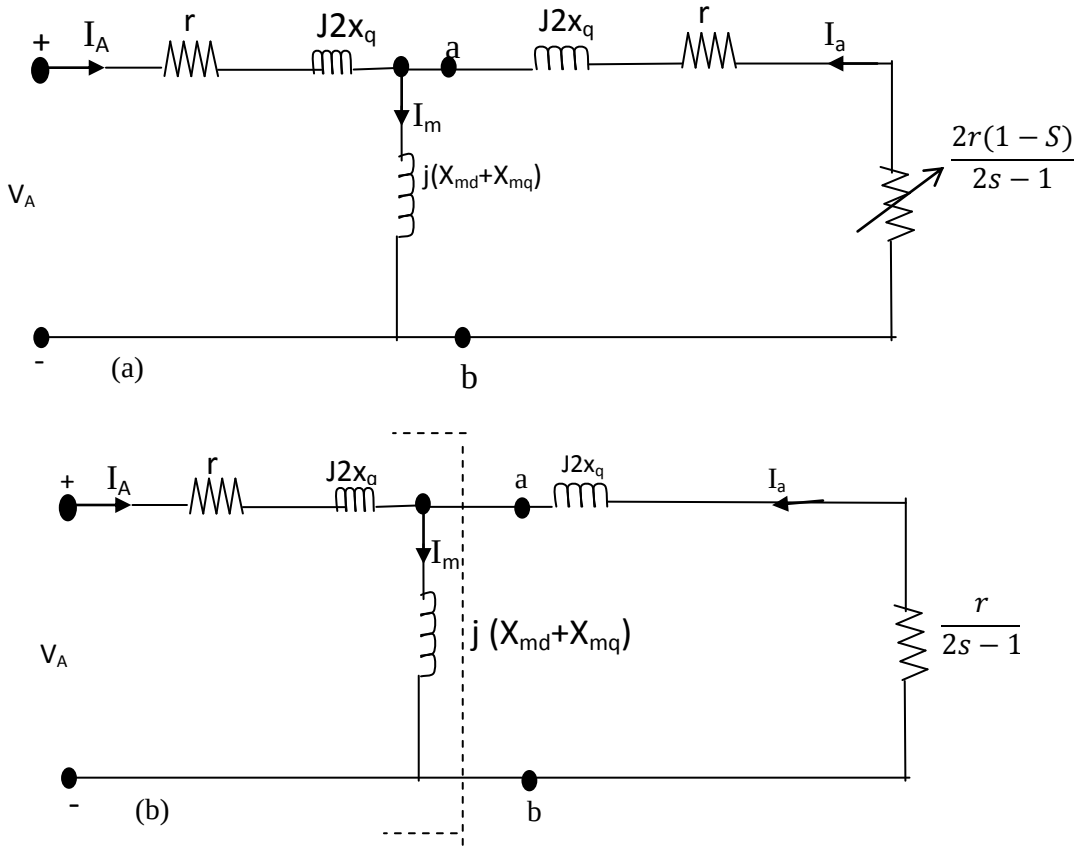

Fig 3.13 (a and b) – Modified per phase steady-state T- equivalent circuit of a 3-phase transfer field reluctance motor without rotor windings.

From figure 3.13a, the V_{TH} (voltage across a-b) is given by;

$$V_{TH} = \left[\frac{j\ (X_{md} - X_{mq})}{j\ (X_{md} - X_{mq}) + (r + j2X_q)}\right] V_A \quad \text{volts}$$

$$= \left[\frac{j\ (X_{md} - X_{mq})}{r + j\ (X_{md} - X_{mq} + 2X_q)}\right] V_A \quad \text{volts} \qquad (3.80)$$

If $r << j\ (x_{md} - x_{mq} + 2x_q)$, then equation (3.80) becomes;

$$V_{TH} = \left[\frac{j\ (X_{md} - X_{mq})}{j\ (X_{md} - X_{mq} + 2X_q)}\right] V_A \quad \text{volts} \qquad (3.81)$$

$$\Rightarrow V_{TH} = \left[\frac{(X_{md} - X_{mq})}{(X_{md} - X_{mq} + 2X_q)}\right] VA \quad \text{volts}$$

Also $Z_{TH} = \frac{j\ (X_{md} - X_{mq})(r + j\ 2X_q)}{j\ (X_{md} - X_{mq}) + (r + j2X_q)}$

$$= \frac{j\ (X_{md} - X_{mq})(r + j2X_q)}{r + j\ (X_{md} - X_{mq}\ + 2X_q)} \qquad (3.82)$$

If r<< j (r_{md}-x_{mq}) + $2x_q$), then equation (3.82) become;

$$Z_{TH} = \frac{j\ (X_{md} - X_{mq})(r + j2X_q)}{j\ (X_{md} - X_{mq} + 2X_q)}$$

$$= \frac{(X_{md} - X_{mq})(r + j2X_q)}{(X_{md} - X_{mq} + 2X_q)}$$

$$= \frac{r\ (X_{md} - X_{mq}) + j2X_q\ (X_{md} - X_{mq})}{(X_{md} - X_{mq} + 2X_q)}$$

$$= \frac{r\ (X_{md} - X_{mq})}{(X_{md} - X_{mq} + 2X_q)} \quad + \quad \frac{j\,(2X_q (X_{md} - X_{mq})}{(X_{md} - X_{mq} + 2X_q)} \qquad (3.83)$$

But $Z_{TH} = R_{TH}$ (Real Component) + X_{TH} (Imaginiry component)

Hence, $R_{TH} = \frac{r\ (X_{md} - X_{mq})}{X_{md} - X_{mq} + 2X_q}$ (3.84)

$$X_{TH} = \frac{j[(2X_q (X_{md} - X_{mq})]}{X_{md} - X_{mq} + 2X_q} \qquad (3.85)$$

The circuit of figure (3.13), then reduces to that of figure 3.14, in which it is convenient to take V_{TH} as the reference voltage

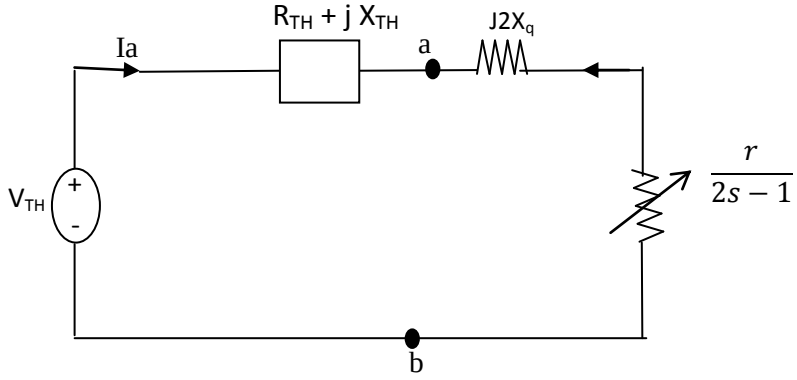

Fig 3.14 Thevenin equivalent of 3 – phase transfer field reluctance motor circuit model

From figure 3.14,

$$I_a = \frac{V_{TH}}{\left(R_{TH} + \frac{r}{2s-1}\right) + j\,(X_{TH} + 2x_q)} \quad \text{Amperes} \qquad (3.86)$$

$$\Rightarrow (I_a)^2 = \frac{(V_{TH})^2}{\left(R_{TH} + \frac{r}{2s-1}\right)^2 + (X_{TH} + 2x_q)^2} \quad \text{Amperes} \qquad (3.87)$$

The expression for the steady state electromagnetic torque is given by;

$T_e = \frac{P_m}{\omega_r} = \left(\frac{6(I_a)^2 r}{\omega_r}\right)\left(\frac{1-s}{2s-1}\right)$

$= \left(\frac{6(I_a)^2 r}{\omega\,(1-s)}\right)\left(\frac{1-s}{2s-1}\right) = \frac{6(I_a)^2 r}{\omega(2s-1)}$ N-m (3.88)

Hence, putting equation (3.87) into equation (3.88) yields;

$T_e = \left(\frac{6}{\omega}\right)\frac{(V_{TH})^2}{\left(R_{TH}+\frac{r}{25-1}\right)^2 + (X_{TH}+2x_q)^2}\left(\frac{r}{2s-1}\right)$ N-m (3.89)

3.2.15 Torque/Slip characteristics of a conventional 3-phase transfer field reluctance motor

The torque/slip characteristic of the motor is analysis using equation 3.89 for the Matlab plot, as shown in figure 4.1a.

3.2.16 Efficiency/Slip characteristics of 3-phase transfer field reluctance motor without rotor windings

The efficiency/slip relationship for a conventional 3-phase transferred field reluctance motor without rotor windings can be investigated using the per phase steady-state equivalent circuit of a 3-phase transfer field machine of fig 3.13(b).

From fig 3.13(b);

The input impedance looking through the input terminals is;

$Z = r + j2x_q + \left[\frac{j\left(X_{md}-X_{mq}\right)\left(j\,2x_q+\frac{r}{25-1}\right)}{\frac{r}{25-1}+j\left(2x_q+\left(X_{md}-X_{mq}\right)\right)}\right]$ (3.90)

Also, the current in the main winding (I_A) is given by;

$I_A = \frac{V_A}{Z}$ (3.91)

The current in the auxiliary winding is given by;

$I_a = \left[\frac{j\left(X_{md}-X_{mq}\right)}{\frac{r}{25-1}+j\left(2x_q+\left(X_{md}-X_{mq}\right)\right)}\right]I_A$ (3.92)

The copper losses in the main and auxiliary windings = $3r(I_A + I_a)^2$ (3.93)

Input power = Output power + the copper losses, excluding windage and friction losses.

From equation 3.79,

The machine input power = $6r\left(\frac{1-s}{2s-1}\right)(I_a)^2 + 3r(I_A + I_a)^2$

$$= 3r\left[2\left(\frac{1-s}{2s-1}\right)(I_a)^2 + (I_A + I_a)^2\right] \quad (3.94)$$

Hence, the machine Efficiency $\varepsilon = \frac{output\ \ power}{input\ \ power} = \frac{2\left(\frac{1-s}{2s-1}\right)(I_a)^2}{2\left(\frac{1-s}{2s-1}\right)(I_a)^2+(I_A+I_a)^2}$ (3.95)

3.2.17 Power factor/Slip characteristics of 3-phase transfer field reluctance motor without rotor windings

From the Thevenin equivalent of a 3-phase transfer field machine circuit model of fig 3.14, the machine's power factor (cosθ) is given by;

Power factor $(\cos\theta) = \frac{Real\ (Z)}{\sqrt{Real\ (Z)^2 + Imag\ (Z)^2}}$ 3.96

$$= \frac{R_{TH} + \frac{r}{2s-1}}{\sqrt{\left(R_{TH} + \frac{r}{2s-1}\right)^2 + \left(X_{TH} + 2x_q\right)^2}} \quad 3.97$$

3.2.18 Auxiliary current (I_a)-slip(s) Characteristics of conventional 3-phase transfer field machine.

Using equation 3.86, a plot of auxiliary current (I_a) against slip(s) is obtained as in figure 4.4a.

3.3 ANALYSIS OF THREE-PHASE TRANSFER-FIELD RELUCTANCE MOTOR WITH THE INTRODUCTION OF ROTOR WINDINGS

3.3.1 Introduction/Background

The ultimate feature of every electrical rotating machine, be it a generator or a motor is its output characteristics. It is the yard-stick upon which the machine is evaluated. Obviously, the output characteristics of all three phase transfer field reluctance motors are much inferior to that of a three-phase induction motor of comparable size and ratings.

This is the attribute of their low direct axis reactance to quadrature axis reactance ratio, coupled with the excessive leakage reactance from the quadrature axis reactance. These are as a result of the salient nature of their rotor pole structures. To ameliorate these set-backs, their rotor designs need to be improved. The new configuration of three phase transfer field reluctance motor is intended to minimize the excessive leakage reactance for a better output performance of the motor.

In this study, the rotor windings are wound at the periphery of the rotor pole structures connecting the two machine sets (A and B). Just as in the auxiliary windings, the rotor windings are transposed between the machine sets, and then connected then in parallel with the auxiliary windings.

The use of short-circuited rotor windings, would lead to considerable improvements in its performance. The rotor windings do not only give rise to an increase in the induced e.m.f but also augment output power by effectively lowering the synchronous reactance of the output windings, thus leading to a higher output and greater synchronous stability. Hence, there is the necessity to raise the output of the cage-less three phase transfer field machine by way of

using circuits on the structure (shaft), so as to augment the effect of saliency (E.S Obe and A. Binder 2011).

Additionally, the windings in the rotor of a three-phase transfer field reluctance motor could go a long way to improving its performance characteristics and a better ability to preserve the voltage wave shape following a sudden addition or removal of load than does a three-phase transfer field reluctance motor without rotor windings. Also, the three-phase transfer field reluctance motor without rotor windings is only capable of yielding less than half the rated power while the T.F machine with a rotor windings is able to produce more than two-thirds of the rated power. This is due to the inability of the three-phase transfer field reluctance motor without rotor windings to excite at capacitance value high enough to circulate the rated current in the machine windings. Unlike the T.F motors with windings at the rotor, the counterpart without rotor windings produces a lower voltage and lower load current and, hence can only yield lower power.

In its normal running condition, the operation of the transfer field motor is asyndronous, that is, the rotor speed is different from that of the field. It follows therefore that the winding impedances will be influenced by closed electric circuit in the rotor (L.A Agu 1984). A short circuited full rotor cage or poly-phase winding will reduce the effective reactance of the primary winding in the same way that it would in a conventional induction motoroperating at a slip. The rotor winding being almost wholly inductive; the rotor current produce a field which is nearly totally demagnetizing with respect to the applied primary field; additional primary current is drawn from the supply to balance the rotor current. In terms of the supply therefore, the primary reactance is effectively reduced. If the rotor is connected to a capacitive load such that the rotor current is leading, the rotor field will act in the direction of the applied

field, and the total current drawn from the supply will be reduced. So in supply terms, this will amount to an increase in primary reactance.

The rotor winding can be split into two separate d-axis and q-axis windings. The d-axis winding has its axis along the direct axis of the salient pole rotor, and the q-axis winding has its axis along the quadrature axis of the salient pole rotor. The d-axis and q-axis have been shown in fig 3.15. The direct (d)-axis and quadrature (q)-axis flux path involve two small air gaps and two large air gaps respectively. The first is path of minimum reluctance, where as the second is the path of maximum reluctance (Smarajit Ghosh (2007).

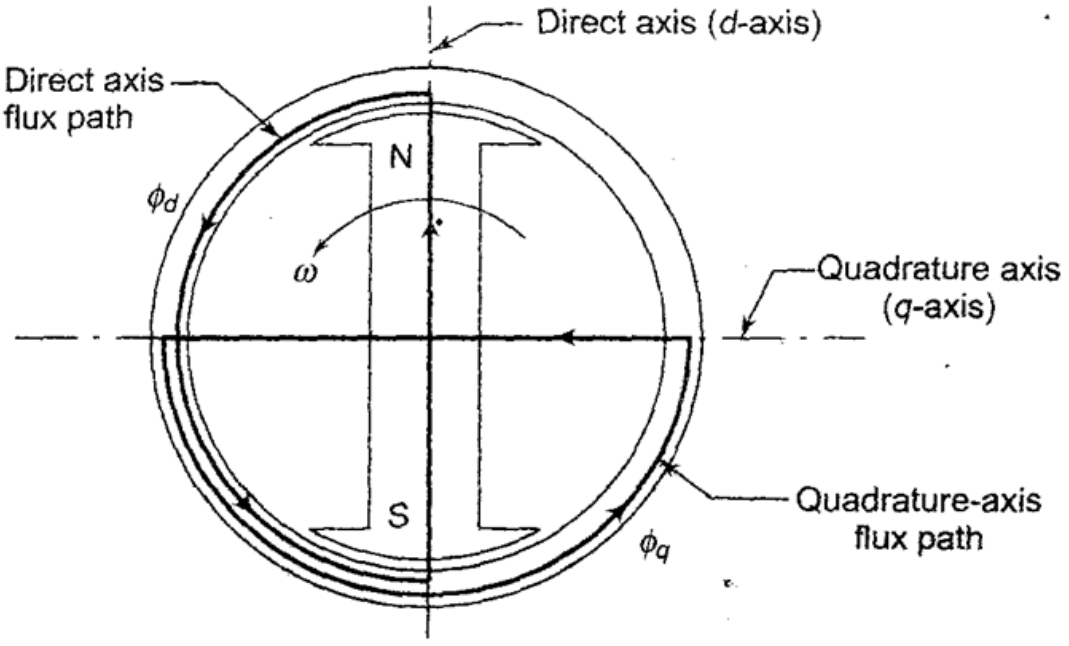

Fig 3.15 Direct (d) axis and quadrature (q) axis of two-pole salient pole rotor

A single phase d-axis rotor winding will have no influence on the reactance of the primary winding, the latter's axis concides with the q-axis of the rotor, but will have the must effect when the winding axis concides with the rotor d-axis. Similarly, a q-axis rotor winding will

have the most effect on the quadrature axis reactance of the primary winding and non on the direct axis reactance. If the current induced by the primary winding in the d-axis rotor magnetic field will assist the primary field; ansd so, for given applied voltage the primary current will be less than it would be if the rotor coils were absent. The primary winding d-axis rotor winding, lagging power factor (pf) currents in the d-axis rotor winding will reduce the primary d-axis reactance. The primary q-axis reactance is lowered by induced reactive currents in the q-axis rotor windings. It can be deduced therefore that a combination of d-axis rotor winding with leading power factor (pf) currents and q-axis rotor windings, with lagging power factor (pf) current will raise the effective X_d to X_q ratio of the transfer field (TF) machine.

3.3.2 The three-phase transfer field reluctance motor with rotor windings descriptions

The structural arrangement of the motor under study is shown in fig 3.16. Unlike the existing three phase transfer field reluctance motor without rotor windings counterpart, the three-phase transfer field reluctance motor with rotor windings comprised two identical poly-phase reluctance machine with moving conductors (rotor windings), whose salient poles rotor are mechanically coupled together, such that their d-axis are in space quadrature. As depicted in fig 3.16, the stator windings, are integrally wound. Each machine element has three sets of windings. Two sets out of the three sets of windings of the machine are identical and are housed in the stator. These are called the main (primary) and the auxiliary windings. The main windings of the machine carry the excitation current, while the auxiliary windings, carry the circulating current. The (2s-1) ω_0 low frequency current is confined in the auxiliary winding without interfering with the supply. The main windings of the machine sets are connected in series while the auxiliary windings, though also in the stator are transposed between the two machine stacks. They are wound for the same pole number and both are star connected. The

third set of windings known as the rotor (cage) windings are wounded at the periphery of the rotor shaft connecting the two machine sets. Just as in the auxiliary windings, the rotor (cage) windings are also transposed between the two machine stacks and then connected in parallel with the auxiliary windings (see fig 3.17a).

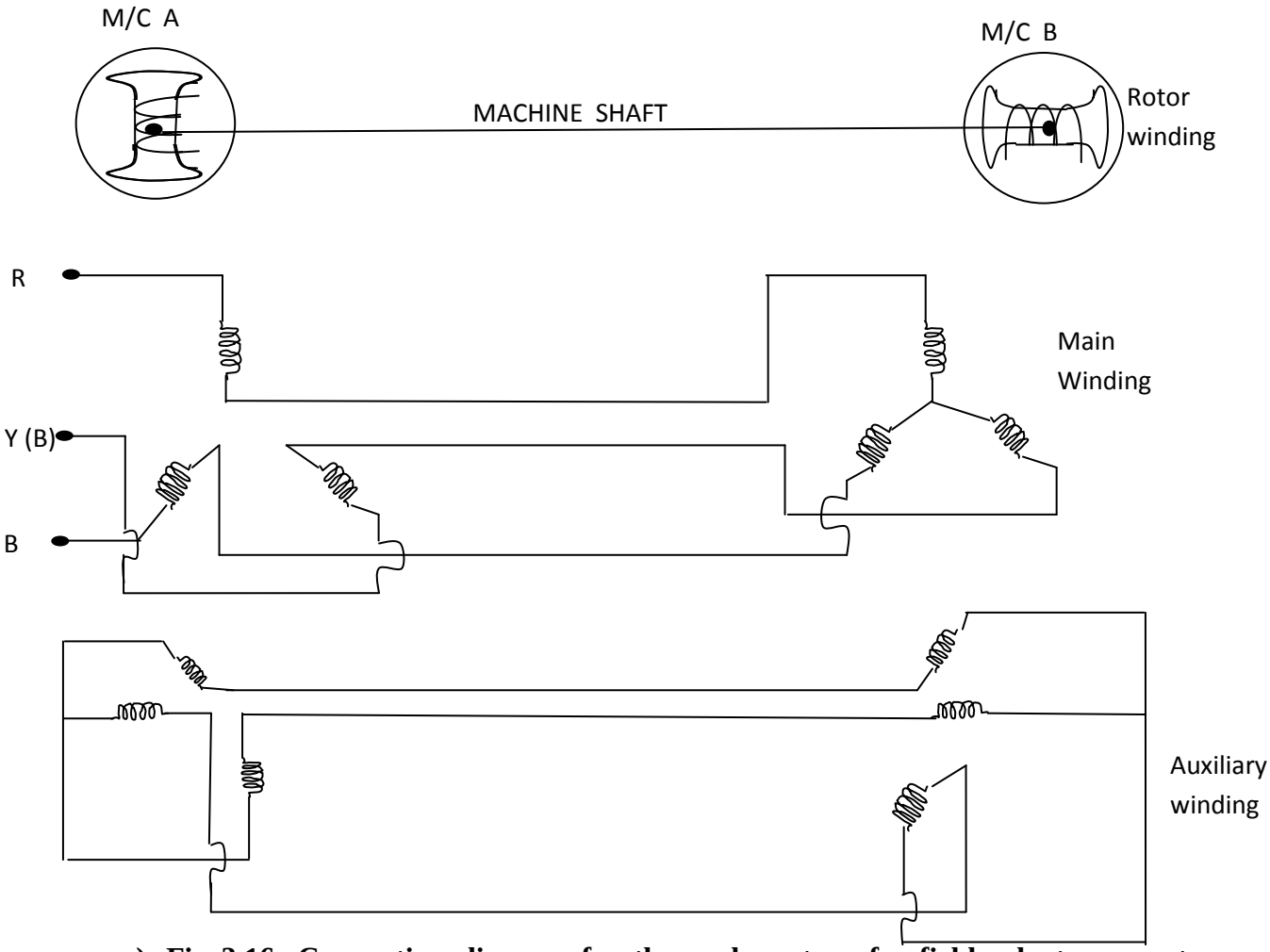

a) Fig 3.16: Connection diagram for three phase transfer field reluctance motor with rotor winding

3.3.3: Steady state analysis of the configured 3-phase transfer-field reluctance motor with rotor windings.

The steady state analysis of the configured motor can be done, using the schematic diagram of figure 3.17 below;

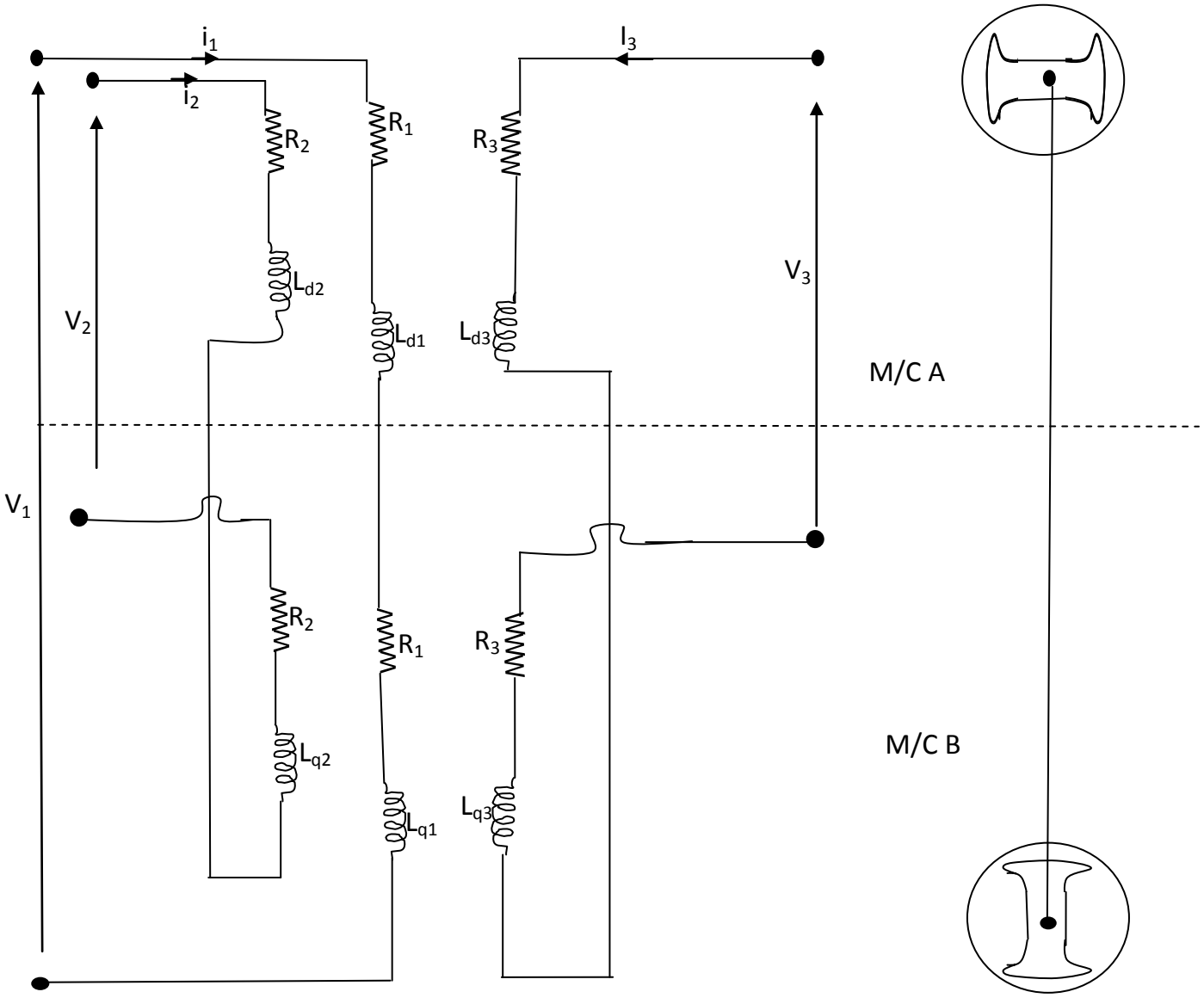

Fig. 3.17(a)- Per phase schematic diagram of 3-phase transfer field reluctance motor with rotor windings.

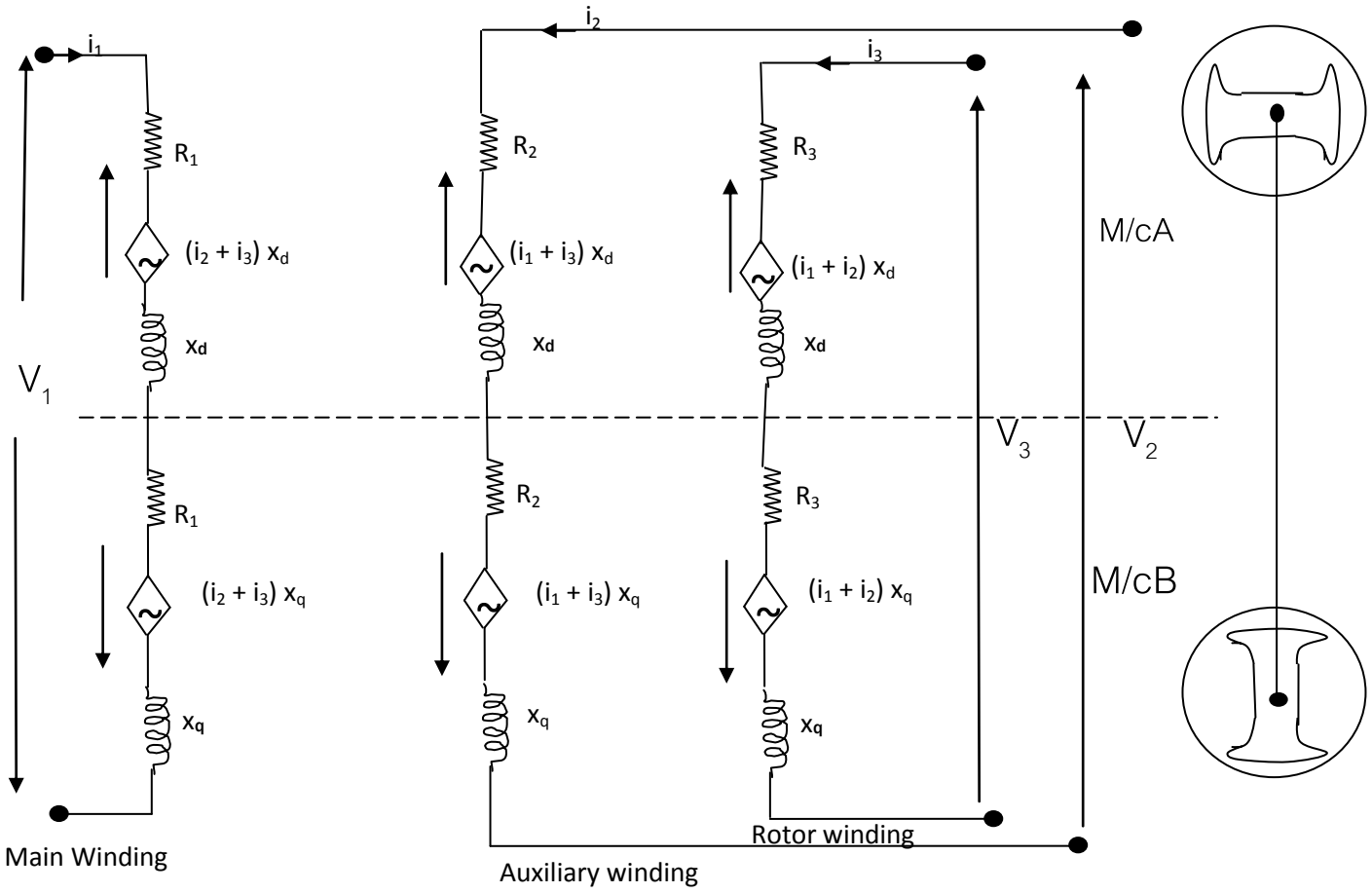

Fig 3.17(b) Modified per phase schematic diagram of the three-phase transfer field reluctance motor with rotor windings under rotor stand-still condition, that is slip(s)=1, N_r=0

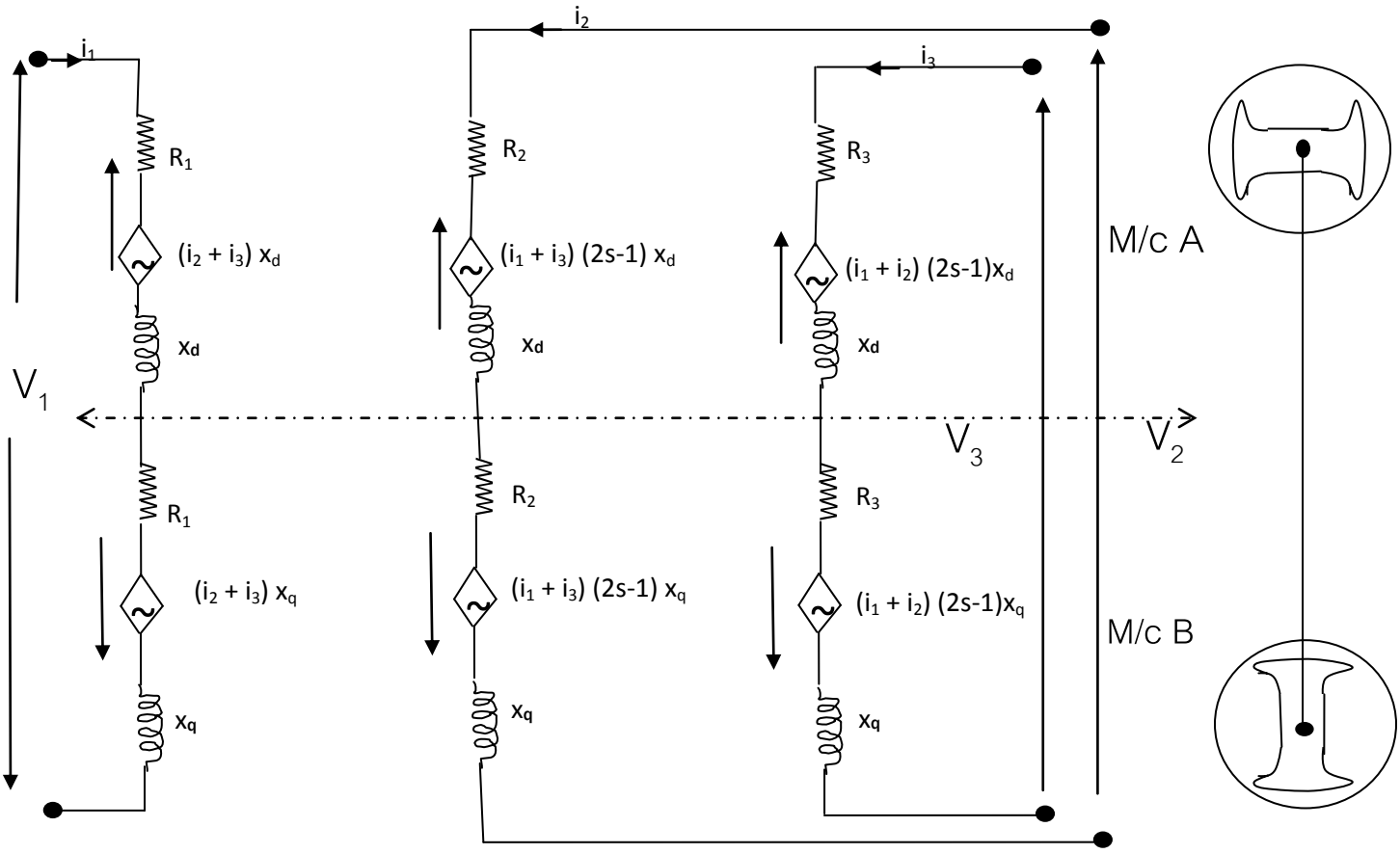

Fig 3.17(c) Modified per phase schematic diagram of the three-phase transfer field reluctance motor with rotor windings under run condition, that is slip = (2s-1).

Where, V_1 = Main winding voltage

V_2 = Auxiliary winding voltage

V_3 = Cage (rotor) winding voltage

$L_{d1} = L_{d2} = L_{d3} = L_d$ = Direct axis inductances

$L_{q1} = L_{q2} = L_{q3} = L_q$ = Quadrature axis inductances

$R_1 = R_2 = R_3 = R$ = Resistance of the machine windings

i_1 = Current at the main windings

i_2 = Current at the Auxiliary windings

i_3 = Current at the rotor windings

Also , $L_{12,}$ L_{13}. L_{21} L_{23} L_{31} and L_{32} are the mutual couplings between coil 1, 2, and 3 at the direct axis.

Similarly, $L_{1\acute{2}}, L_{1\acute{3}}, L_{2\acute{1}}, l_{2\acute{3}}, L_{3\acute{1}}$ and $L_{3\acute{2}}$ are the mutual couplings between coil 1, 2, and 3 at the quadrature axis.

Hence $L_{12} = L_{13} = L_{21} = L_{23} = L_{31} = L_{32} = k\sqrt{L_d}\,L_d = L_d$

Similarly, $L_{1\acute{2}} = L_{1\acute{3}} = L_{2\acute{1}} = L_{2\acute{3}} = L_{3\acute{1}} = L_{3\acute{2}} = k\sqrt{L_q}\,L_q = L_q$

Owing to the fact that the pole structure of the machine is salient in nature as in fig, $L_d \neq L_q$. that is;

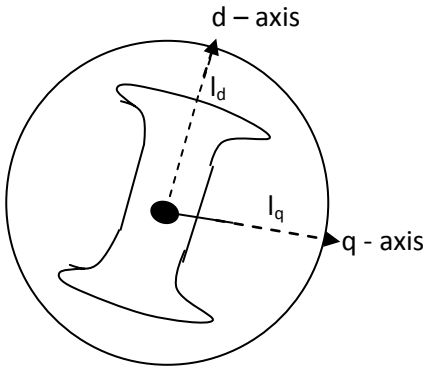

Fig 3.18 – The Salient pole structure of the three-phase transfer field reluctance motor with d-axis and q-axis positions

From figure 3.18,

But $L_d = N^2P_d = \frac{N^2}{S_d}$

$L_q = N^2P_q = \frac{N^2}{S_q}$ (3.98)

$S_d = \frac{l_d}{\mu_A}$

$S_q = \frac{l_q}{\mu_A}$

From fig 3.18, $I_q > l_d$, at constant μ_A and N,

$S_q > S_d$

$\Rightarrow L_d > L_q$

Where

l_d = Direct axis air-gap length

l_q = Quadrature axis air gap length

P_d, S_d = Direct axis permeance and reluctance respectively

P_q, S_q = Quadrature axis permeance and reluctance respectively

L_d = Direct axis inductance

L_q = Quadrature axis inductance

Taking the voltage equation of the machine sections of fig 3.17b, we obtain;

$$V_1 = (R_1 + R_1)\, i_1 + L_d \frac{di_1}{d_t} + L_q \frac{di_1}{d_t} + L_{12} \frac{di_2}{d_t} - L_{1\acute{2}} \frac{di_2}{d_t} + L_{13} \frac{di_3}{d_t} - L_{1\acute{3}} \frac{d_{i3}}{d_t}$$

$$V_1 = (R_1 + R_1)\, i_1 + L_d \frac{di_1}{d_t} + L_q \frac{di_1}{d_t} + L_d \frac{di_2}{d_t} - L_q \frac{di_2}{d_t} + L_d \frac{di_3}{d_t} - L_q \frac{d_{i3}}{d_t}$$

$$V_1 = 2R_1\, i_1 + j\omega L_d\, i_1 + j\omega L_q\, i_1 + j\omega L_d\, i_2 - j\omega L_q\, i_2 + j\omega L_d\, i_3 - j\omega L_q\, i_3$$

$$V_1 = 2R_1\, i_1 + jx_d\, i_1 + jx_q\, i_1 + jx_d\, i_2 - jx_q\, i_2 + jx_d\, i_3 - jx_q\, i_3$$

$$V_1 = 2R_1\, i_1 + j(x_d + x_q - (x_d - x_q)\, i_1 + j(x_d - x_q) i_1 + (x_d - x_q) i_2 + j(x_d - x_q) i_3$$

$$\therefore V_1 = 2R_1\, i_1 + j\,(2x_q) i_1 + (x_d - x_q)\,(i_1 + i_2 + i_3) \qquad (3.99)$$

$$V_2 = (R_2 + R_2) i_2 + L_d \frac{d_{i2}}{d_t} + L_q \frac{d_{i2}}{d_t} + L_{21} \frac{d_{i1}}{d_t} - L_{2\acute{i}} \frac{d_{i1}}{d_t} + L_{23} \frac{d_{i3}}{d_t} - L_{2\acute{3}} \frac{d_{i3}}{d_t}$$

$$V_2 = (R_2 + R_2)\, i_2 + L_d \frac{di_2}{d_t} + L_q \frac{di_2}{d_t} + L_d \frac{di_1}{d_t} - L_q \frac{di_1}{d_t} + L_d \frac{di_3}{d_t} - L_q \frac{d_{i5}}{d_t}$$

$$V_2 = 2R_2\, i_2 + (2s - 1)\,[\, j\omega L_d\, i_2 + j\omega L_q\, i_2 + j\omega L_d\, i_1 - j\omega L_q\, i_1 + j\omega L_d\, i_3 - j\omega L_q\, i_3]$$

$$V_2 = 2R_2\, i_2 + (2s - 1)\,[\, jx_d\, i_2 + jx_q\, i_2 + jx_d\, i_1 - jx_q\, i_1 + jx_d\, i_3 - jx_q\, i_3]$$

$$V_2 = 2R_2\, i_2 + (2s - 1)\,[\, j(x_d + x_q - (x_d - x_q))\, i_2 + j(x_d - x_q) i_2 + j(x_d - x_q) i_1 + j(x_d - x_q) i_3]$$

$V_2 = 2R_2 i_2 + (2s-1)[\, j(2x_q) i_2 + j(x_d - x_q)(i_2 + i_1 + i_3)$

$\therefore \frac{V_2}{2s-1} = \frac{2R_2 i_2}{2s-1} + j(2x_q) i_2 + j(x_d - x_q)(i_1 + i_2 + i_3)$ (3.100)

Also, $V_3 = (R_3 + R_3)i_3 + L_d \frac{di_3}{dt} + L_q \frac{di_3}{dt} + L_{31}\frac{di_1}{dt} - L_{31}\frac{di_1}{dt} + L_{32}\frac{di_2}{dt} - L_{32}\frac{di_2}{dt}$

$V_3 = (R_3 + R_3)i_3 + L_d\frac{di_3}{dt} + L_q\frac{di_3}{dt} + L_d\frac{di_1}{dt} - L_q\frac{di_1}{dt} + L_d\frac{di_2}{dt} - L_q\frac{di_2}{dt}$

$V_3 = 2R_3 i_3 + (2s-1)[\, j\omega L_d i_3 + j\omega L_q i_3 - j\omega L_q i_1 + j\omega L_d i_1 - j\omega L_q i_2 + j\omega L_d i_2]$

$V_3 = 2R_3 i_3 + (2s-1)[\, jx_d i_3 + jx_q i_3 + jx_d i_1 - jx_q i_1 + jx_d i_2 - jx_q i_2]$

$= 2R_3 i_3 + (2s-1)[j(x_d + x_q - (x_d - x_q))i_3 + j(x_d - x_q) i_3 + j(x_d - x_q)i_1 + j(x_d - x_q)i_2$

$= 2R_3 i_3 + (2s-1)[j(2x_q)i_3 + j(x_d - x_q)(i_3 + i_1 + i_2)$

$\Rightarrow \frac{V_3}{2s-1} = \frac{2R_3 i_3}{2s-1} + j(2x_q) i_3 + j(x_d - x_q)(i_1 + i_2 + i_3)$ (3.101)

Equations 3.99 – 3.101 result an equivalent circuit of fig 3.19 below

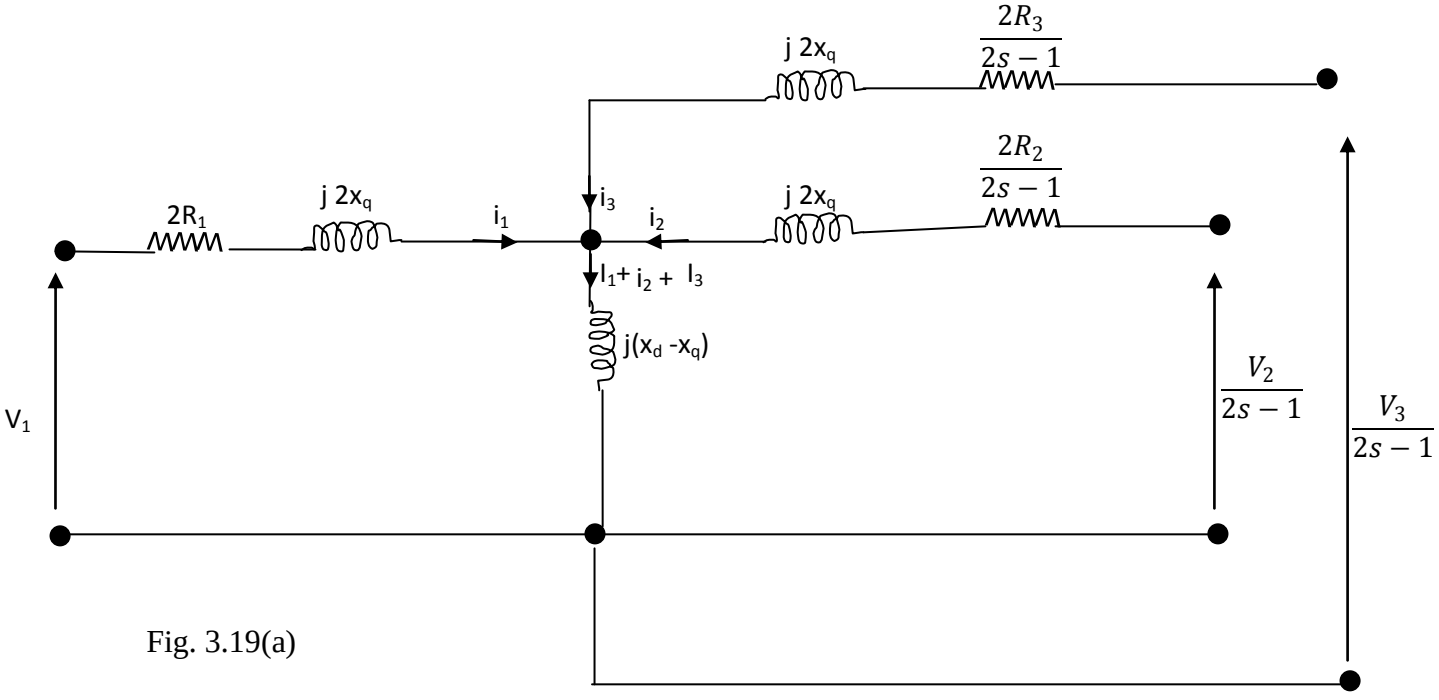

Fig. 3.19(a)

Since the rotor and auxiliary windings are short circuited, $\frac{V_3}{2s-1}$ =0, $\frac{V_2}{2s-1}$ = 0. Hence, fig. 3.19a yields;

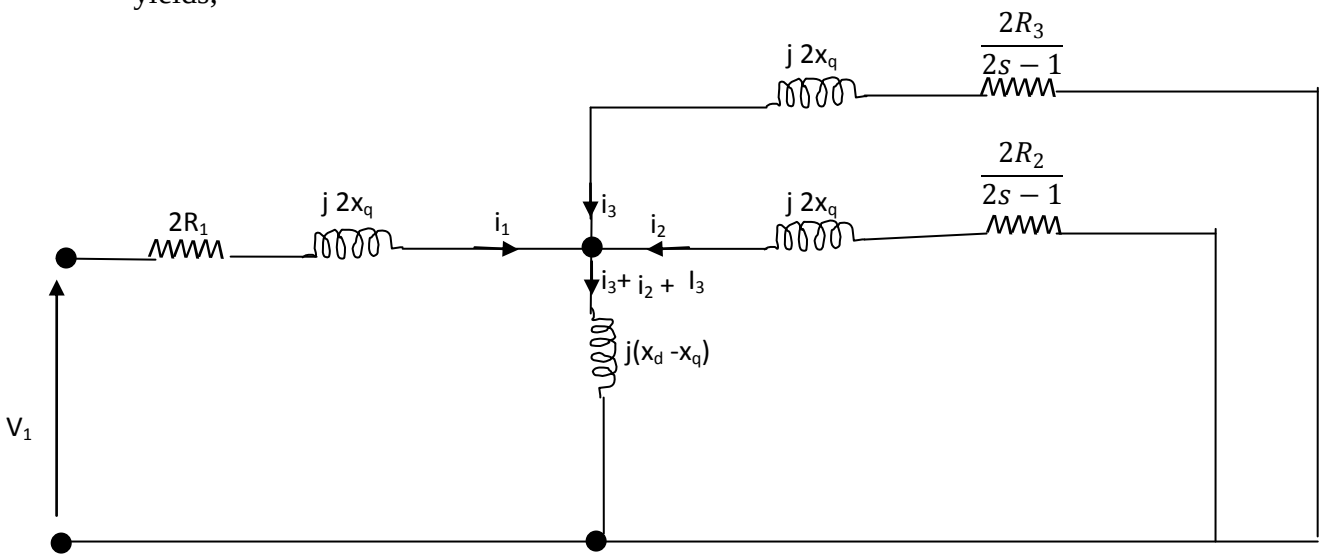

(b)

From fig 3.19b, So far $R_1 = R_2 = R_3 = R$,

$$Z_2 \uparrow\uparrow z_3 = \left[\frac{\left(\frac{2R}{2s-1}\right)+\left(j2\,x_q\right)\left(\frac{2R}{2s-1}\right)+\left(j2\,x\,q\right)}{\left(\frac{2R}{2s-1}\right)+j2\,x_q+\left(\frac{2R}{2s-1}\right)+\left(j2\,x_q\right)}\right]$$

$$= \frac{\left[\left(\frac{2R}{2s-1}\right)+\left(j2\,x_q\right)\right]^2}{2\left[\left(\frac{2R}{2s-1}\right)+\left(j2\,x_q\right)\right]}$$

$$= \frac{\frac{2R}{2s-1}+j2\,x_q}{2}$$

$$= \frac{2R}{2(2s-1)} + \frac{j2\,x_q}{2}$$

$$\therefore Z_2 \uparrow\uparrow z_3 = \frac{R}{2s-1} + j\,x\,q \qquad (3.102)$$

Hence, fig 3.19b can be redrawn as below;

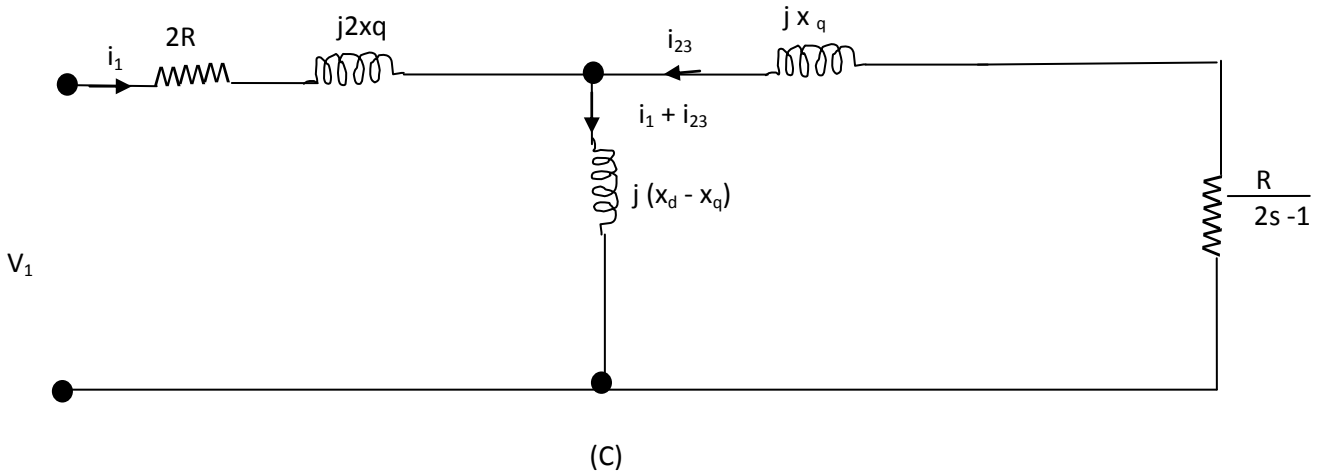

(C)

Fig. 3.19c

Also, $\frac{2R}{2s-1}$ = R + $\frac{2R\ (1-s)}{2s-1}$ (3.103)

Hence, Fig 3.19c becomes;

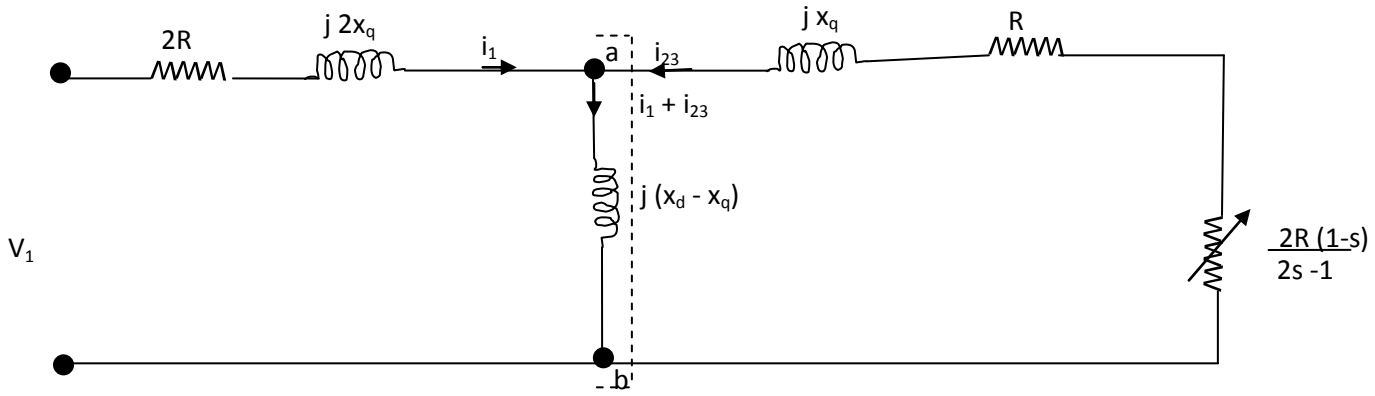

(d)

Fig 3.19(a) – Per-phase steady state equivalent circuit of 3-phase transfer field Reluctance motor with rotor windings

(b) Per phase steady state equivalent circuit of the motor 3-phase transfer field Reluctance motor with rotor windings when V_2 and V_3 are short circuited.

(c|d) – The modified equivalent circuits of the 3-phase transfer field Reluctance motor with rotor windings

From fig 3.19d,

$V_{TH} = \left[\frac{j(x_d - x_q)}{j(x_d - x_q) + (2R + j2\,x_q)}\right] V_1$

$= \left[\frac{j(x_d - x_q)}{2R + j\,(x_d - x_q + 2x_q)}\right] V_1$ (3.104)

If $2R << j\,(x_d - x_q + 2\,x_q)$, we have;

$V_{TH} = \left[\frac{j(x_d - x_q)}{j(x_d - x_q + 2x_q)}\right] V_1$

$\therefore V_{TH} = \left[\frac{x_d - x_q}{x_d + x_q}\right] V_1$ volts (3.105)

Also

$Z_{TH} = \frac{j\,(x_d - x_q)(2R + j2\,x_q)}{j\,(x_d - x_q)(2R + j2\,x_q)}$

$= \frac{j\,(x_d - x_q)(2R + j2\,x_q)}{2R + j\,(x_d - x_q + 2x_q)}$ (3.106)

If $2R <<< j\,(x_d - x_q + 2\,x_q)$, then;

$Z_{TH} = \frac{j\,(x_d - x_q)(2R + j2\,x_q)}{j(x_d - x_q + 2x_q)}$

$= \frac{(x_d - x_q)(2R + j2\,x_q)}{(x_d + x_q)}$ (3.107)

But $(x_d - x_q)\,(2R + j2\,x_q) = 2R\,(x_d - x_q) + j(2x_q\,(x_d - x_q))$

$= 2R\,(x_d - x_q) + j(2x_q\,x_d - 2x_q\,x_q))$ (3.108)

$\therefore Z_{TH} = \frac{2R\,(x_d - x_q)}{(x_d + x_q)} + \frac{j\left(2x_q\,x_d - 2(x_q)^2\right)}{(x_d + x_q)}$

But $Z_{TH} = R_{TH} + X_{TH}$

Hence $R_{TH} = \frac{2R\,(X_d - X_q)}{(X_d + X_q)}$ - Real value of Z_{TH} (3.109)

$X_{TH} = \frac{j\,(2xq\;xd - 2(x_q)^2)}{(X_d + X_q)} = \frac{j2x_q\,(X_d - X_q)}{(X_d + X_q)}$ - Imaginary value of Z_{TH} (3.110)

Hence fig 3.19d reduces to;

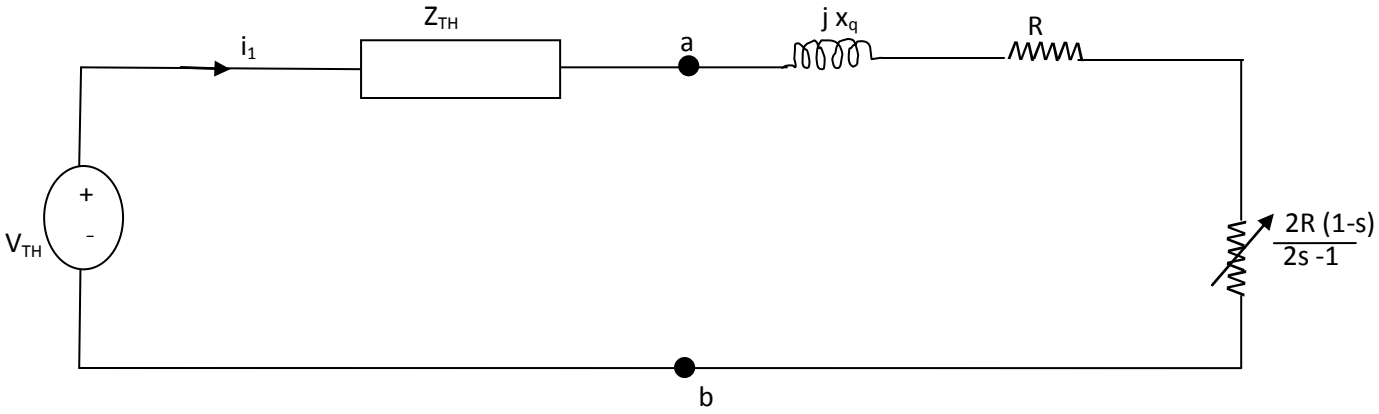

Fig 3.19(e) Thevenin equivalent of three phase transfer field reluctance motor with rotor winding circuit model

From fig 3.19e,

$$i_1 = \frac{V_{TH}}{Z_{TH}} = \frac{V_{TH}}{\left(R_{TH} + R + \frac{2R(1-s)}{2s-1}\right) + j\,(X_{TH} + X_q)}$$

$$= \frac{V_{TH}}{\left(R_{TH} + \frac{R}{2s-1}\right) + j\,(X_{TH} + X_q)} \qquad (3.111)$$

$$\Rightarrow i_1^2 = \frac{(V_{TH})^2}{\left[\left(R_{TH} + \frac{R}{2s-1}\right) + j\,(X_{TH} + X_q)\right]^2}$$

$$= \frac{(V_{TH})^2}{\left(R_{TH} + \frac{R}{2s-1}\right)^2 + (X_{TH} + X_q)^2} \qquad (3.112)$$

3.3.4 Power Across Air –gap, Torque and Power Output in three-phase transfer field reluctance motor with rotor winding

With regards to the equivalent circuit of fig 3.19(d), the power crossing the terminal **ab** in the circuit is the power that is transferred from the stator windings to then auxiliary and cage windings, through the machine air-gap magnetic field. This is called the power across the air gap or simply air-gap power, whose three phase value is shown below;

$$P_G = 3\,(i_{23})^2\,\frac{R}{2s-1} \quad \text{Watts} \qquad (3.113)$$

Auxiliary/rotor windings copper P_c (aux/rotor) $= 3(i_{23})^2 R$ (3.114)

Putting equation 3.114 into equation 3.113, we have;

$P_G = \frac{P_{c(aux\ /rotor\ )}}{2s-1}$

$\Rightarrow P_{c\ (aux/rotor)} = (2s\text{-}1)\ P_G$ Watts (3.115)

But Mechanical Output (gross) Power (P_m) of the machine is given by;

$P_m = P_G - P_c$ (aux/rotor)

$\Rightarrow P_m = \left[3(i_{23})^2\ \frac{R}{2s-1}\right]$ - $\left[3(i_{23})^2\ R\right]$

$= 6\ (i_{23})^2\ R\ \frac{(1-S)}{2s-1}$ Watts

$\Rightarrow P_m = 2P_G(1\text{-}s)$ Watts (3.116)

From equation 3.115 and 3.116, it can be inferred that high slip operation of the machine will favour auxiliary/rotor winding copper losses $P_{c(aux/rotor)}$ at the detriment of the mechanical output (gross) Power (P_m), and would make the machine highly inefficient. Hence, the machine is particularly designed to operate at low slip, even at full load.

3.3.5 Torque/slip Characteristic of 3-phase transfer field reluctance motor with rotor windings

From fig 3.19e, The expression for the steady-state electromagnetic torque of the machine is given as below;

$T_e = \frac{P_m}{\omega_m} = \frac{P_m}{\omega(1-s)}$ (3.117)

$= [6\ (i_{23})^2\ R\ \frac{(1-S)}{2s-1}\ x\ \frac{1}{\omega(1-s)}]$

$= \frac{6(i_{23})^2 R}{\omega\ (2s-1)}$

$= \frac{6(i_{23})^2 R}{\omega\ (2s-1)}$ N-m (3.118)

Putting equation 3.112 into equation 3.118, we have;

$T_e = \frac{6}{\omega}\ \left(\frac{R}{2s-1}\right)\left[\frac{(V_{TH})^2}{\left(R_{TH}+\frac{R}{2s-1}\right)^2 + (X_{TH}+X_q)^2}\right]$ N-m (3.119)

Equation 3.119 is the expression for torque developed as a function of voltage (V_{TH}) and slip (s).

3.3.6 Efficiency/slip characteristics of the 3-phase transfer field reluctance motor with rotor windings.

The efficiency/slip relationship for the 3-phase transfer field reluctance motor with rotor windings can be studied for better, using the per phase steady-state equivalent circuit of the machine as in fig 3.19d

The input impedance looking through the input terminals is;

$$Z = 2R + j2x_q + \left[\frac{j(X_d - X_q)\,(jx_q + \frac{R}{2s-1})}{\frac{R}{2s-1} + j(x_q + (X_d - X_q))}\right]$$

$$= 2R + j2x_q + \left[\frac{j(X_d - X_q)\,(jx_q + \frac{R}{2s-1})}{\frac{R}{2s-1} + jx_d}\right] \quad (3.120)$$

The current I_1 in the main winding;

$$\Rightarrow i_I = \frac{V_1}{Z} \quad (3.121)$$

Similarly, the current in the auxiliary and rotor windings (i_{23}) is given by;

$$i_{23} = \left[\frac{j(X_d - X_q)}{\frac{R}{2s-1} + j(x_q + (X_d - X_q)}\right] i_1 \quad (3.122)$$

The copper losses in the main, auxiliary and rotor winding = $3[2R(i_1)^2 + R(i_{23})^2]$

$$= 3R[2(i_1)^2 + (i_{23})^2] \quad (3.123)$$

But, Input Power = Output Power + Copper losses in the main, auxiliary and rotor winding, excluding windage and friction losses;

$$\therefore \text{ Input Power} = 6R\left(\frac{1-s}{2s-1}\right)(i_{23})^2 + 3R\,(2(i_1)^2 + (i_{23})^2)$$

$$= 3R\left[2\left(\frac{1-s}{2s-1}\right)(i_{23})^2 + 2(i_1)^2 + (i_{23})^2\right] \quad (3.124)$$

$$\therefore \text{ The machine efficiency } (\varepsilon) = \frac{2\left(\frac{1-s}{2s-1}\right)(i_{23})^2}{2\left(\frac{1-s}{2s-1}\right)(i_{23})^2 + 2(i_1)^2 + (i_{23})^2} \quad (3.125)$$

3.3.7 Power factors/Slip characteristic of the 3-phase transfer field reluctance motor with rotor windings

From the Thevenin equivalent of the configured machine of fig 3.19d the machine's power factor (cosθ) is given by;

$$\text{Power factor } (\cos\theta) = \frac{Real\ (Z)}{\sqrt{Real\ (Z)^2 + Imag\ (Z)^2}}$$

$$= \frac{R_{TH} + \frac{R}{2s-1}}{\sqrt{\left(R_{TH} + \frac{R}{2s-1}\right)^2 + \left(X_{TH} + X_q\right)^2}} \qquad (3.126)$$

3.3.8 Rotor current (i_{23}) – Slip(s) characteristic of 3-phase transfer field reluctance motor with rotor windings

Using equation 3.111, a plot of rotor current (i_{23}) against slip(s) can be obtained.

3.4 Dynamic Model of 3-Phase transfer Field reluctance motor with rotor windings

For us to derive the dynamic equations of the circuit model of the configured transfer field reluctance machine it is paramount to take a look at the variation of inductances with rotor position since the rotor has salient poles. In general, the permeance along the d and q axes is not the same.

Since the rotor is of salient poles, its mmfs are always directed along the d and q axes. Also, the direction of the resultant mmf of the stator windings relative to these two axes will vary with the power factor. A common approach to handling the magnetic effect of the stator's result an mmf is to resolve it along the d and q axes, where it could be dealt with systematically. Let us consider the magnetic effect of current flowing in phase **a**of the stator. The resolved components of the a-phase mmf F_a, will produce the flux components:

$\phi_d = P_d F_a \sin\theta_r$ and $\phi_q = P_q F_a \cos\theta_r$ along the d and q axes respectively.

Where P = peameance

The linkage of these resolved flux components with the a-phase windings is;

$\lambda_{aa} = N_s (\phi_d \text{ Sin } \theta_r + \phi_q \cos \theta_r)$ Wb turn.

$= N_s F_a (P_d \sin^2\theta_r + P_q \cos^2\theta_r)$

$= N_s F_a (\frac{p_d+p_q}{2} - \frac{p_d-p_q}{2} \cos 2\theta_r)$ (3.127)

Similarly, the linkage of the flux component, ϕ_d and ϕ_q by the b - phase winding that is $\frac{2\pi}{3}$ ahead may be written as:

$\lambda_{ba} = N_s F_a (P_d \sin \theta_r \sin (\theta_r - \frac{2\pi}{3}) + p_q \cos \theta_r \cos (\theta_r - \frac{2\pi}{3}))$

$= N_s F_a (-\frac{p_d+p_q}{4} - \frac{p_d-p_q}{2} \cos 2(\theta_r - \frac{\pi}{3}))$ (3.128)

Based on the functional relationship of λ_{aa} with the rotor angle, θ_r, we can deduce that the self inductance of the stator a-phase winding, excluding the leakage has the form;

$L_{aa} = L_o - L_{ms} \cos 2 \theta_r$ H

Where;

$L_o = \frac{L_{md}+L_{mq}}{2}$ and $L_{ms} = \frac{L_{md}+L_{mq}}{2}$

Those of the b – and c – phases, L_{bb}, L_{cc} are similar to that of L_{aa} but with θ_r replaced by $(\theta_r - \frac{2\pi}{3})$ and $(\theta_r + \frac{2\pi}{3})$, respectively.

Similarly, it can be deduced from equation 3.35, that the mutual inductance between the **a** and **b** phase of the stator is of the form,

$L_{ab} = L_{ba} = \frac{L_o}{2} - L_{ms} \cos 2 (\theta_r - \frac{2\pi}{3})$ H (3.129)

Similarly, expression for L_{bc} and L_{ac} can be obtained by replacing θ_r with $(\theta_r - \frac{2\pi}{3})$ and $(\theta_r + \frac{2\pi}{3})$ respectively.

Since a conventional T.F. effect machine is composed of two components with two windings each, if the parameter referring to the main winding is inscrived with the subscript A, B, C (ie phase quantities) while that referring to the auxiliary winding will have subscript a, b, c, the the dynamic model can be derived as follows:

$$\left.\begin{aligned} V_{ABC} &= r_{ABC}\, i_{ABC} + P\lambda_{ABC} \\ V_{abc} &= r_{abc}\, i_{abc} + P\lambda_{abc} \\ V_{dqrABC} &= r_{dqrABC}\, i_{dqrABC} + P\lambda_{dqrABC} \\ V_{dqrabc} &= r_{dqrabc}\, i_{dqrabc} + P\lambda_{dqrabc} \end{aligned}\right\} \quad (3.130)$$

Where $P \frac{d}{dt}$, λ = flux

R_{ABC} = diag $[(r_A\ r_B\ r_C)]$ and r_{abc} = diag $[(r_a\ r_b\ r_c)]$

The flux linkages are expressed as;

$$\lambda_{ABC} = L_{GG}\, i_{ABC} + L_{GH}\, i_{abc}$$

$$\lambda_{abc} = L_{HG}\, i_{ABC} + L_{HH}\, i_{abc} \quad (3.131)$$

where L_{GG}, L_{GH}, L_{HG} and L_{HH} are inductance matrices obtained from the inductance sub matrices of the two components machines as shown below.

Let L_{11} be the self inductance of the main winding and L_{22} be the self inductance of the auxiliary winding; then the mutual inductance between the main and the mutual inductance between the main and the auxiliary winding will be L_{12} or L_{21} as the case may be;

Now; $L_{11} = \begin{bmatrix} L_{AA} & L_{AB} & L_{AC} \\ L_{BA} & L_{BB} & L_{BC} \\ L_{CA} & L_{CB} & L_{CC} \end{bmatrix}$ $\quad L_{12} = \pm \begin{bmatrix} L_{Aa} & L_{Ab} & L_{Ac} \\ L_{Ba} & L_{Bb} & L_{Bc} \\ L_{Ca} & L_{Cb} & L_{Cc} \end{bmatrix}$

$L_{21} = \pm \begin{bmatrix} L_{aA} & L_{aB} & L_{aC} \\ L_{bA} & L_{bB} & L_{bC} \\ L_{cA} & L_{cB} & L_{cC} \end{bmatrix}$ $\quad L_{12} = \pm \begin{bmatrix} L_{aa} & L_{ab} & L_{ac} \\ L_{ba} & L_{bb} & L_{bc} \\ L_{ca} & L_{cb} & L_{cc} \end{bmatrix}$

So far the main and the auxiliary winding are identical,

L_{GG} = L_{11} (Machine A) + L_{11} (Machine B)

= $L_{11}^{A} + L_{11}^{B}$

The individual inductance expressions are as follows;

$L_{AA} = L_{a1} + L_{a2} \cos 2\theta_r$

$L_{AB} = L_{BA} = -\frac{1}{2} L_{a1} \pm L_{a2} \cos(2\theta_r - \alpha)$

$L_{AC} = L_{CA} = -\frac{1}{2} L_{a1} \pm L_{a2} \cos(2\theta_r + \alpha)$

$L_{BC} = L_{CB} = -\frac{1}{2} L_{a1} \pm L_{a2} \cos 2\theta_r$

$L_{BB} = \frac{1}{2} L_{a1} \pm L_{a2} \cos(2\theta_r - \alpha)$

$L_{CC} = \frac{1}{2} L_{a1} \pm L_{a2} \cos(2\theta_r + \alpha)$

$L_{aa} = \frac{1}{2} L_{a1} \pm L_{a2} \cos 2\theta_r$

$L_{ab} = L_{ba} = \frac{1}{2} L_{a1} \pm L_{b2} \cos(2\theta_r - \alpha)$

$L_{bc} = L_{cb} = \frac{1}{2} L_{b1} \pm L_{b2} \cos 2\theta_r$

$L_{bb} = \frac{1}{2} L_{b1} \pm L_{b2} \cos(2\theta_r - \alpha)$

$L_{cc} = \frac{1}{2} L_{a1} \pm L_{b2} \cos(2\theta_r + \alpha)$

$L_{Aa} = L_{aA} = \frac{1}{2} L_{b12} \pm L_{b12} \cos 2\theta_r$

$L_{Ab} = L_{bA} = \frac{1}{2} L_{a12} \cos\alpha \pm L_{b12} \cos(2\theta_r - \alpha)$

$L_{Ac} = L_{cA} = \frac{1}{2} L_{a12} \cos\alpha \pm L_{b12} \cos(2\theta_r + \alpha)$

$L_{Ba} = L_{ab} = \frac{1}{2} L_{a12} \cos\alpha \pm L_{b12} \cos(2\theta_r - \alpha)$

$L_{Bb} = L_{bB} = \frac{1}{2} L_{a12} \cos\alpha \pm L_{b12} \cos(2\theta_r + \alpha)$

$L_{Bc} = L_{cB} = \frac{1}{2} L_{a12} \cos\alpha \pm L_{b12} \cos 2\theta_r$

$L_{Ca} = L_{aC} = \frac{1}{2} L_{a12} \cos\alpha \pm L_{b12} \cos(2\theta_r + \alpha)$

$L_{Cb} = L_{bC} = \frac{1}{2} L_{a12} \cos\alpha \pm L_{b12} \cos 2\theta_r$

$L_{Cc} = L_{cC} = \frac{1}{2} L_{a12} \cos\alpha \pm L_{b12} \cos(2\theta_r - \alpha)$

Where , $\alpha = \frac{2\pi}{3}$, and; $L_{a11} = L_{a22} = L_{a12} = \frac{1}{2}(L_{md} + L_{mq})$

$$L_{b11} = L_{b22} = L_{b12} = \frac{1}{2}(L_{md} - L_{mq})$$

However, the expressions for the individual inductances above, can further be used for the inductance matrix for the main windings for both machines A and B.

For machine A, the inductance matrix for the main winding is;

$$L_{11}^{A} = \begin{bmatrix} L_{ls} + L_a - L_{ms}\cos 2\theta_r & -\frac{1}{2}L_o - L_{ms}\cos 2\left(\theta_r - \frac{\pi}{3}\right) & -\frac{1}{2}L_o - L_{ms}\cos 2\left(\theta_r + \frac{\pi}{3}\right) \\ -\frac{1}{2}L_o - L_{ms}\cos 2\left(\theta_r - \frac{\pi}{3}\right) & L_{ls} + L_a - L_{ms}\cos 2\left(\theta_r + \frac{2\pi}{3}\right) & -\frac{1}{2}L_o - L_{ms}\cos 2(\theta_r - \pi) \\ -\frac{1}{2}L_o + L_{ms}\cos 2\left(\theta_r + \frac{\pi}{3}\right) & -\frac{1}{2}L_o + L_{ms}\cos 2(\theta_r - \pi) & L_{ls} + L_a - L_{ms}\cos 2\left(\theta_r - \frac{2\pi}{3}\right) \end{bmatrix}$$

For machine B, the inductance matrix for the main winding is;

$$L_{11}^{B}=\begin{bmatrix} L_{ls}+L_a+L_{ms}\cos 2\theta_r & -\frac{1}{2}L_o+L_{ms}\cos 2\left(\theta_r-\frac{\pi}{3}\right) & -\frac{1}{2}L_o+L_{ms}\cos 2\left(\theta_r+\frac{\pi}{3}\right) \\ -\frac{1}{2}L_o+L_{ms}\cos 2\left(\theta_r-\frac{\pi}{3}\right) & L_{ls}+L_a+L_{ms}\cos 2\left(\theta_r+\frac{2\pi}{3}\right) & -\frac{1}{2}L_o+L_{ms}\cos 2(\theta_r-\pi) \\ -\frac{1}{2}L_o+L_{ms}\cos 2\left(\theta_r+\frac{\pi}{3}\right) & L_o+L_{ms}\cos 2(\theta_r-\pi) & L_{ls}+L_a+L_{ms}\cos 2\left(\theta_r-\frac{2\pi}{3}\right) \end{bmatrix}$$

Hence $L_{GG} = L_{11}^{A} + L_{11}^{B}\begin{bmatrix} 2L_{LS}+2L_O & -L_O & -L_O \\ -L_O & 2L_{LS}+2L_O & -L_O \\ -L_O & -L_O & 2L_{LS}+2L_O \end{bmatrix}$

Where L_{Ls} = leakage inductance, and $L_o = \frac{L_{md}+L_{mq}}{2}$

$$\therefore L_{GG}=\begin{bmatrix} 2L_{LS}+L_{md}+L_{mq} & -\frac{1}{2}\left(L_{md}+L_{mq}\right) & -\frac{1}{2}\left(L_{md}+L_{mq}\right) \\ -\frac{1}{2}\left(L_{md}+L_{mq}\right) & 2L_{LS}+L_{md}+L_{mq} & -\frac{1}{2}\left(L_{md}+L_{mq}\right) \\ -\frac{1}{2}\left(L_{md}+L_{mq}\right) & -\frac{1}{2}\left(L_{md}+L_{mq}\right) & 2L_{LS}+L_{md}+L_{mq} \end{bmatrix} \quad (3.132)$$

Now for mutual inductance

For machine A, the mutual inductance matrix is given as;

$$L_{12}^{A} =$$

$$\begin{bmatrix} L_{ls}+L_a-L_{ms}\cos 2\theta_r & L_o-L_{ms}\cos(2\theta_r-\alpha) & L_o\cos\alpha-L_{ms}\cos(2\theta_r+\alpha) \\ L_o\cos\alpha-L_{ms}\cos(2\theta_r-\alpha) & L_{ls}+L_a-L_{ms}\cos(2\theta_r+\alpha) & L_o\cos\alpha-L_{ms}\cos 2\theta_r \\ L_o\cos\alpha-L_{ms}\cos(2\theta_r+\alpha) & L_o\cos\alpha-L_{ms}\cos 2\theta_r & L_{ls}+L_a-L_{ms}\cos(2\theta_r-\alpha) \end{bmatrix}$$

Likewise, for machine B, the mutual inductance matrix is given as;

$$L_{12}^{B} =$$

$$\begin{bmatrix} L_{ls}+L_a+L_{ms}\cos 2\theta_r & L_o+L_{ms}\cos(2\theta_r-\alpha) & L_o\cos\alpha+L_{ms}\cos(2\theta_r+\alpha) \\ L_o\cos\alpha+L_{ms}\cos(2\theta_r-\alpha) & L_{ls}+L_a+L_{ms}\cos(2\theta_r+\alpha) & L_o\cos\alpha+L_{ms}\cos 2\theta_r \\ L_o\cos\alpha+L_{ms}\cos(2\theta_r+\alpha) & L_o\cos\alpha+L_{ms}\cos 2\theta_r & L_{ls}+L_a+L_{ms}\cos(2\theta_r-\alpha) \end{bmatrix}$$

But $L_{GH} = L_{12}^{A} + L_{12}^{B}$

$$\therefore L_{GH} = \begin{bmatrix} -2L_{ms}\cos 2\,\theta_r & -2L_{ms}\cos\,(2\theta_r - \alpha) & -2L_{ms}\cos\,(2\theta_r + \alpha) \\ -2L_{ms}\cos\,(2\theta_r - \alpha) & -2L_{ms}\cos(2\theta_r + \alpha) & -2L_{ms}\cos\,2\theta_r \\ -2L_{ms}\cos\,(2\theta_r + \alpha) & -2L_{ms}\cos 2\theta_r & -2L_{ls}\cos(2\theta_r - \alpha) \end{bmatrix}$$

$$\Rightarrow L_{GH} = -2L_{ms}\begin{bmatrix} \cos 2\,\theta_r & \cos\,(2\theta_r - \alpha) & \cos\,(2\theta_r + \alpha) \\ \cos\,(2\theta_r - \alpha) & \cos(2\theta_r + \alpha) & \cos\,2\theta_r \\ \cos\,(2\theta_r + \alpha) & \cos 2\theta_r & \cos(2\theta_r - \alpha) \end{bmatrix}$$

But $L_{ms} = \frac{L_{md} - L_{mq}}{2}$

$\therefore$ - $2L_{ms} = \frac{2(L_{md} - L_{mq})}{2}$ = s

$$\therefore L_{GH} = L_{mq} - L_{md}\begin{bmatrix} \cos 2\,\theta_r & \cos\,(2\theta_r - \alpha) & \cos\,(2\theta_r + \alpha) \\ \cos\,(2\theta_r - \alpha) & \cos(2\theta_r + \alpha) & \cos\,2\theta_r \\ \cos\,(2\theta_r + \alpha) & \cos 2\theta_r & \cos(2\theta_r - \alpha) \end{bmatrix} \quad (3.133)$$

Where, $\alpha = \frac{2\pi}{3}$

Since the main and auxiliary winding for machine A and B are identical, L_{HG} and L_{HH} will be the same as L_{GH} and L_{GG} respectively.

3.4.1 – Rotor Winding Inductance

The stages of transformation of the voltage equations are to first transform the a.b.c. phase variables into **q-d-o** frame where the quantities are in stationary reference fame. Secondly is to convert the stationary reference **q-d-o** frame into the rotor reference frame ie $\mathbf{d}_r$ and $\mathbf{q}_r$. Since the rotor of this machine is salient pole, the axis of the rotor quantities are already in the **q** and **d** axis, so that the **q-d-o** transformation need only by applied to the stator quantities.

3.4.2 The Machine Model in Arbitrary q-d-o Reference Frame

In order to remove the rotor position dependence on the inductances seen in equation 3.133, the voltage equations in equation 3.130 need to be transferred to q-d-o reference frame. The technique is to transform all the stator variable to an arbitrary reference frame.

Here, all the stator variable will be transform to the rotor. In the voltage equations for the main and auxiliary windings of the transfer field machine of equation 3.130, there is no need to include the rotor equation here since our intension is to adopt rotor reference frame.

Hence, the voltage equations of equation 3.130 will after the transformation yield (Chee-Mumo, 1997);

$$V_Q = \omega\lambda_D + \rho\lambda_Q + ri_Q$$
$$V_D = \omega\lambda_Q + \rho\lambda_D + ri_D \quad (3.134)$$
$$V_O = \rho\lambda_O + ri_O$$

Doing like – wise for the auxiliary and cage (rotor) windings, we have,

$$V_q = (\omega\text{-}2\omega_r)\,\lambda_d + \rho\lambda_q + ri_q$$
$$V_d = (\omega\text{-}2\omega_r)\,\lambda_q + \rho\lambda_d + ri_d$$
$$V_o = \rho\lambda_o + ri_o \quad (3.135)$$
$$V_{q\acute{r}} = (\omega\text{ -}2\omega_r)\ \lambda_{d\acute{r}} + \rho_{\lambda\acute{q}r} + r_{q\acute{r}}\ i_{q\acute{r}}$$
$$V_{d\acute{r}} = (\omega\text{ -}2\omega_r)\ \lambda_{q\acute{r}} + \rho_{\lambda\acute{d}r} + r_{d\acute{r}}\ i_{d\acute{r}}$$

3.4.3 Transformation of flux Linkages

The **ABC** and **abc** subscripts denote variables and parameters associated with the main and auxiliary windings respectively. Both r_{ABC} and r_{abc} are diagonal matrices each with equal non zero elements. For a magnetically linear system, the flux linkages may be expressed as;

$$\begin{bmatrix}\lambda_{ABC}\\ \lambda_{abc}\end{bmatrix} = \begin{bmatrix}L_{GG} & L_{GH}\\ L_{HG} & L_{HH}\end{bmatrix}\begin{bmatrix}i_{ABC}\\ i_{abc}\end{bmatrix}\text{Wb turns} \quad (3.135)$$

Where G = main winding, H = Auxiliary winding.

To transform the above equation in respect to the cage winding, we have as follows,

$$\begin{bmatrix}\lambda_{ABC}\\ \lambda_{abc}\\ \lambda_{dqr\,1}\\ \lambda_{dqr\,2}\end{bmatrix} = \begin{bmatrix}L_{GG} & L_{GH} & L_{GRA} & L_{GRB}\\ L_{HG} & L_{HH} & L_{HRA} & L_{HRB}\\ L_{RAG} & L_{RAH} & L_{RARA} & L_{RARB}\\ L_{RBG} & L_{RBH} & L_{RBRA} & L_{RBRB}\end{bmatrix}\begin{bmatrix}i_{ABC}\\ i_{abc}\\ i_{dqr\,1}\\ i_{dqr\,2}\end{bmatrix} \quad (3.137)$$

The inductance matrix terms L_{GG}, L_{GH}, L_{HG} and L_{HH} are obtained from inductance sub-matrices L_{11}, L_{12}, L_{21} and L_{22} for machine A and B.

L_{GRA} is the mutual inductance matrix between main winding of machine A and rotor winding of machine A.

L_{GRB} is the mutual inductance matrix between main winding of machine B nd rotor winding of machine B.

L_{HRA} is the mutual inductance matrix between auxiliary winding of machine A and rotor winding of machine A

L_{HRB} is the mutual inductance matrix between auxiliary winding of machine B nd rotor winding of machine B.

L_{RARA} is the inductance matrix of rotor winding of machine A.

L_{RARB} is the mutual inductance matrix between the rotor winding of machine A and the rotor winding of machine B.

Similar definitions apply to other inductance matrix terms in equation 10

3.4.4 – Stator Winding inductances

To reduce the mathematical complexities of equation 3.136, it is rewritten in q-d-o frame as;

$$\begin{bmatrix}\lambda_Q & \lambda_D & \lambda_O \\ \lambda_q & \lambda_d & \lambda_o\end{bmatrix}^T = \begin{bmatrix}K_G\, L_{GG}\, K_G^{-1} & K_G\, L_{GH}\, K_H^{-1} \\ K_H\, L_{HG}\, K_G^{-1} & K_G\, L_{HH}\, K_H^{-1}\end{bmatrix}\begin{bmatrix}i_Q & i_D & i_O \\ i_q & i_d & i_o\end{bmatrix} \quad (3.138)$$

$$\text{Where } K_G = \frac{2}{3}\begin{bmatrix}\cos\theta & \cos(\theta-\alpha) & \cos(\theta+\alpha) \\ \sin\theta & \sin(\theta-\alpha) & \sin(\theta+\alpha) \\ \frac{1}{2} & \frac{1}{2} & \frac{1}{2}\end{bmatrix} \quad (3.139)$$

$$K_G^{-1} = \begin{bmatrix}\cos\theta & \sin\theta & 1 \\ \cos(\theta-\alpha) & \sin(\theta-\alpha) & 1 \\ \cos(\theta+\alpha) & \sin(\theta+\alpha) & 1\end{bmatrix} \quad (3.140)$$

$$K_H = \frac{2}{3}\begin{bmatrix} cos\beta & \cos(\beta-\alpha) & \cos(\beta+\alpha) \\ sin\beta & \sin(\beta-\alpha) & \sin(\beta+\alpha) \\ \frac{1}{2} & \frac{1}{2} & \frac{1}{2} \end{bmatrix} \quad (3.141)$$

$$K_H^{-1} = \begin{bmatrix} cos\beta & \sin\beta & 1 \\ \cos(\beta-\alpha) & \sin(\beta-\alpha) & 1 \\ \cos(\beta+\alpha) & \sin(\beta+\alpha) & 1 \end{bmatrix} \quad (3.142)$$

Where $\beta = \theta - =$ Speed of rotation of the arbitrary reference frame

θ_r = Angular rotor position

Therefore the flux linkage of equation 11 is now expressed as;

$\lambda_Q = (2L_L + L_{mq} + L_{md})\, i_Q - (L_{md} - L_{mq})\,(i_q + i_{q\acute{r}})$

$= 2L_L\, i_Q + L_{mq}\, i_Q + L_{md}\, i_Q - L_{md}\,(i_q + i_{q\acute{r}}) + L_{mq}\,(i_q + i_{q\acute{r}})$

$= 2L_L\, i_Q + L_{mq}\, i_Q + L_{md}\, i_Q + L_{md}\, i_Q - L_{md}\, i_Q - L_{md}\,(i_q + i_{q\acute{r}}) + L_{mq}\,(i_q + i_{q\acute{r}})$

$= 2L_L\, i_Q + 2L_{md}\, i_Q + L_{mq}\, i_Q - L_{md}\, i_Q - (i_q + i_{q\acute{r}}) + L_{mq}\,(i_q + i_{q\acute{r}})$

$= 2\,(L_L + L_{md})\, i_Q + [i_Q(L_{mq} - L_{md}) + (i_q + i_{q\acute{r}})\,(L_{mq} - L_{md})]$

$= 2\,(L_L + L_{md})\, i_Q + (i_Q + i_q + i_{q\acute{r}})\,(L_{mq} - L_{md})$

$\therefore \lambda_Q = 2\,(L_L + L_{md})\, i_Q + (L_{mq} - L_{md})\,(i_Q + i_q + i_{q\acute{r}})$ (3.143)

Similarly;

$\lambda_D = (2L_L + L_{mq} + L_{md})\, i_D + (L_{md} - L_{mq})\,(i_d + i_{d\acute{r}})$

$= 2\,(L_L + L_{mq})\, i_D + (L_{md} - L_{mq})\,(i_D + i_d + i_{d\acute{r}})$ (3.144)

$\lambda_O = 2L_L\, i_O$ (3.145)

Also, $\lambda_q = (2L_L + L_{mq} + L_{md})\, i_q - (L_{md} - L_{mq})\,(i_Q + i_{q\acute{r}})$

$= 2\,(L_L + L_{md})\, i_q + (L_{mq} - L_{md})\,(i_Q + i_q + i_{q\acute{r}})$ (3.146

$\lambda_d = (2L_L + L_{mq} + L_{md})\, i_d + (L_{md} - L_{mq})\,(i_D + i_{d\acute{r}})$

$= 2\,(L_L + L_{mq})\, i_d + (L_{md} - L_{mq})\,(i_D + i_d + i_{d\acute{r}})$ (3.147)

$\lambda_o = 2L_L\, i_o$ (3.148)

Also; $\lambda_{q\acute{r}} = (L_{Lqr} + L_{mq} + L_{md})\, i_{q\acute{r}} - (L_{md} - L_{mq})\,(i_Q + i_q)$

$= (L_{Lqr} + 2L_{md})\, i_{q\acute{r}} + (L_{mq} - L_{md})\,(i_Q + i_q + i_{q\acute{r}})$ (3.149)

$$\lambda_{d'r} = (L_{Ldr} + L_{mq} + L_{md})\, i_{d'r} - (L_{md} - L_{mq})\,(i_D + i_d)$$

$$= (L_{Ldr} + 2L_{mq})\, i_{d'r} + (L_{md} - L_{mq})\,(i_d + i_{d+}\, i_{d'r}) \quad (3.150)$$

NB: Upper case letters represent the main winding parameters, while the lower case letters and the primed lower case letters represent the auxiliary winding parameters and rotor winding parameters respectively

As before equations 3.143 - 3.145 represent the flux linkages of the main winding circuit while equations 3.146 -3.148 represent the flux linkages of the auxiliary winding circuit. Also equations 3.149 - 3.150 represent the flux linkages of the caged (rotor) winding circuit t, and r in equations 3.134 and 3.135 is the sum of the resistances of the main, auxiliary and rotor windings in both machine halves. Hence equations 3.413 - 3.150 can be put into equations 3.134 and 3.135 to yield;

$$V_Q = \omega\lambda_D + \rho\,[2\,(L_L + L_{md})\, i_Q + (L_{mq} - L_{md})\,(i_Q + i_{q+}\, i_{q'r})] + r i_Q \quad (3.151)$$

$$V_q = (\omega - 2\omega_r)\,\lambda_d + \rho\,[2\,(L_L + L_{md})\, i_q + (L_{mq} - L_{md})\,(i_Q + i_q + i_{q'r})] + r i_q \quad (3.152)$$

$$V_{q'r} = (\omega - 2\omega_r)\,\lambda_{d'r} + \rho[(L_{Lqr} + 2L_{md})\, i_{q'r} + (L_{mq} - L_{md})\,(i_Q + i_{q+}\, i_{q'r}) + r i_{q'r} \quad (3.153)$$

$$V_D = \omega\lambda_Q + \rho\,[2\,(L_L + L_{mq})\, i_D + (L_{md} - L_{mq})\,(i_D + i_d + i_{d'r})] + r i_D \quad (3.154)$$

$$V_d = (\omega - 2\omega_r)\,\lambda_q + \rho\,[2(L_L + L_{mq})\, i_d + (L_{md} - L_{mq})\,(i_D + i_d + i_{d'r})] + r i_d \quad (3.155)$$

$$V_{d'r} = (\omega - 2\omega_r)\,\lambda_{q'r} + [\rho\,(L_{Ldr} + 2L_{mq})\, i_{d'r} + (L_{md} - L_{mq})\,(i_d + i_{d+}\, i_{d'r})] + r i_{d'r} \quad (3.156)$$

Also for O-variables;

$$V_O = \rho\lambda_O + r i_O$$

$$= \rho(2L_L\, i_O) + r i_O \quad (3.157)$$

$$V_O = \rho\lambda_o + r i_o$$

$$= \rho(2L_L\, i_o) + r i_o \quad (3.158)$$

$$V_{o'r} = \rho\lambda_{o'r} + r i_{o'r}$$

$$= \rho(L_r\, i_{o'r}) + i_{o'r} \quad (3.159)$$

Equations 3.151 – 3.153 result the equivalent circuit shown in figure 3.20 below;

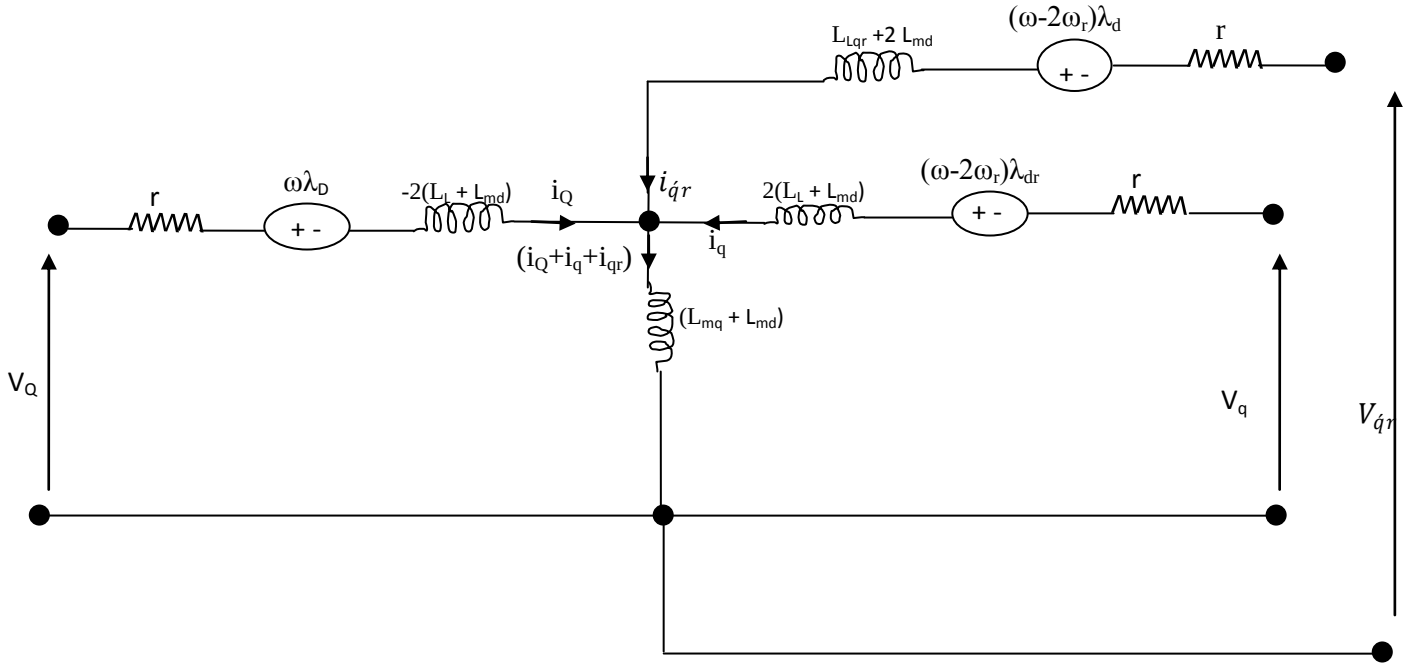

Fig 3.20 Arbitrary reference frame equivalent circuit for a 3-phase symmetrical transfer field reluctance motor with rotor windings in the q-variable.

Also, equations 3.154 -3.156 result the equivalent circuit shown in fig 3.21 below

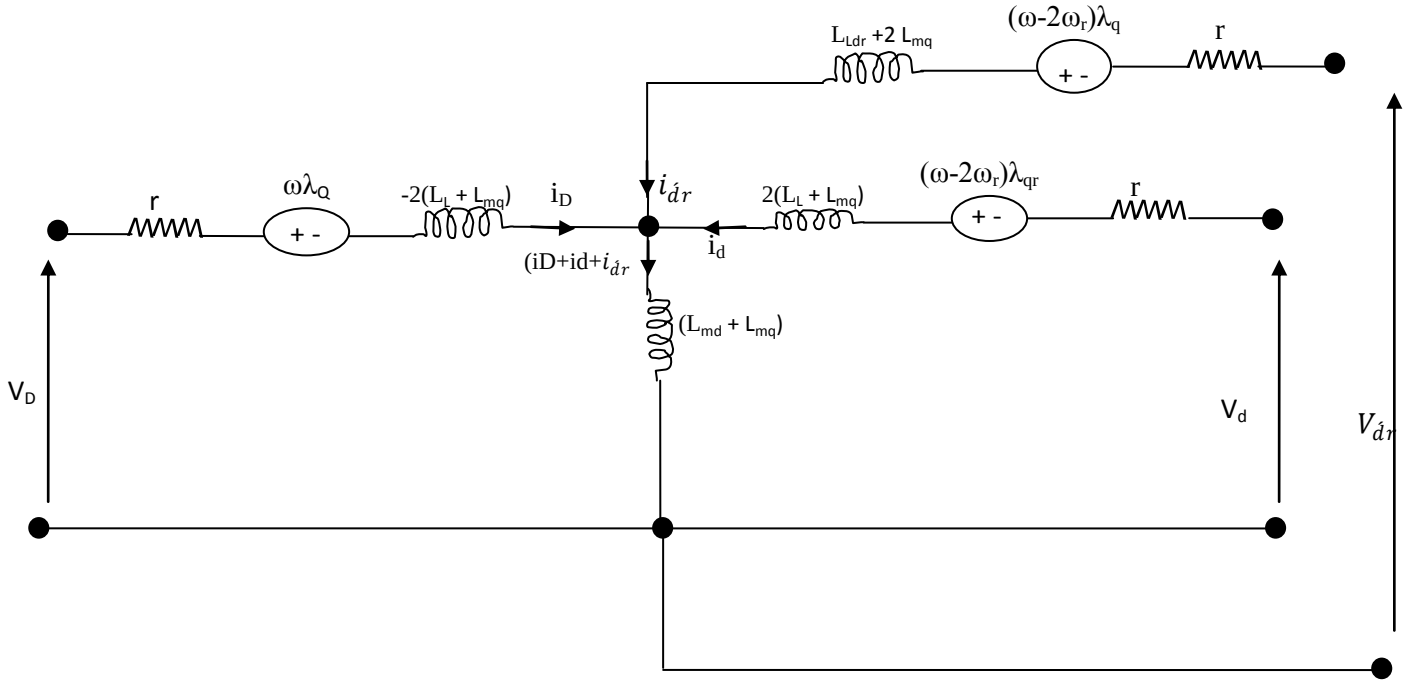

Fig 3.21 Arbitrary reference frame equivalent circuit for a 3-phase symmetrical transfer field reluctance motor with rotor windings in the d-variable.

Similarly, equations 3.157 – 3.159 combines to yield the equivalent circuit shown in fiig 3.22 below

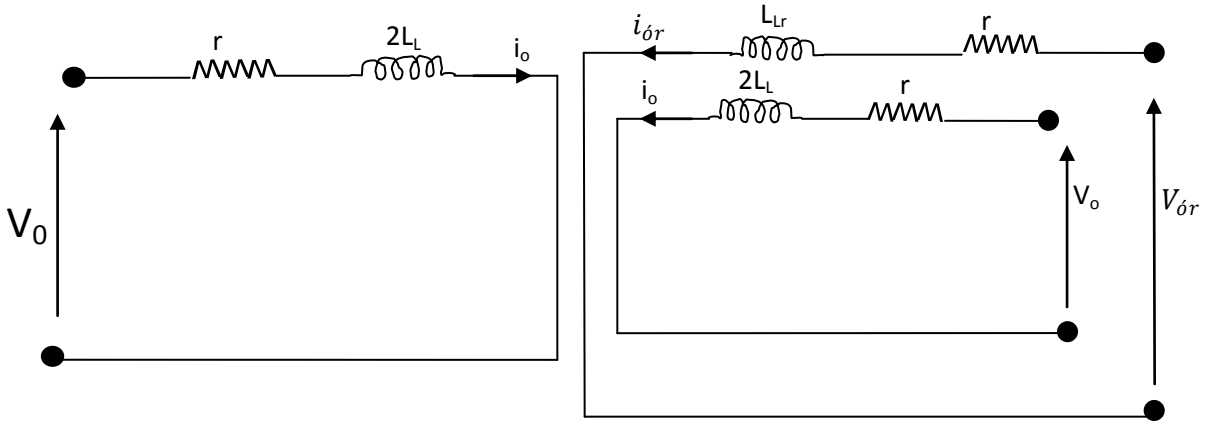

Fig 3.22 Arbitrary reference frame equivalent circuit for a 3-phase symmetrical transfer field reluctance motor with rotor windings in the O-variable.

3.4.5 – Rotor to stator winding inductances

Obviously, both rotors of the machine halves are identical. Therefore, they possess equal and similar parameters. Let us consider the complying between the rotor winding, and the stator windings of machine A. The winding placements are depicted in fig3.23 below

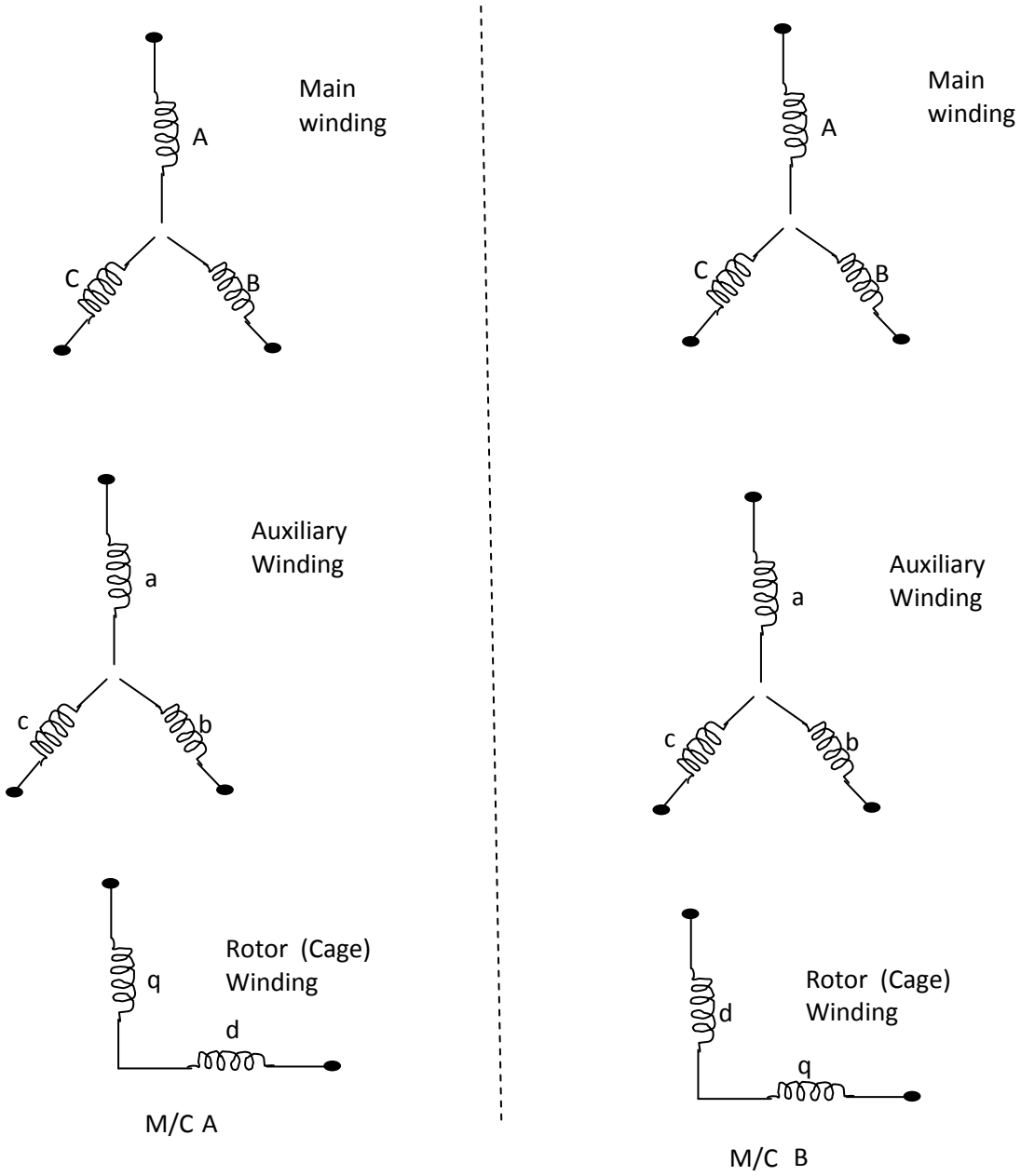

Fig 3.23 Rotor to Stator winding inductances

From figure 3.23 above;

$$L_{GRA} = L_{RAG} = \begin{bmatrix} L_{Aq} & L_{Ad} \\ L_{Bq} & L_{Bd} \\ L_{Cq} & L_{Cd} \end{bmatrix} \quad (3.160)$$

$$L_{HRB} = L_{RBH} = \begin{bmatrix} L_{aq} & L_{ad} \\ L_{bq} & L_{bd} \\ L_{cq} & L_{cd} \end{bmatrix}$$

NB $L_{GRA} = L_{HRB}$ on the account if the identity of the two machine halves.

Also

$L_{aq} = L_{Aq} = L_{mq} \cos \theta r$

$L_{ad} = L_{Ad} = L_{md} \sin \theta r$

$L_{bq} = L_{Bq} = L_{mq} \cos (\theta r - \frac{2\pi}{3})$

$L_{bd} = L_{Bd} = L_{md} \sin (\theta r - \frac{2\pi}{3})$ (3.161)

$L_{cq} = L_{Cq} = L_{mq} \cos (\theta r - \frac{4\pi}{3})$

$L_{cd} = L_{Cd} = L_{md} \sin (\theta r - \frac{4\pi}{3})$

3.4.6 Rotor to Rotor Winding inductances

On the account of identity of the two machine halves;

$$L_{RARA} = L_{RBRB} = \begin{bmatrix} L_{ldr} + L_{md} & O \\ O & L_{ldr} + L_{md} \end{bmatrix} \quad (3.162)$$

3.4.7 The torque equation of the 3-phase transfer field reluctance motor with rotor windings

The torque equation of the configured machine is obtained by integrating the rotor winding parameters into the derived torque equation of the conventional 3-phase transfer field machine with no rotor winding.

The expression for the torque equation of three-phase transfer field motor with cage winding is given as;

$$T_e = \frac{3}{2}\left(\frac{P}{2}\right)\left[\left(i_{Qs} + i_{qs}\right) X_{mq} \left(i_{Ds} + i_{ds} + i_{\acute{d}s}\right]\right.$$

$$\left. - \left[\left(i_{Ds} + i_{ds}\right) X_{mq} \left(i_{Qs} + i_{qs} + i_{\acute{q}s}\right)\right]\right. \quad (3.163)$$

Where,

i_{Qs} is the q-axis stator current in the main winding of TF machine

i_{qs} is the q-axis stator current in the auxiliary winding of T.F machine

i_{Ds} is the d-axis stator current in the main winding of T.F machine

i_{ds} is the d-axis stator current in the auxiliary winding of TF machine $i\acute{d}r$ is the d-axis rotor current in the (cage) rotor of T.F machine.

$i_{\acute{q}r}$ is the q-axis rotor current in the (cage) rotor of T.F machine.

CHAPTER FOUR

RESULT AND DISCUSSION

4.1 Steady state simulations of the 3-phase transfer field reluctance motor with/without rotor windings

After the modification of the conventional three phase transfer field reluctance motor, its analaysis was carried out to ascertain its characteristics through simulation.

4.1.1 Torque/slip characteristics of the 3-phase transfer field reluctance motor with/without rotor windings

In the composite machines, the interaction between the main, auxillary and the rotor windings currents produce the fluxes which are responsible for the torque production. Given the machine parameters as in table 4.1, we can use equations 3.89 and 3.119 to produce Plots for the torques developed at various ranges of slips for the two motors respectively.

Table 4.1: The Machine Parameters

S/No	Parameter	Value
1	L_{md}	133.3mH
2	L_{mq}	25.6mH
3	$L_{Ls} = L_{ia} = L_{er}$	0.6mH
4	$r_m = r_a = r_r = 2R$	3.0Ω
5	J	$1.98x10^{-3}kgm^3$
6	V	220V
7	F	$50H_Z$
8	P	2

The Matlab plots for the torque developed against slips are shown in figure 4.1a and 4.1b

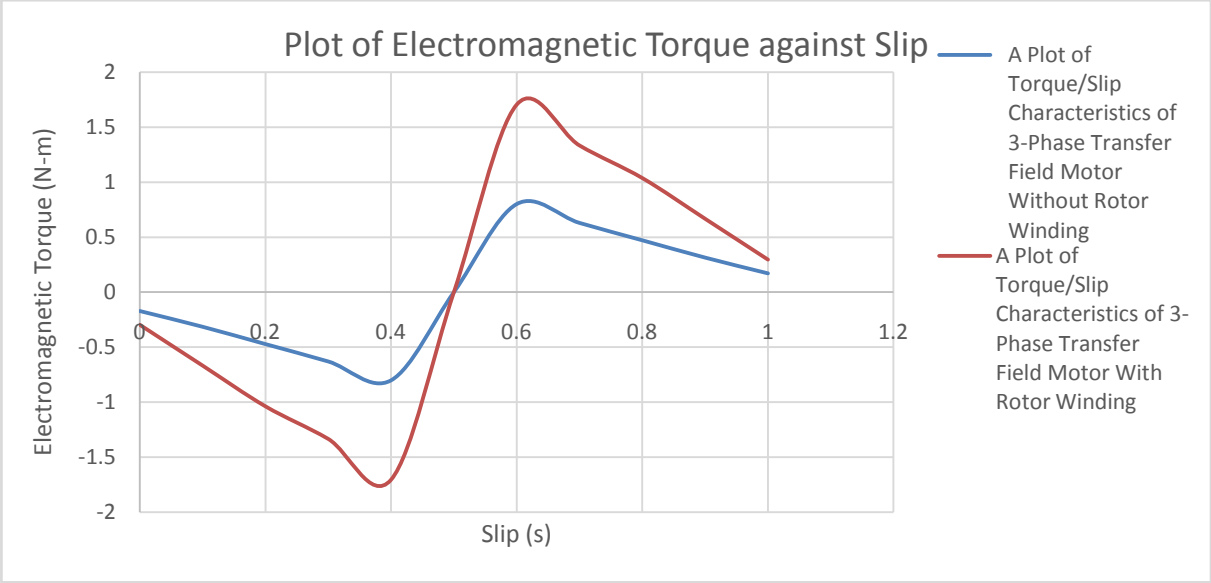

Fig 4.1 A plot of torque developed against ranges of slip(s) for 3-phase transfer field reluctance motor with and without rotor windings

4.1.2 Power factor/slip characteristics of the 3-phase transfer field reluctance motor with and without rotor windings

The plots of the power factor (cos θ)/slip relationships for 3-phase transfer field reluctance motor with and without rotor windings are obtained using equations 3.97 and 3.126 respectively. Their plots are depicted in figure 4.2

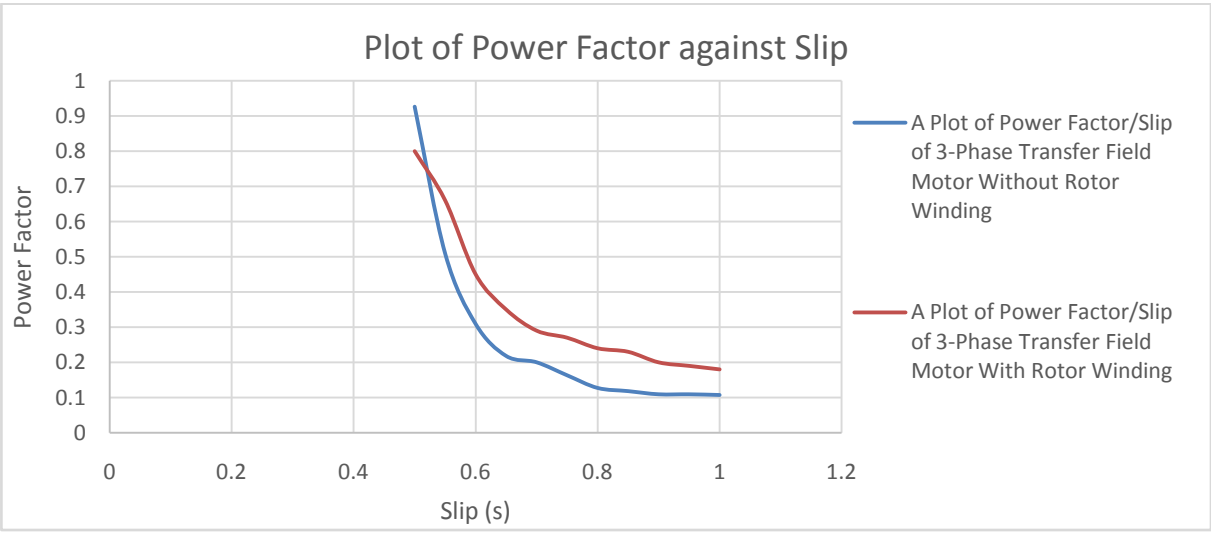

Fig. 4.2 Power factor/slip characteristics of 3-phase transfer field reluctance motor with and without rotor windings

4.1.3. Induced current/slip characteristics for 3-phase transfer field reluctance motor with and without rotor windings

The plots of the induced current (I_a and I_{23})/slip relationship for the existing and the improved motors are obtained using equations 3.86 and 3.111 respectively. Their respective plots are shown in figure 4.3.

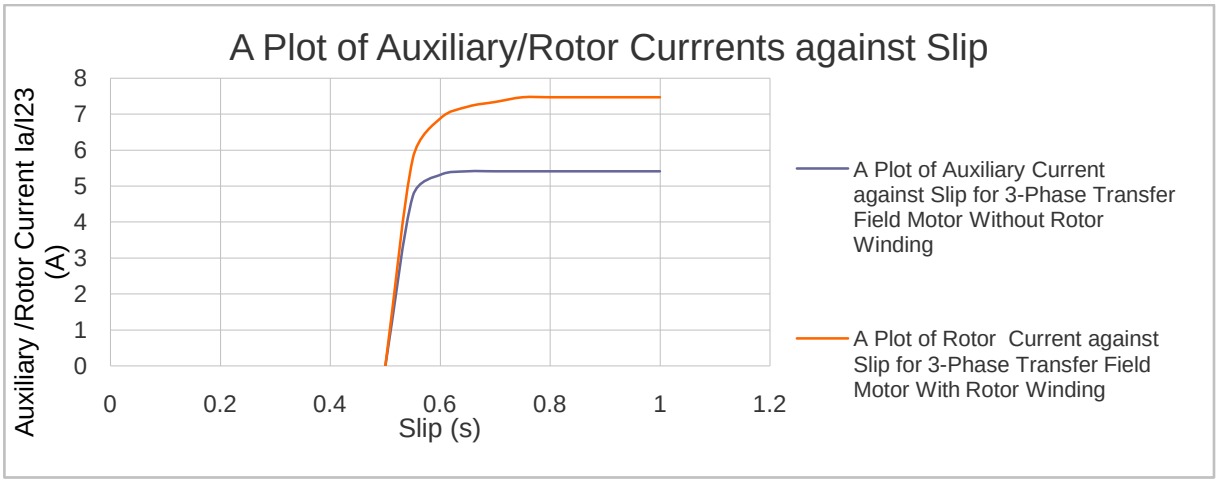

Figure 4.3: A plot of auxiliary current against slip for 3-phase transfer field reluctance motor with and without rotor windings.

4.2 Dynamic-state simulations of the 3-phase transfer field reluctance motor with and without rotor windings

Using equation 3.48 through equation 3.68 and equations 3.163 and values for circuit parameters of table 4.1, the dynamic simulation plots of 3-phase transfer field reluctance motor without rotor windings and that of 3-phase transfer field reluctance motor with rotor winding are shown in figure 4.4a, 4.5a and figure 4.4b, 4.5b respectively.

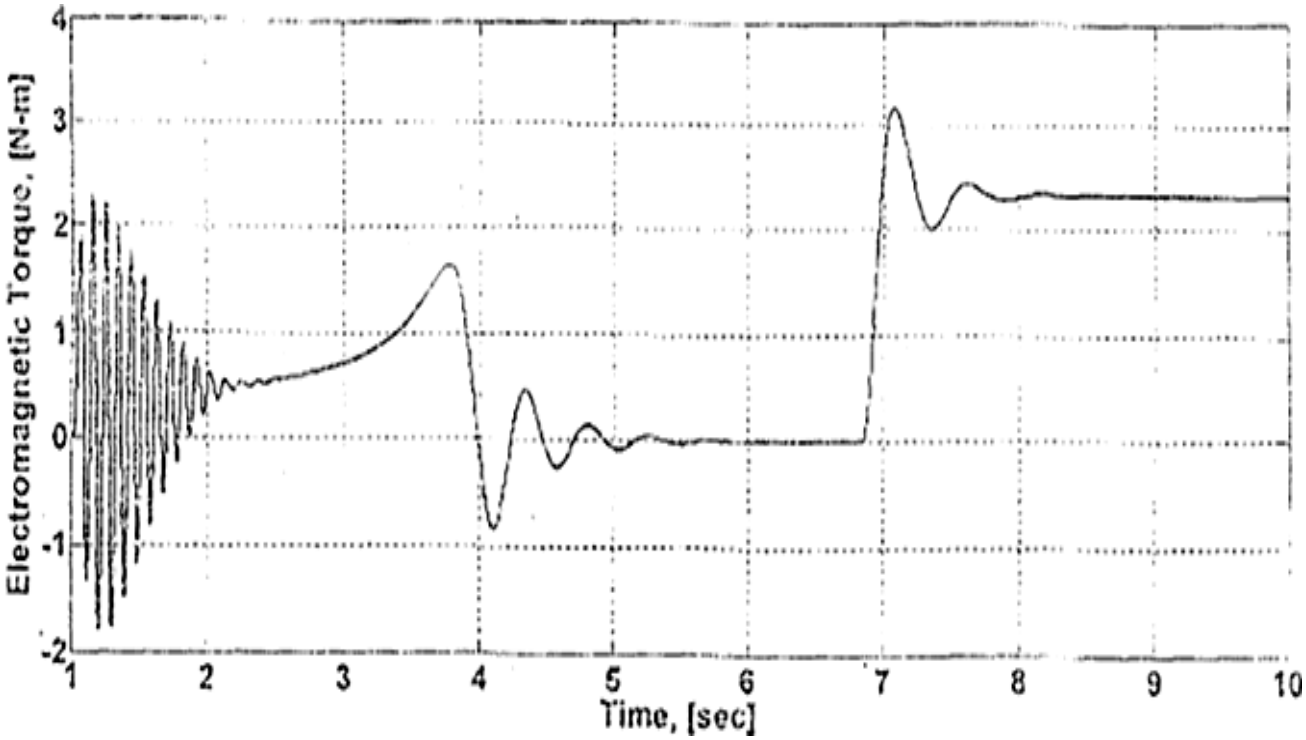

Fig. 4.4a: The Electromagnetic Torque against time for three-phase transfer field reluctance motor without rotor windings

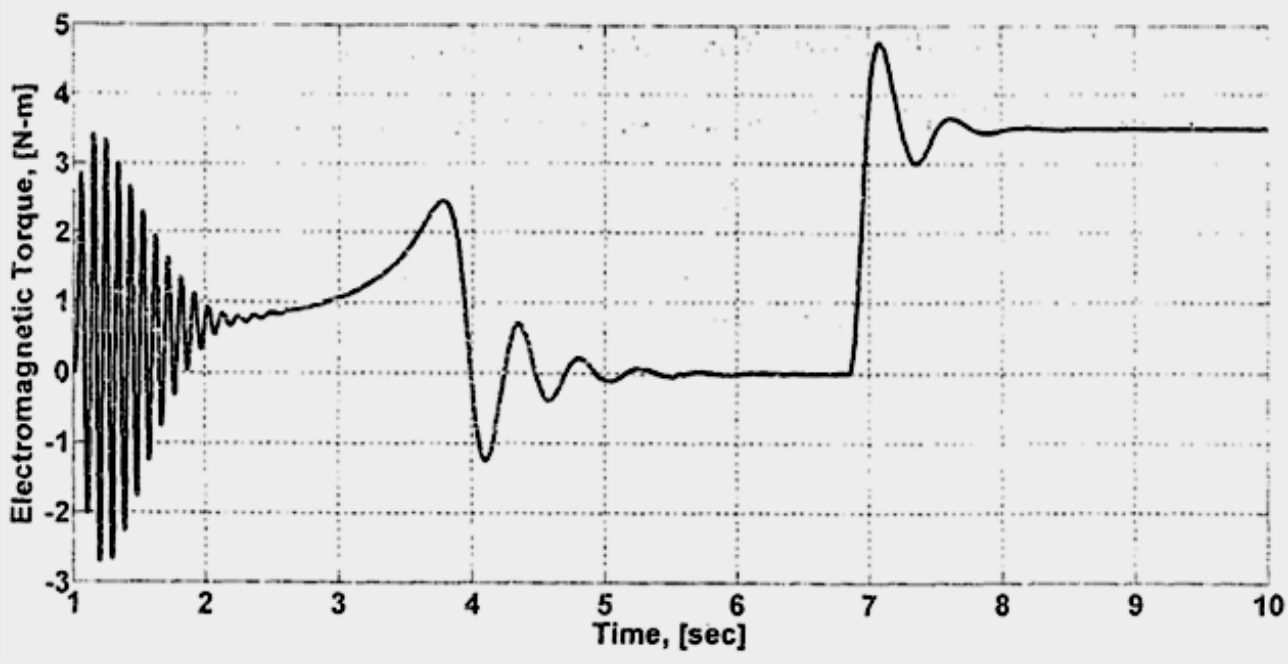

Fig 4.4b: A Plot of Electromagnetic torque verses Time for three-phase transfer field reluctance motor with rotor windings.

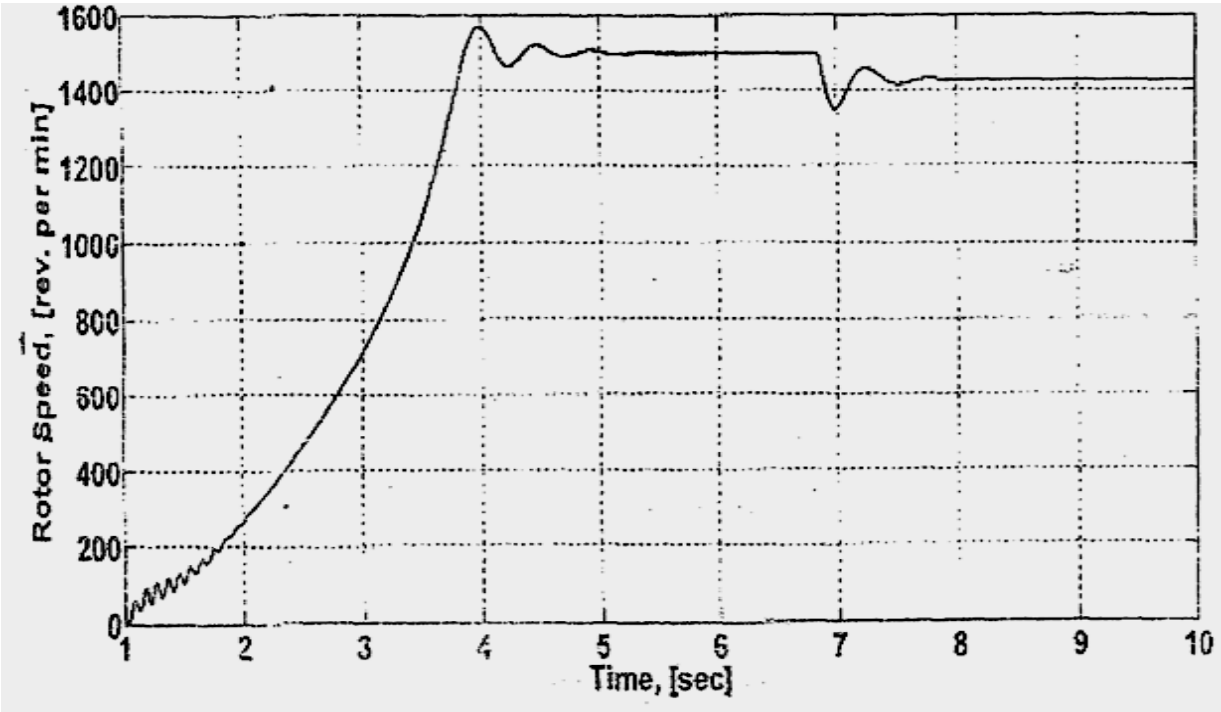

Fig 4.5a Auxiliary winding (rotor) speed (ω_r) against time for three-phase transfer field reluctance motor without rotor windings

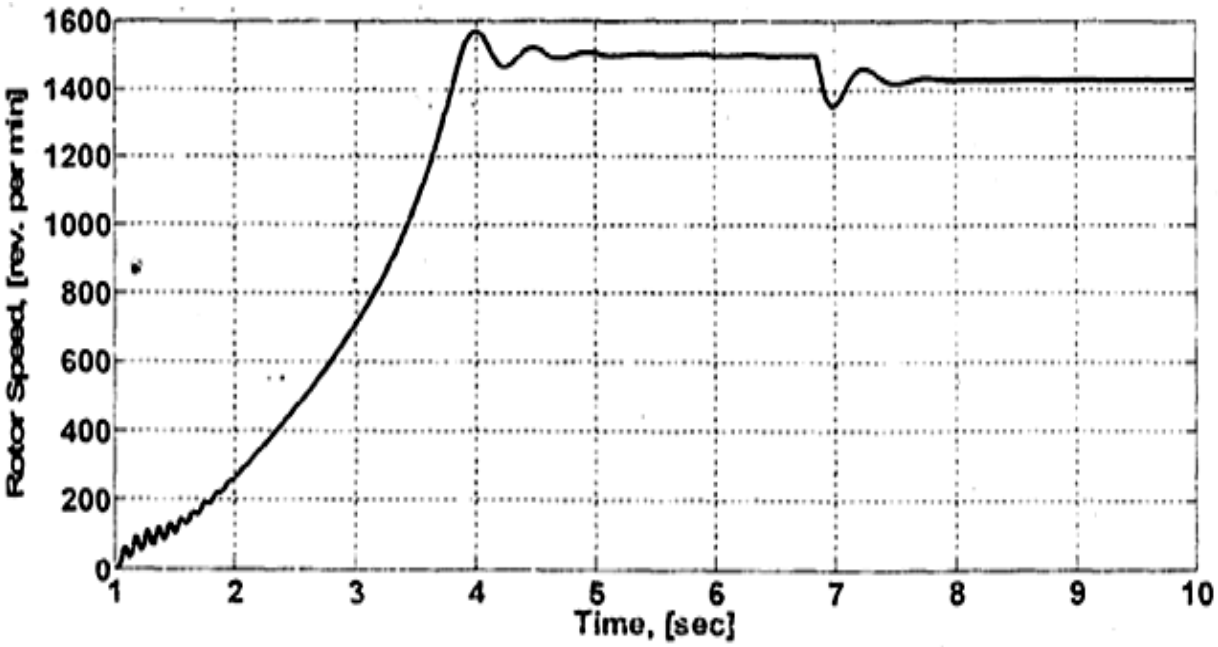

Fig 4.5b: Rotor speed run up plot for the configured motor for three-phase transfer field reluctance motor with rotor windings

4.3 Analysis of Results

4.3.1 Steady-state electromagnetic torques of the motors

From the steady-state electromagnetic torque versus slip characteristics plots for both motors of the results reveals a good similarity to that of the conventional three-phase transfer field reluctance motor without rotor windings (see figure 4). At slip of 0.5, the injected voltage at the auxiliary and rotor windings is zero. Hence, necessitating a zero torque. However, torque may be developed at this slip if the two windings are excited with direct current, hence, making the machine run at synchronous mode. The steady-state analysis of the configured motor was analyzed using dynamic model and circuit theory (Thevenin's) approaches. The results of the steady-state equations, circuit diagrams and simulations using the two approaches married together.

The starting torque of the steady-state electromagnetic torque of the 3-phase transfer field reluctance motor with rotor windings was observed to be approximately 0.296 N-m, while the

maximum torque was 1.57N-m see fig. 4.1b. Similarly, the starting and maximum torques of the **3-phase transfer field reluctance motor without rotor windings** were 0.171N-m and 0.80N-m respectively.

. However, the similarity that exists between the machines is that at low slip (near synchronous speed), the torque is approximately inversely proportional to the slip. At synchronous speed (Ns), s = 0.5 for and torque decays to zero.

4.3.2 Machines power factors

In the plot of power factor/slip curve, of figure 4.3, it is observed that there is an improvement in the power factor of the **3-phase transfer field reluctance motor with rotor windings** as compared to that of the conventional three phase transfer field reluctance motor without rotor windings. At stand still of the rotor (i.e. Nr = 0, s = 1), the power factor of the improved (configured) motor is seen to be 0.180 while for the conventional transfer field reluctance motor without rotor windings, the power factor is seen to be 0.107.

4.3.3 Machines starting currents (I_{au} & I_{23})

Further still, owing to the influence of the rotor windings there is an improvement in the induced auxiliary starting current (I_a) of the conventional **3-phase transfer field reluctance motor without rotor windings**. From figure 4.3, it is observed that due to the additional rotor windings, the induced starting currents rose from 5.409A to 7.475A respectively for the two motors. This brings about a concomitant boost in the maximum and starting torques of the improved machine and at better power factor. For the two motors, at synchronous speeds (s = 5) currents decayed to zero, but at zero speed (N_r = 0, s = 1), starting currents are maximum.

However, the improvements on the output characteristics of the improved motor which was examined by comparing the outputs of the two motors are summarized as tabulated below;

Table 4.2: Summary on the improvement on the output characteristics of 3-phase transfer field reluctance motor with and without rotor windings

Output characteristics	3-phase trasnsfer field relucatnace motor without rotor windings	3-phase trasnsfer field relucatnace motor with rotor windings	Percentage improvement
Electromagnetic torque against slip	Has starting torques of 0.171N-m	Has starting torques of 0.296N-m	73.09%
Power factor against slip	The power factor at start is 0.107	The power factor at start is 0.180	68%
Auxiliary/rotor currents against slip	Induced auxiliary current as start is 5.409A	Induced rotor current as start is 7.475A	38%

4.3.4 Result Analysis of the motors under dynamic state conditions

For the dynamic operation of the machines, the rotor speed run-up plot against time for the **3-phase transfer field reluctance motor with and without rotor windings** is as shown in figure 4.5b and 4.5a. There was a little transient at different stages while rotor speed builds up before an application of load at 7 seconds. After another little transient, the rotor speed now settles to a steady-state at about 1410N-m. The above results infer that the rotor run-up plot for both machines are almost the same.

Also, the graph of Electromagnetic torque against time for both motors with and without windings with oscillations noticed at different stages are shown in figure 4.4b and 4.4a. It is observed that on no-load, value for electromagnetic torque is zero. On application of load torque at 6.9 seconds to **3-phase transfer field reluctance motor with and without rotor windings**, they oscillate and settled to a steady-states of 3.4N-m and 2.25N-m respectively.

CHAPTER FIVE

CONCLUSION AND RECOMMENDATION

5.1 Conclusion

Analysis of the effect of induced rotor current on the improvement of the output performance of 3-phase transfer field reluctance motor due to influence of rotor windings has been concluded. The rotor windings were incorporated into the conventional 3-phase transfer field reluctance motor with a view to attenuating the excessive leakage reactance with a concomitant increase in rotor current of the machine. The equivalent circuit of the improved motor was derived and then analyzed based on circuit theory (Thevenin's approach) concept and d-q-0 analysis. The output power/torque and power factor of the improved motor (3-phase transfer field reluctance motor with rotor windings) were compared with those of the conventional (3-phase transfer field reluctance motor without rotor windings) motor without rotor windings. It was shown that though they exhibited related characteristics, 3-phase transfer field reluctance motor with rotor windings is superior to that of the conventional 3-phase transfer field reluctance motor with rotor windings.

From the results obtained it is important to state the accelerated rotor current is a consequence of the rotor windings added to the rotor of the existing motor. Also the increased induced rotor current is responsible for the improved output power, electromagnetic torque and power factor of the existing motor.

Though the transfer field electric machine is an asynchronous machine, the machine is capable of synchronous operation when the auxiliary windings run at half the source frequency or when the slip is 0.5 and a direct current is injected into the auxiliary windings to

produce a direct field at a speed when the rotor speed is half of the synchronous speed. In this mode, the motor will operate as a synchronous machine utilizing one side of the coupled transfer field machine.

The self inductance matrix of the two machines are derived and both shown to be independent of the rotor angular position. However, the mutual coupling inductance in both cases are dependent on rotor angular position. For the transfer field machine, in addition to rotor angle dependence, it also depends on the difference between the direct and quadrature axes reactances. Consequently, the machine produces reluctance torque as a result of the rotor pole – axis trying to alian with the axis of the maximum flux. But that of induction motoris by alignment of fields, that is, the rotating magnetic field of the rotor trying to catch up with that of the stator. Under steady-state performance, the transfer field machine exhibited a lower pull out and starting torque as well as lower efficiency than the induction machine. In dynamic mode, the torque versus speed characteristics of both machines are very identical which is akin to what obtains in the steady-state simulation. Also the starting current of the transfer field machine is not high – a feature that makes it possible for the transfer field machine to tolerate a longer starting time without any major disturbance to the supply unlike the induction machine.

5.2 Recommendation

The transfer field effect machine in general is a low speed machine operating at half the speed of a conventional induction machine. It is envisaged that improved conventional three phase transfer field reluctance motor with rotor windings for enhanced output power and power factor will have future in a variety of special applications such as low speed fixed frequency drives, linear motors for small scale transport systems and small brushless motors etc. It is

common knowledge that a low speed motor will find applications in domestic appliances requiring low speed drives such as grinding motors for perishables.

It is also recommended that more research should be carried out on the output power to size ratio of the transfer field reluctance motors of various ratings necessary for industrial and domestic applications as obtainable in old and well known induction motors.

5.3 Contribution to knowledge

The addition and proper connections of rotor windings to the rotor poles structures of the existing three-phase transfer field reluctance motor without rotor windings, contributed immensely to the enhancement on the output characteristics (such as the output torque, output power, power factor, efficiency etc) of the motor. This new model of 3-phase transfer field reluctance motor can replace the usual 3-phase induction motors for better performance at relative negligible cost.

REFERENCES

Agu, L. A. & Anih**,** L. U. (2002). Couple Poly phase reluctance machine without rotating windings. A technical Transactions of Nigeria society of Engineers. Pp. 37, 46 – 53.

Agu, L. A. (1978). *The transfer field machine, Electric Machine and Electro Mechanics*. pp 403-418.

Agu, L. A. (1984). Output enhancement in the transfer-field machine using rotor circuit induced currents. *Nigeria Journal of Technology* Vol. 8, No. 1. Pp. 7 – 11.

Alger P. (1970). *The nature of induction motor*2nd edition, Gordon & Breach New York

Ani, L.U. et al **(**2012). The steady-state performance characteristics of single **phase** transfer field machine operating in the asynchronous mode. *Nigeria Journal of Technology* vol.31, No 3, November 2012 pp 219-226

Anih, L. U. (2009). Magnetic of an idealized Asynchronous reluctance machine with no moving conductors. *The Pacific Journal of Science and Technology* Vol. 10 Pp 3-4

Anih, L. U. & Obe E. S **(**2001). *Performance analysis of a composite Dual winding machine*. Pp 23 of 18

Anih, L. U. et al (2004). Modelling and Performance of a hybrid synchronous reluctance machine with adjustable $\frac{Xd}{Xq}$ ratio. A publication of the IET Electric Power Applications.

Anih,. L. U. & Agu, L. A. (2008). Mechanism of Torque production in a coupled polyphase reluctance machine. *Nigerian Journal of Technology* Vol. 27 No. 1. Pp 29 – 38.

Bhatta, C. S. K. (2009). Electrical machines (second edition). Published by Tasta McGraw-hill Publishing Ltd 7 West Pastel Nagar, New Delhi 110008 pp495

Brodway, A. R. W. & Tan, S.C.F. (1973). *Brushless stator - controlled synchronous induction machine.* Pp 120, 860-866

Chee-mun O. (1997). *Dynamic Simulation of Electric Machinery using Matlab/simulink*. Prentice Hall PTR, New Jersey.

Eleanya, M.N. (2015). *Comparative Analysis of a transfer field machine and induction machine*. Thesis submitted to the Department of Electrical Engineering University of Nigeria Nsukka pp 72

Fitzgerald, A. E; Charles, K. Jr. & Stephen, D. U. (2003). *Electric Machinery,* Tata McGraw-Hill

Gapta, J. B. (2006). *Theory and performance of Electrical machine*. S.K Katania and Sons 4424/6 Guru Namak Market, Naisarak Delhi-110006, pp. 578-579.

Gupta, J. B. (2000). *A course in Power Systems*. Published by Sanjeev Kumar Kataria and Sons. 6 Guru Nanak Market, Nai Sarak, Delhi – 11006. Tenth edition. Pp. 66 – 69.

Ijeomah, C. N. et al (1996). Torque Enhancement of a reluctance effect machine by step-frequency secondary voltage injection method.

Krishnan, R. (2000). *Electric Motor drives: Modeling, analysis and cont*rol, Prentice Hall, New Jersey.

Lipo T. A. & Chang, K. C. (1985). *A new approach to flux and Torque Sensing in induction machines* IEEE IAS annual meeting.

Menta, V.K. & Rotit M. (2000). "*Principles of Electrical Machines*" published by S. Chand and Company Ltd. Rann Nagar, New Delhi – 110055 pp 386

Okozi, S. O. et al (2017) Starting, steady-state modeling and simulation studies of single-phase transfer field reluctance motor, operating in the asynchronous mode. *International journal of scientific research publications* vol. 7 issue 1 Jan 2017 pp **182-188**

Eleanya, M. N. et al (2016). Analytical determination of steady state performance indices of single-phase induction motor, using symmetrical components of unbalanced voltages of 3-phase system. *International journal of recent advances in multi disciplinary research* vol.03, issue 11 November pp 1913 – 1918.

Smarajit, G. (2005). "*Electrical Machine*" Published by Dorling Kindersley (India) PVT. Ltd. Pp. 375.

Stephen J. C. (2007). "*Electric Machinery Fundamental*". 1221 Avenue Americas New York McGraw Hill Inc, New York 10020. Forth edition

APPENDICES

Appendix A: Matlab program for steady state torque of the three phase transfer field reluctance motor without rotor windings using Thevenin's Equivalent circuit approach.

```
F=50;  V1=220; R=1.5; w=2*3.142*F;
Ls=0.6e-3;Lr=0.6e-3;
Lmq=25.6e-3; Lmd=133.3e-3;
Xmq=w*Lmq;  Xmd=w*Lmd; Xlr=w*Lr; Xq=w*(Ls+Lmq);
Rth=R*(Xmd-Xmq)/(Xmd-Xmq+2*Xq);
Xth=2*(Xq*Xmd-Xq*Xmq)/(Xmd-Xmq+2*Xq);
Vth=((Xmd-Xmq)/(Xmd-Xmq+2*Xq))*V1;
s= [0.4,0.3,0.2,0.1,0,0.5,1,0.9,0.8,0.7,0.6];
A=6*R./w*(2*s - 1);
B=(Vth^2);
C=Rth+(R./(2*s-1));
D=Xth+2*Xq;
Te=A.*(B./(C.^2+D^2));
s = 0:0.1:1;
s_interp = linspace(min(s), max(s));
Te_interp = interp1(s,Te,s_interp, 'spline');
plot(s_interp,Te_interp);

title('Plot of Electromagnetic Torque against Slip');
xlabel('Slip (s)');
ylabel('Electromagnetic Torque Te (N-m)');
```

Appendix B: Matlab program for steady state torque of the Three phase transfer field Reluctance motor with rotor windings, Using Thevenin's equivalent circuit approach

```
F=50;  V1=220; R=1.5; w=2*3.142*F;
Ls=0.6*10^-3;Lr=0.6*10^-3;
Lmq=25.6*10^-3; Lmd=133.3*10^-3;
Xd = w*Lmd;
Xq = w*(Ls+Lmq);
s= [0.4,0.3,0.2,0.1,0,0.5,1,0.9,0.8,0.7,0.6];
Vth = ((Xd-Xq)/(Xd+Xq))*V1;
Rth = (2*R*(Xd-Xq))/(Xd+Xq);
Xth = (2*Xq*(Xd-Xq))/(Xd+Xq);
A=(6*R./w)*(2*s - 1);
B = Vth^2;
C=Rth+(R./(2*s-1));
D=Xth+Xq;
Te=A.*(B./(C.^2+D^2));
s = 0:0.1:1;
s_interp = linspace(min(s), max(s));
Te_interp = interp1(s,Te,s_interp, 'spline');
plot(s_interp,Te_interp);

title('Plot of Electromagnetic Torque against Slip');
xlabel('Slip (s)');
ylabel('Electromagnetic Torque Te (N-m)');
```

Appendix C: Matlab program for the efficiency of the Three-phase transfer field reluctance motor without rotor windings.

```
F=50;  Va=220; R=1.5; w=2*3.142*F;
Ls=0.6e-3;Lr=0.6e-3;
Lmq=25.6e-3; Lmd=133.3e-3;
Xmq=w*Lmq;  Xmd=w*Lmd; Xlr=w*Lr; Xq=w*(Ls+Lmq);
s = 1:-0.1:0.5;
Az = R + 2* Xq*1j;
rs1 = (R./ (2*s - 1));
Bz = (Xmd - Xmq)*1j *(2*Xq*1j + rs1);
Cz = rs1 + (2*Xq + (Xmd - Xmq))*1j;
Z = Az + (Bz./Cz);

IA = Va./Z;

Ai = (Xmd - Xmq)*1j;
Bi = (2*Xq + (Xmd - Xmq)) * 1j;
Ia = (Ai ./(rs1 + Bi)).* IA;

rs2 = (1 - s)./( 2*s - 1);

eff = (2 * rs2 .* (Ia.^2))./(2*(rs2.*Ia.^2) + (IA +
Ia).^2);
eff(6) = 0.1 ;

s_interp = linspace(min(s), max(s));
eff_interp = interp1(s,eff,s_interp, 'spline');
plot(s_interp,eff_interp);

grid on;
title('Plot of Efficiency against Slip');
xlabel('Slip (s)');
ylabel('Efficiency');
```

Appendix D: Matlab program for the efficiency of the three phase transfer field reluctance motor with rotor windings

```
F=50;  V1=220; R=1.5; w=2*3.142*F;
Ls=0.6*10^-3;Lr=0.6*10^-3;
Lmq=25.6*10^-3; Lmd=133.3*10^-3;
Xd = w*Lmd;
Xq = w*(Ls+Lmq);
Vth = ((Xd-Xq)/(Xd+Xq))*V1;
Rth = (2*R*(Xd-Xq))/(Xd+Xq);
Xth = (2*Xq*(Xd-Xq))/Xd+Xq);

s = 0.5:0.05:1;
Az = 2*R + 2* Xq*1j;
rs1 = (R./ (2*s - 1));
Bz = (Xd - Xq)*1j *(Xq*1j + rs1);
Cz = rs1 + Xd*1j;
Z = Az + (Bz./Cz);

I1 = V1./Z;

I23 = ((Xd - Xq)*1j./(rs1 + (1j*Xd))).*I1;
rs2 = (1 - s)./( 2*s - 1);

Aeff = (rs2 .*I23).^2;
Beff = (rs2 .*(I23.^2)) + (I1+I23).^2;
eff = Aeff./Beff;
eff = abs(eff);
eff(1) = 0.1;

s_interp = linspace(min(s), max(s));
eff_interp = interp1(s,eff,s_interp,'spline');
plot(s_interp,eff_interp);
title('Plot of Efficiency against Slip');
xlabel('Slip (s)');
ylabel('Efficiency');
```

Appendix E: Matlab program for power factor of the Three-phase transfer field reluctance motor without rotor windings

```
F=50;  V1=220; R=1.5; w=2*3.142*F;
Ls=0.6e-3;Lr=0.6e-3;
Lmq=25.6e-3; Lmd=133.3e-3;
Xmq=w*Lmq;  Xmd=w*Lmd; Xlr=w*Lr; Xq=w*(Ls+Lmq);
Rth=R*(Xmd-Xmq)/(Xmd-Xmq+2*Xq);
Xth=2*(Xq*Xmd-Xq*Xmq)/(Xmd-Xmq+2*Xq);
s = 0.5:0.05:1;
rs1 = (R./ (2*s - 1));
A=Rth + rs1;
B=Xth + (2*Xq);
pf = A./((A.^2 + B.^2).^0.5);

s_interp = linspace(min(s), max(s));
pf_interp = interp1(s,pf,s_interp, 'spline');
plot(s_interp,pf_interp);

title('Plot of Power factor against Slip');
xlabel('Slip (s)');
ylabel('Power Factor');
```

Appendix F: Matlab program for power factor of the Three-phase transfer field reluctance motor with rotor windings

```
F=50;  V1=220; R=1.5; w=2*3.142*F;
Ls=0.6e-3;Lr=0.6e-3;
Lmq=25.6e-3; Lmd=133.3e-3;
Lmq=25.6*10^-3; Lmd=133.3*10^-3;
Xd = w*Lmd;
Xq = w*(Ls+Lmq);
Rth = (2*R*(Xd-Xq))/(Xd+Xq);
Xth = (2*Xq*(Xd-Xq))/(Xd+Xq);
s = 0.5:0.05:1;
rs1 = (R./ (2*s - 1));
A=Rth + rs1;
B=Xth + Xq;
pf = A./((A.^2 + B.^2).^0.5);
pf(1) = 0.8;
s_interp = linspace(min(s), max(s));
pf_interp = interp1(s,pf,s_interp, 'spline');
plot(s_interp,pf_interp);

title('Plot of Power factor against Slip');
xlabel('Slip (s)');
ylabel('Power Factor');
```

Appendix J: Matlab program for Auxiliary current against slip for the Three-phase transfer field reluctance motor without rotor windings

```
F=50;  V1=220; R=1.5; w=2*3.142*F;
Ls=0.6e-3;Lr=0.6e-3;
Lmq=25.6e-3; Lmd=133.3e-3;
Xmq=w*Lmq;  Xmd=w*Lmd; Xlr=w*Lr; Xq=w*(Ls+Lmq);
Rth=R*(Xmd-Xmq)/(Xmd-Xmq+2*Xq);
Xth=2*(Xq*Xmd-Xq*Xmq)/(Xmd-Xmq+2*Xq);
Vth=((Xmd-Xmq)/(Xmd-Xmq+2*Xq))*V1;

s = 0.5:0.05:1;
A=Rth+(R./(2*s-1));
B=Xth+2*Xq;

Ia = Vth./sqrt(A.^2 + B.^2);

s_interp = linspace(min(s), max(s));
Ia_interp = interp1(s,Ia,s_interp, 'spline');
plot(s_interp,Ia_interp);
xlabel('slip (S)');
ylabel('Ia (A)');
```

Appendix H: Matlab program for rotor current against slip for the Three-phase transfer field reluctance motor with rotor windings

```
Ls=0.6*10^-3;Lr=0.6*10^-3;
Lmq=25.6*10^-3; Lmd=133.3*10^-3;
Xd = w*Lmd;
Xq = w*(Ls+Lmq);
Vth = ((Xd-Xq)/(Xd+Xq))*V1;
Rth = (2*R*(Xd-Xq))/(Xd+Xq);
Xth = (2*Xq*(Xd-Xq))/(Xd+Xq);

s = 0.5:0.05:1;
A = Rth + (R./(2*s-1));
B = Xth+Xq;

I23 = Vth./(sqrt(A.^2 + B.^2));
s_interp = linspace(min(s), max(s));
I23_interp = interp1(s,I23,s_interp, 'spline');
plot(s_interp,I23_interp);
xlabel('slip (S)');
ylabel('I_23 (A)');
```

Appendix I: Matlab Programm for the Dynamic Simulation of the Three-phase transfer field reluctance motor without rotor windings

```
function [diQ,diD,diq,did,iA,iABC,ia,iabc,FQ,FD,Fq,Fd,Te,dwm] =
fcn(iQ,iD,iq,id,Va,Vb,...
    Vc,wm)
%#eml

 Vm = 179.63; P = 4;
r =6.0;
lmd = 133.3e-3; lmq = 25.6e-3; lls = 6e-3;
J = 0.00198; Tl = 0;
% p=number of poles
% Vm = 179.63; P = 4;
% r = 6.0;
% lmd = 133.3e-3; lmq = 25.6e-3; lls = 6e-3;
% J = 0.00198; Tl = 0;
ld = (lmq + lmd)/2;
ls = lls + ld;
lm = lmd - lmq;


%w is the electrical speed of the rotor

% wr = wm * P/2;
wr = 100*pi;
R = [r 0 0 0; 0 r 0 0; 0 0 r 0; 0 0 0 r];
L = [2*ls 0 -lm 0; 0  2*ls 0 lm; -lm 0 2*ls 0; 0 lm 0 2*ls];
wL = [0          2*ls*wr        0          lm*wr;
    -2*ls*wr      0           lm*wr         0;
     0          wr*lm          0         -2*wr*ls;
     lm*wr        0           2*ls*wr      0];


Vabc = Vm * [Va; Vb; Vc];
kk = 2*pi/3; tt = 0;
K = (2/3)*[-sin(tt) -sin(tt - kk) -sin(tt + kk);...
          cos(tt) cos(tt - kk) cos(tt + kk);...
          1/2    1/2     1/2];
VQD = K * Vabc;
vQ = VQD(1); vD = VQD(2);
vq = 0; vd = 0;
Vqd0 = [vQ; vD; vq; vd];
i = [iQ; iD; iq; id];
di = L \ (Vqd0 - (R + wL)*i);
diQ = di(1); diD = di(2); diq = di(3); did = di(4);

Te = (3/4) * P * lm *(iQ*conj(id) - iD*conj(iq));
```

```
dwm = 4*(Te - Tl )/J;

iABC = K\ [iQ; iD; 0];
iA = iABC(1); iB = iABC(2); iC = iABC(3);

iabc = K\ [iq; id; 0];
ia = iabc(1); ib = iabc(2); ic = iabc(3);

II = [iQ; iD; iq; id];
LL = [2*ls 0 -lm 0; 0 2*ls 0 lm; -lm 0 2*ls 0; 0 lm 0 2*ls];

F = LL * II;
FQ = F(1); FD = F(2); Fq = F(3); Fd = F(4);



clear; clc;
load dual_obe
t=linspace(0,2,20006);

figure (1);
plot(t,IA,'k-','linewidth',2); xlabel('Time, [sec]'); ylabel('Main Winding current, I_A_S,
[A]');
grid on

figure (2);
plot(t,Ia,'k-','linewidth',2); xlabel('Time, [sec]'); ylabel('Aux. Winding current, I_a_s,
[A]');
grid on

figure (3);
plot(t,speed,'k-','linewidth',2); xlabel('Time, [sec]'); ylabel('Rotor Speed, \omega_r,
[rads/sec]');
grid on

figure (4);
plot(t,torque,'k-','linewidth',2); xlabel('Time, [sec]'); ylabel('Electromagnetic Torque,
T_e, [N-m]');
grid on

figure (5);
plot(speed,torque,'k-','linewidth',2); xlabel('Rotor Speed, \omega_r');
ylabel('Electromagnetic Torque, T_e, [N-m]');
grid on
```

APPENDIX J - LISTS OF PLATES

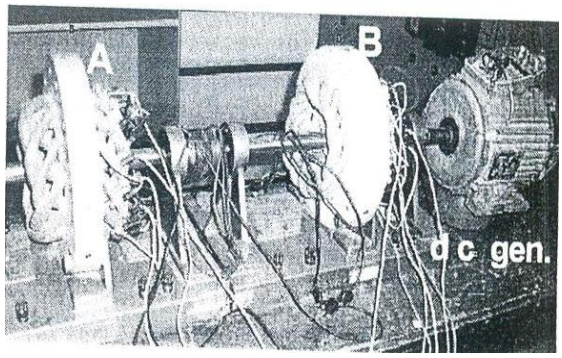

Plate 1 – Pictorial view of a transfer field reluctance machine. Courtesy of machine laboratory, University of Nigeria Nsukka

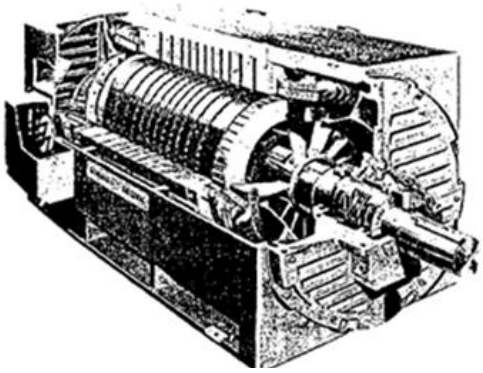

Plate 2: Cutaway view of a Squirrel cage induction motor

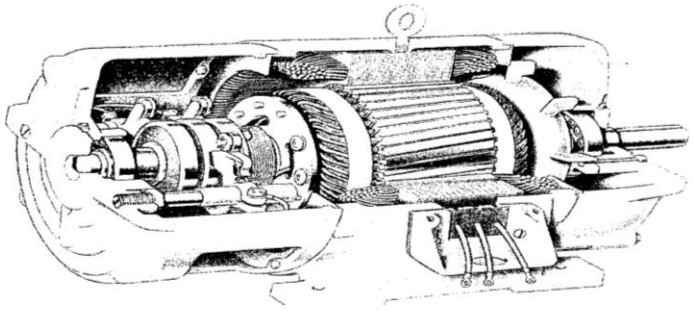

Plate 3: Cutaway view of a Wound rotor induction motor.

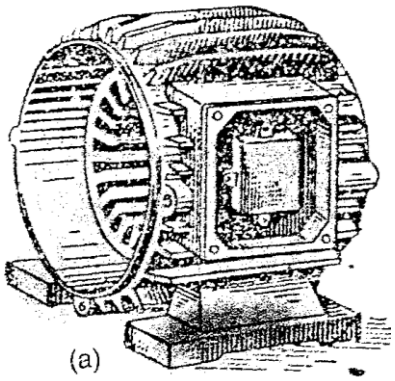

Plate 4: Induction motor frame with unwound stator

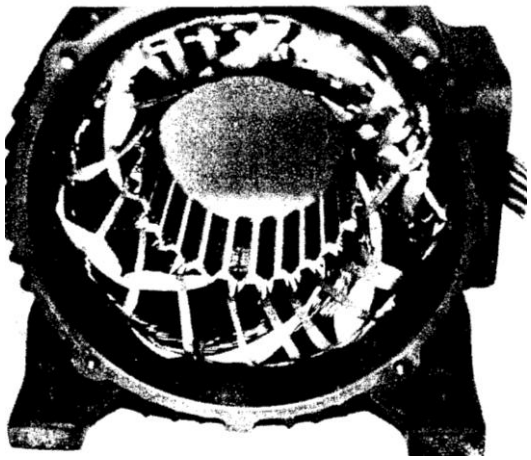

Plate 5: Induction motor frame with wound stator

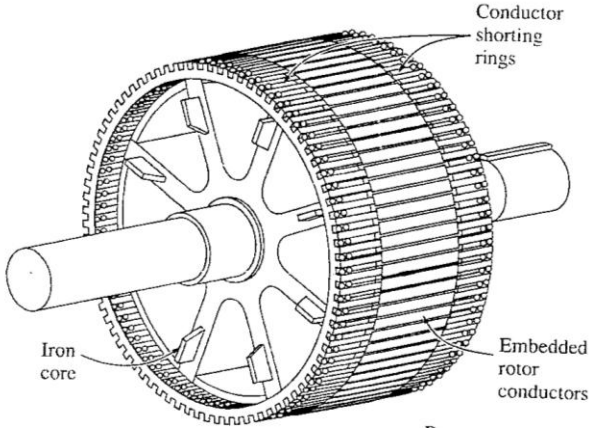

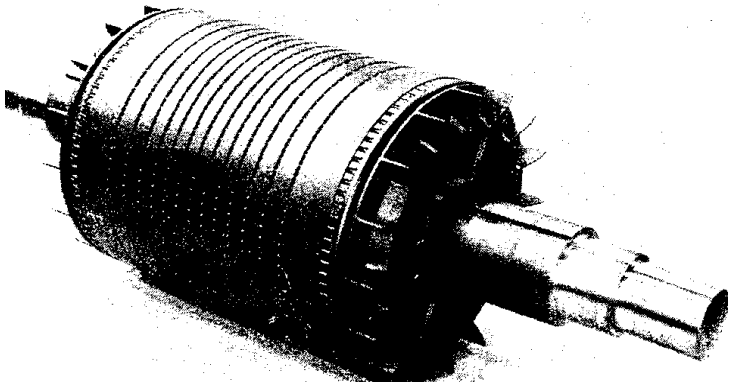

Plate 6(a/b): Typical squirrel-cage rotor

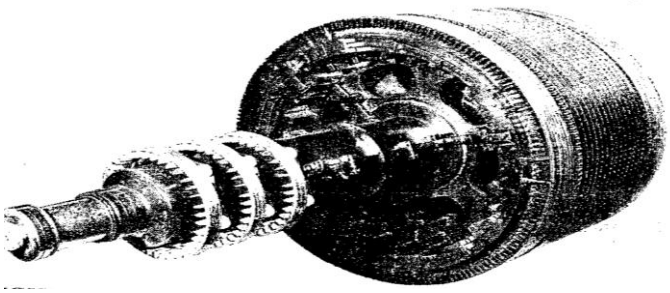

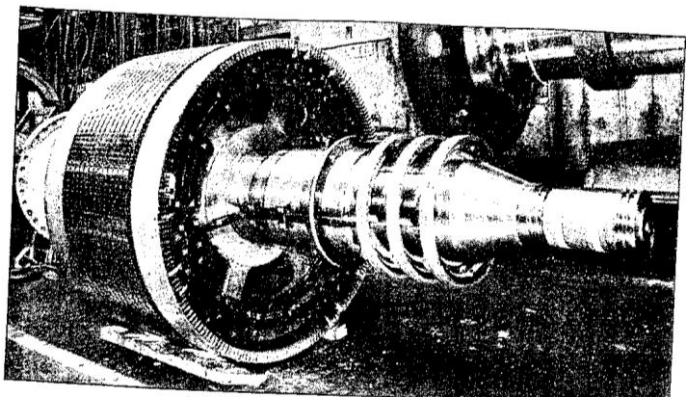

Plate 7(a/b) Typical wound (slip rings) rotors